UNIVERSITY OF SOUTHAMPTON

FACULTY OF MEDICINE

CANCER SCIENCES

VOLUME 1 OF 1

The effect of histone deacetylase inhibitors on Notch signalling in the epidermis

By

Charlotte Cotter

Thesis for the degree of Master of Philosophy

October 2014

1. Abstract

The skin is regenerated every 2-3 weeks by a tightly regulated process which depends on keratinocyte stem cells at the innermost layer proliferating, differentiating and migrating upwards to form the suprabasal layers. As cells differentiate they typically undergo epigenetic changes to their DNA. Histone acetylation is one type of epigenetic modification that can alter gene expression patterns. Therefore, to assess how keratinocyte cell fate is modulated by histone regulation we assessed HDAC expression in keratinocytes and subsequently treated primary human keratinocytes with a panel of histone deacetylase inhibitors (HDACi) to assess their proliferation and differentiation characteristics. One of these HDACi, valproic acid (VPA) significantly inhibited keratinocyte proliferation and differentiation. As Notch signalling plays a key role in commitment of keratinocytes to terminal differentiation the expression of Notch1 in VPA-treated keratinocytes was assessed next by qPCR. Notch1 levels were reduced 24h post-treatment with VPA while expression of its downstream target Hes1 was reduced by 3-fold within 6h. In contrast, two Notch co-factors Hey1 and Mastermind (MAML1) were upregulated by 20.8- and 7.8-fold, respectively. These data demonstrate that the HDACi VPA inhibits epidermal differentiation by modifying the levels of Notch1 signalling molecules. Specific upregulation of Hey1 and MAML1 coupled with downregulation of Notch1 and Hes1, suggest that VPA does not interfere with canonical Notch signalling but rather affects Notch signalling via an independent route which bypasses Notch activation and instead directly modulates the downstream signalling molecules. With this knowledge it may be possible to specifically target components of the epidermal proliferation and differentiation networks without consequent side effects.

Table of Contents

List of Figures

Declaration of Authorship

I, Charlotte Cotter, declare that this thesis and the work presented in it are my own and has been generated by me as the result of my own original research.

The effects of histone deacetylase inhibitors on Notch signalling in the epidermis

I confirm that:

1. This work was done wholly or mainly while in candidature for a research degree at this University;
2. Where any part of this thesis has previously been submitted for a degree or any other qualification at this University or any other institution, this has been clearly stated;
3. Where I have consulted the published work of others, this is always clearly attributed;
4. Where I have quoted from the work of others, the source is always given. With the exception of such quotations, this thesis is entirely my own work;
5. I have acknowledged all main sources of help;
6. Where the thesis is based on work done by myself jointly with others, I have made clear exactly what was done by others and what I have contributed myself;
7. None of this work has been published before submission.

Signed:.....

Date:.....

Acknowledgements

I would like to thank Team Lemon for all their help with my lab work, particularly Dr Sarah Bailey, and for the continual laughs which brighten up the days when nothing works. I would also like to thank Dr Franco Conforti for sharing his expertise in culturing primary human keratinocytes and performing various assays. Huge thanks are extended to Dr Berna Sayan for her continual patience and guidance, I'm sure I drive her mad. I would also like to thank Professor Paul Townsend and Professor Mark Cragg for their input into my PhD project and the Medical Research Council for funding my work. Last but not least I'd like to thank my rugby and American football girls who have kept me sane over the last few years.

Abbreviations

ADAM A disintegrin and metalloprotease

ANK Ankyrin repeats

AP-2γ Activating enhancer binding protein 2 gamma

BSA Bovine serum albumin

cDNA Complementary DNA

CRE Cre recombinase

D0 Day 0

DAPT *N*-[(3,5-Difluorophenyl)acetyl]-L-alanyl-2-phenyl]glycine-1,1-dimethylethyl ester

DMEM Dulbecco's modified Eagle medium

DNA Deoxyribonucleic acid

E8.5 Embryonic day 8.5

ECM Extracellular matrix

ED Ectodermal dysplasia

EGF Epidermal growth factor

EPU Epidermal proliferation unit

FBS Foetal bovine serum

GSK3β Glycogen synthase kinase 3 beta

HaCaT Human adult low calcium high temperature

HATs Histone acetyltransferases

HD Heterodimerisation domain

HDACs Histone deacetylases

HDACi Histone deacetylase inhibitor

Hes1 Hairy/enhancer of split-1

Hey1 Hairy/enhancer-of-split related with YRPW motif 1

HRP Horseradish peroxidase

IFE Interfollicular epidermis

K1 Keratin 1

K5 Keratin 5

K8 Keratin 8

K10 Keratin 10

K14 Keratin 14

K18 Keratin 18

KO Knockout

LNR Lin-12-Notch repeats

MAML1 Mastermind-like 1

nHEKs Neonatal human epidermal keratinocytes

NECD Notch extracellular domain

NICD Notch intracellular domain

NLS Nuclear localisation sequence

NMSC Non-melanoma skin cancer

NRR Negative regulatory region

PBS Phosphate-buffered saline

PCR Polymerase chain reaction

PEST Proline/glutamic acid/serine/threonine-rich

PI Propidium iodide

PUMA p53-upregulated modulator of apoptosis

RAM RBP-jκ association module

RNA Ribonucleic acid

qPCR Quantitative polymerase chain reaction

SCs Stem cells

SCCs Squamous cell carcinomas

SDS Sodium dodecyl sulphate

SpiA Spiruchostatin A

TA Transit-amplifying

TAD Transactivation domain

TBST Tris-buffered saline with 0.1% Tween-20

TM Transmembrane

TNFα Tumour necrosis factor α

TP63 Tumour protein p63

TSA Trichostatin A

UK United Kingdom

VPA Valproic acid

2. Introduction

2.1 General Background

The skin is the body's first line of defence against dehydration and external pathogens so its integrity is critical for survival. Many conditions exist which can compromise the barrier function hence more research into this area is fundamental for future healthcare.

2.1.1 Existing dermatological concerns

Millions of people around the world suffer from a variety of dermatological disorders ranging from mild conditions such as acne to more severe ones such as epidermolysis bullosa where light frictional or mechanical trauma of the skin and mucous membranes results in painful blistering (Coulombe and Lee 2012). Burns are another health concern with approximately 250,000 incidences in the UK each year, with almost half of these being sustained by children under 12 years (Hettiaratchy and Dziewulski 2004).

2.1.2 Skin malignancies

Skin is the site for a number of life-threatening cancers. Both melanoma and non-melanoma skin cancers are becoming increasingly prevalent. Non-melanoma skin cancer (NMSC) is extremely common, with 99,549 cases registered in the United Kingdom (UK) in 2010 according to the Office for National Statistics. Of these cases the large majority occur in patients aged 60 and over (http://www.cancerresearchuk.org/cancer-info/cancerstats/types/skin/). Squamous cell carcinomas (SCCs) are the most common ectodermal cancers and the sixth most common cancer in the world, accounting for over 300,000 deaths per year (Madan, Lear et al. 2010). They arise from stratified epithelium of the skin, lung, oropharynx, larynx and oesophagus among other tissues (Agrawal, Frederick et al. 2011). Despite new therapeutics, five year survival remains around 50% (Boldrup, Coates et al. 2011). Given the aging demographic in developed countries more cases are diagnosed each year, increasing the financial burden on national health services. These conditions can be incredibly debilitating, severely affecting a patient's quality of life, often resulting in cosmetic deformities, intense pain and impairment of functions such as walking and breathing, as well as death however many of the underlying mechanisms remain poorly understood necessitating more research in these areas (Goudas, Bloch et al. 2005).

2.2 Skin development and structure

The skin is the largest organ in the human body and has the essential role of providing a waterproof barrier to protect against dehydration, infection and physical insults. It undergoes significant expansion and remodelling during embryonic development, continuous growth during the postnatal period and is then maintained throughout the adult lifetime.

2.2.1 Embryonic epidermal development

Mammalian skin has a stratified epidermis and an underlying dermis. The epidermal tissues arise from the ectoderm during embryonic development and include the interfollicular epidermis (IFE), hair follicles and sebaceous glands (Blanpain and Fuchs 2009). This study focuses on the IFE, a stratified epithelium composed of a proliferative basal layer adjacent to the basement membrane, and three non-dividing suprabasal layers (Blanpain and Fuchs 2009). In mouse around embryonic day 8.5 (E8.5) a single layer of epidermal cells expressing keratins 8 (K8) and 18 (K18) exists (Medawar, Virolle et al. 2008). At this time, expression of the epidermal lineage-determining transcription factor p63 is induced. p63 is expressed throughout embryonic development, first in the ectoderm prior to stratification and later becomes restricted to the basal layer of the epidermis where it maintains proliferation of keratinocytes (Koster, Dai et al. 2007). p63 is expressed either as full length (TAp63) isoforms containing an N-terminal transactivation domain or as truncated isoforms lacking this domain (ΔNp63). The TAp63α isoform is required for the commitment to stratification and induces expression of activating enhancer binding protein 2 gamma (AP-2γ) which is necessary for expression of keratin 14 (K14), while ΔNp63α is essential in the maintenance of proliferation (Koster, Kim et al. 2006).

At approximately E9.5 stratification is initiated as demonstrated by the expression of keratins 5 (K5) and K14, markers of the innermost (basal) layer of the IFE. Basal cells produce an extracellular matrix (ECM)-rich basement membrane which the epidermis adheres to. An intermediate cell layer then forms between the basal layer and the periderm (Byrne, Tainsky et al. 1994). Cells within this layer express the suprabasal marker keratin 1 (K1) but also continue to proliferate for a limited number of cell divisions, a characteristic which is unique to this transient period of development.

These intermediate keratinocytes then proceed to exit the cell cycle and become non-proliferative suprabasal keratinocytes (Koster and Roop 2008).

Stratification is usually complete by E17.5 and ultimately culminates in the IFE. Keratinocytes comprising the suprabasal layers undergo specific transcriptional changes as they migrate to the skin surface resulting in the spinous layer, the granular layer and the outer cornified layer (stratum corneum) (Figure 2.1).

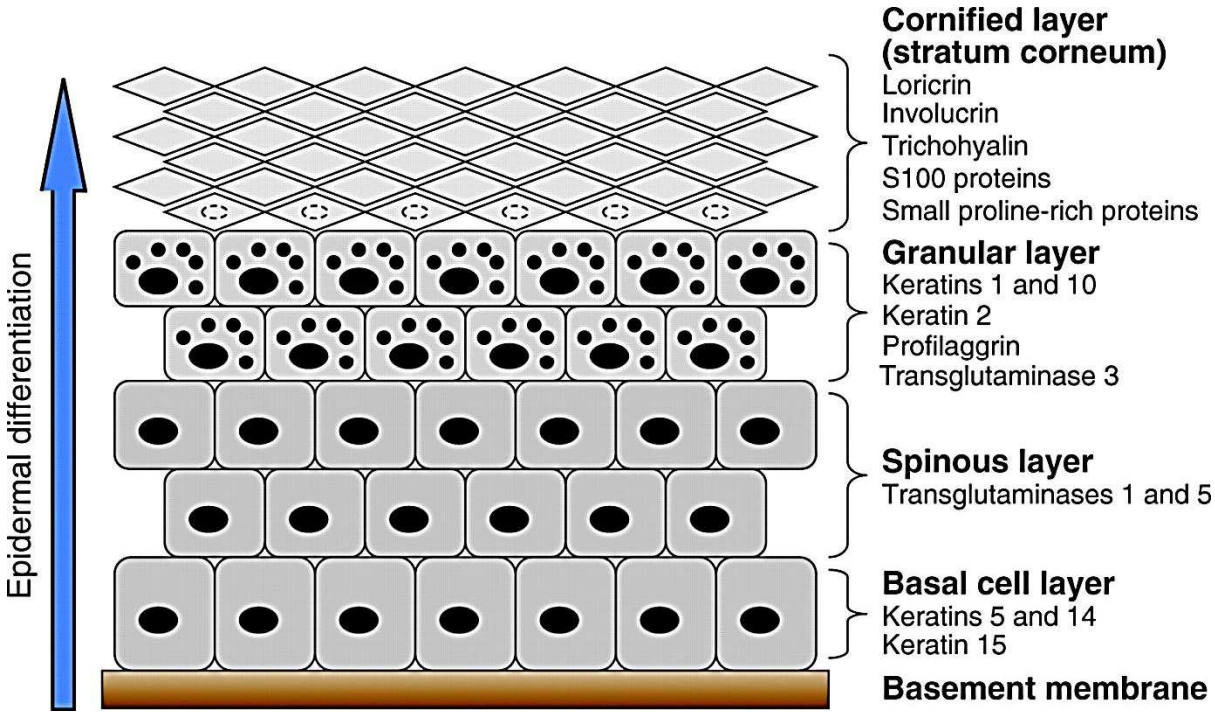

Figure 2.1. The four layers of the skin and the markers they express at each stage of differentiation. The interfollicular epidermis is a stratified epithelium composed of the innermost basal layer which contains the only mitotically active cells and expresses markers such as keratins 5 and 14. These undergo asymmetric cell divisions producing skin stem cells and transit-amplifying cells which have a limited number of cell divisions before moving to the first suprabasal layer, the spinous layer which expresses transglutaminase enzymes, keratin 1 and Hes1. Cells continue to migrate outwards, differentiating along the way, to the granular layer which expresses structural proteins including keratins and profilaggrin and finally to the outermost cornified layer where they are sloughed off. Adapted from (Sandilands, Sutherland et al. 2009).

2.2.2 Epidermal homeostasis

In adult epidermis there is a very high turnover of cells as terminally differentiated squames in the outer cornified layer are constantly sloughed off, therefore epithelial homeostasis is essential to sustain the barrier function. The process of epidermal homeostasis relies on maintaining a pool of proliferative progenitors which give rise to the suprabasal layers continually moving outwards and being lost (Blanpain and Fuchs 2009; Barker, Bartfeld et al. 2010). Migration of the cells from the basal layer to the surface of the skin takes 2-3 weeks, however this period extends with age (Blanpain and Fuchs 2009).

Embryonic lineage tracing experiments using Sox9CRE labelled hair follicles but not the IFE, demonstrating the existence of multiple distinct adult stem cell populations within the epidermis (Nowak, Polak et al. 2008). Additionally, label retaining studies point towards the existence of a population of quiescent stem cells within the IFE which comprise 5% of basal cells (Mascre, Dekoninck et al. 2012). These stem cells divide at a rate 12 times slower than progenitors so their contribution to epidermal homeostasis is minimal (Mascre, Dekoninck et al. 2012). A delicate balance between proliferation and differentiation of the skin stem cells must be established as deregulation of this process can result in cancers, particularly carcinomas (Van Keymeulen and Blanpain 2012).

2.2.3 Symmetric and asymmetric cell divisions

Basal cell division can be planar or perpendicular. Planar cell divisions occur with the mitotic spindle parallel to the basement membrane and result in two basal progeny, whereas if cell division occurs with the mitotic spindle perpendicular to the basement membrane one basal cell and one suprabasal cell are generated (Roshan and Jones 2012). Planar (symmetric) divisions are predominant prior to E12.5, however are rapidly superseded by perpendicular (asymmetric) cell divisions at this stage in line with the formation of the intermediate cell layer. Divisions return to being mainly planar after this stage, with almost all cell divisions in the adult IFE being planar.

Contrastingly, it was proposed that the large majority of divisions in adult epidermis are planar however the progeny have asymmetric fate; one daughter remains proliferating while the other stratifies and leaves the basal layer (Clayton, Doupe et al. 2007). This was further examined using lineage tracing experiments between E14.5 and E15.5 and

the authors discovered that the progeny of a basal cell have the capacity to undergo symmetric or asymmetric cell division (Clayton, Doupe et al. 2007). This was explained in more detail by a study years earlier which labelled basal cells in S phase with H^3-thymidine and followed the progeny cell pairs. By 48h three types of cell pairs were observed: two basal cells, one basal and one suprabasal cell or two suprabasal cells, leading to the conclusion that all cycling cells had an equal chance of differentiating or continuing to divide (Marques-Pereira and Leblond 1965).

Furthermore, basal cells labelled with a fluorescent protein reporter showed an increase in clone size as cells proliferated and the wide range of clone sizes observed over the course of the experiment was consistent with the outcome of each cell division being random (Doupe, Klein et al. 2010). This process is fundamental to adult epidermal homeostasis and the decision to stratify versus proliferate is likely to be linked to whether the surrounding cells are dividing or differentiating such that a constant number of cells within the basal layer is maintained.

2.2.4 Epidermal proliferation units

Small, hexagonal shaped units of proliferation called epidermal proliferation units (EPU) are responsible for ensuring proper proliferation and differentiation of cells in the IFE. Early observations in dorsal murine skin revealed 10.6 basal nuclei beneath a column of cells, with the central nucleus exhibiting different behaviour to the rest including earlier and more efficient responses to stimulation, slower cycling and periods out of cycle (Potten 1974). This led to the prediction that these basal units contain one skin stem cell and around 10 transit-amplifying (TA) cells. TA cells undergo three rounds of cell divisions before they embark on a programme of terminal differentiation (Doupe, Klein et al. 2010).

Fate mapping studies employing retroviral vectors encoding *lacZ* to mark adolescent mouse skin *in situ* demonstrated that columns of β-galactosidase-expressing keratinocytes exist from the basal layer to the top of the cornified layer. These β-galactosidase-expressing EPUs persist for approximately 37 epidermal turnovers after the initial clonal labelling which concurs with the presence of long-lived SCs within the epidermis, specifically as part of an EPU (Ghazizadeh and Taichman 2001). This notion has been challenged, however, by Jones et al. who propose that columns are not formed

by clonal units but rather by a mixture of post-mitotic cells from different progenitors which assemble into columns (Doupe, Klein et al. 2010).

2.2.5 Keratinocyte maturation to form the suprabasal layers of the IFE

The cells within the basal layer are the only mitotically active cells and so the barrier function of skin is dependent upon their self-renewal capacity. In order to replace cells lost at the skin surface TA cells within the basal layer lose their self-renewal property and start to divide asymmetrically. One cell remains attached to the basal layer via integrins in an undifferentiated state while the other exits the cell cycle and begins to stratify (Blanpain and Fuchs 2009). The differentiating progeny migrate vertically in the suprabasal direction until they reach the skin surface where they are shed (Vanbokhoven, Melino et al. 2011). This is demonstrated by lineage tracing experiments such as those discussed previously (Jones et al. and Ghazizadeh et al.).

As they move into the spinous layer the differentiating keratinocytes switch off expression of K5 and K14 and begin expressing a different set of keratins (K1 and K10) which are joined into intermediate filaments. These in turn help strengthen cell-cell junctions that provide resistance against mechanical stresses the body may encounter (Blanpain and Fuchs 2009). The Notch target gene Hes1 is also abundantly expressed in this layer and will be discussed in more detail in the next section.

Next the cells migrate into the granular layer which expresses structural proteins that become cross-linked, forming a very strong proteinaceous sac. One of these structural proteins is filaggrin which is produced in its precursor form profilaggrin and is the main component in keratohyalin granules within the granular layer (Sandilands, Sutherland et al. 2009). During the granular to cornified layer transition profilaggrin is dephosphorylated and cleaved yielding filaggrin monomers that aggregate and align in keratin bundles, increasing the strength of the cornified layer (Dale, Resing et al. 1985). The resulting proteinaceous sac serves as the scaffold for lipid bilayers that render the skin waterproof. The lipid bilayers are extruded from intracellular lamellar granules and surround the squames of the cornified layer (Blanpain and Fuchs 2009).

As differentiation proceeds transcription and metabolism slow down and eventually cease (Mack, Anand et al. 2005). During the cornification process cells undergo nuclear

extrusion, caspase-3 is activated and structural proteins such as keratins, loricrin and involucrin are cross-linked by transglutaminase enzymes to form a hard cornified envelope which provides the strength to protect the organism against environmental assaults (Mack, Anand et al. 2005). The resulting squames in the outermost layer are flattened, dead cells encased by the cornified envelope and are surrounded by lipids (Blanpain and Fuchs 2009).

The molecular mechanisms governing epidermal proliferation and differentiation are not fully understood but seem to involve several signalling pathways. These include the Notch pathway and involvement of the transcription factor p63 among others, but these two appear to be the key regulators of the switch from proliferation to stratification. In particular, evidence from mouse genetics has highlighted p63 as a master regulator of epidermal cell fate and will be discussed below.

2.3 p63 and its isoforms

p63 is a transcription factor and its expression during development marks cells for an epidermal lineage. It governs many aspects of proliferation and differentiation in epidermal cells, and is vital in the regulation of epidermal homeostasis (Candi, Amelio et al. 2014). *p63* is part of the *p53* gene family and shares significant sequence and structural homology with both p53 and p73 (Figure 2.2A) (Mills 2006). All three transcription factors bind directly to DNA as tetramers. Phylogenetic and functional analyses show that p63 is the ancestral member of this family of transcription factors (Figure 2.3) (Yang, Kaghad et al. 2002).

2.3.1 Structure of p63 isoforms

The *TP63* gene is transcribed from two alternate promoters generating full length (TA) isoforms and isoforms lacking an N-terminal transactivation domain (ΔN) (Candi, Rufini et al. 2006). The second promoter is located in the third intron over 30kb downstream of the TAp63 promoter (Yang, Kaghad et al. 2002). The fourth exon (3') therefore encodes the 14 amino acids comprising the N-terminus of ΔNp63 isoforms which has been shown to possess transactivation activity (Bergholz and Xiao 2012). Additional isoform heterogeneity is generated via alternative splicing at the C-terminus, resulting in ten different isoforms (Figure 2.2B). The specific contribution of each isoform to

epidermal proliferation and differentiation remains to be determined, however genetic complementation studies in mouse (discussed in more detail in 2.3.3) show that each isoform is likely to have its own role in these processes as functional redundancy of isoforms does not exist (Candi, Rufini et al. 2006).

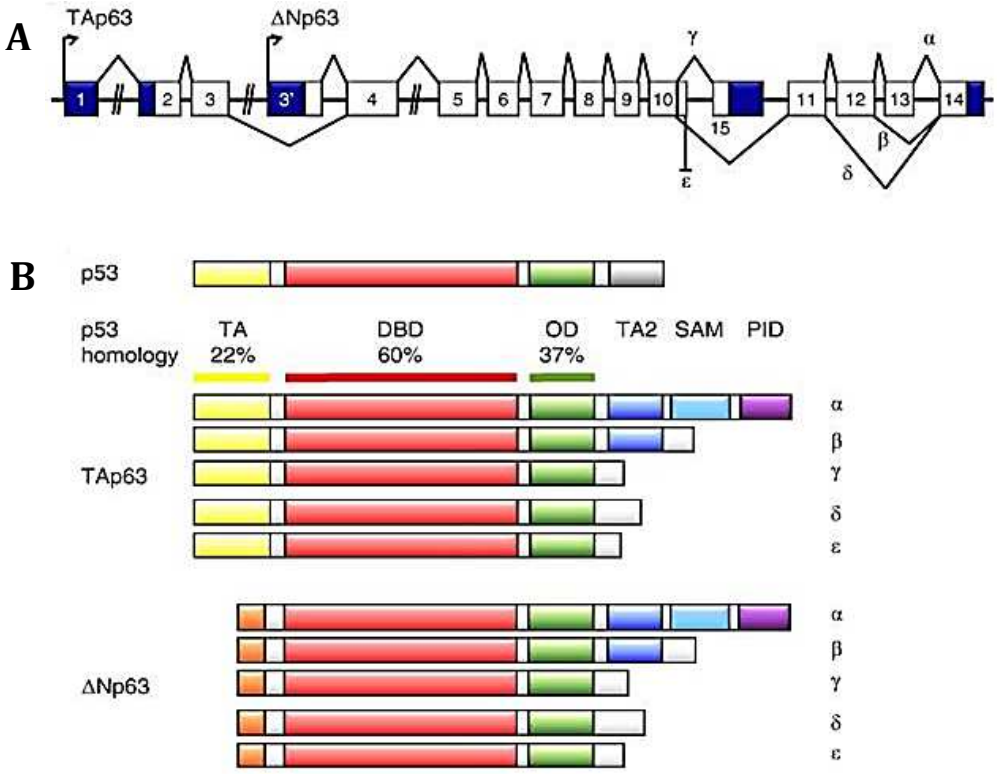

Figure_2.2. The 10 different isoforms of p63 and their homology to p53. (A) The *TP63* gene is transcribed from two alternative promoters and alternative splicing of the C-terminus generates additional isoforms. (B) For comparison, the domain structure of p53 is shown in conjunction with the homology with the p63 isoforms. The domain architecture of all 10 p63 isoforms is displayed. TA, N-terminal transactivation domain; DBD, DNA-binding domain; OD, Oligomerisation domain; TA2, Second transactivation domain; SAM, Sterile alpha motif; PID, Post-inhibitory domain. Adapted from (Bergholz and Xiao 2012)

2.3.2 Roles of TAp63 isoforms

The TA and ΔN isoforms have been described as Janus faces of p63 as their functions often oppose each other during development and in adults (de Fromentel, Aberdam et al. 2012). TAp63 has pro-apoptotic functions, activating genes such as p53-upregulated modulator of apoptosis (*puma*). While p53 is described as being the "guardian of the genome" TAp63 acts as the guardian of oocyte integrity (Kerr, Hutt et al. 2012). TAp63 is primarily expressed in oocytes which it protects against genotoxic insults. If oocytes

are exposed to chemotherapeutic drugs and/or irradiation TAp63 isoforms induce cell death to prevent malformation of a potential developing foetus (Zhu, Li et al. 2012).

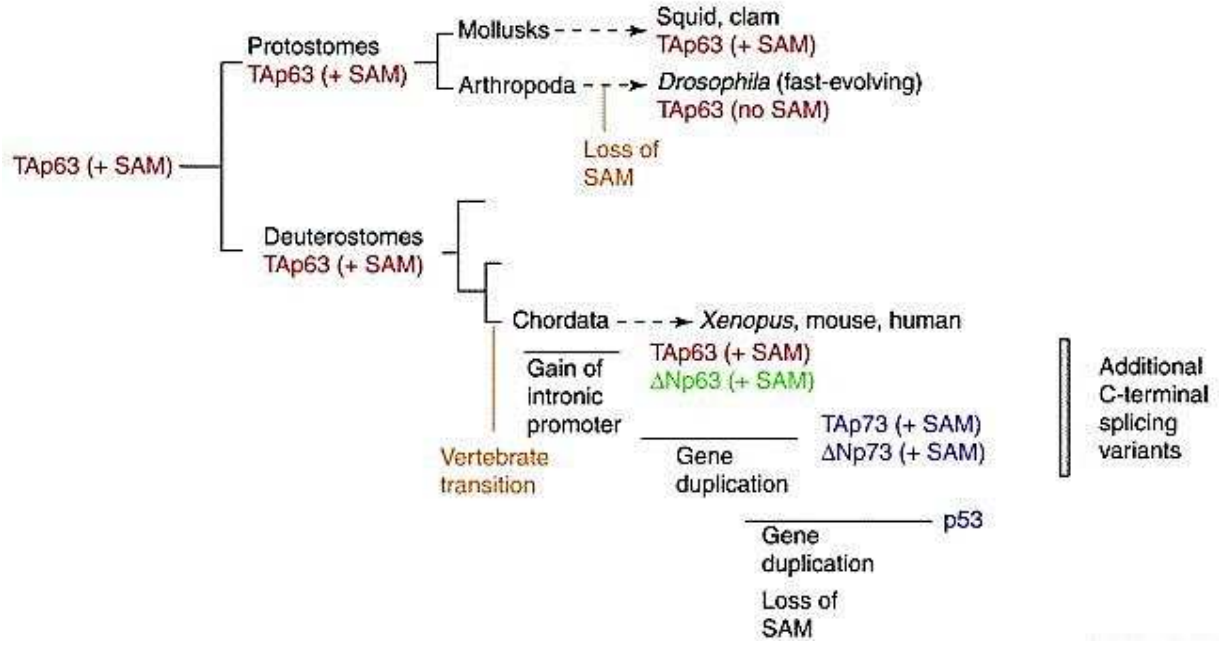

Figure 2.3 Phylogenetic analysis of the p53 family of transcription factors reveals p63 as the ancestral family member. The major branches of metazoan evolution are shown together with the known p53 family members they possess. Both protostomes (represented by mollusks and arthropods such as *Drosophila*) and deuterostomes have TAp63 (+SAM) molecules present signifying that this is likely to be the primordial p53 family member. In protostomes this is the only p53-like molecule present whereas in deuterostomes additional p53-like molecules are observed and are most likely the result of gene duplication throughout evolution. These isoforms are TAp63, ΔNp63, TAp73, ΔNp73 and p53. The p63 and p73 isoforms have additional C-terminal splicing variants as described in Figure 2.2B. SAM, C-terminal sterile alpha motif involved in protein-protein interactions. Adapted from (Yang, Kaghad et al. 2002)

TAp63 isoforms have been shown to be essential for protecting dermal and epidermal progenitor cells from senescence, DNA damage and genomic instability (Paris, Rouleau et al. 2012). TAp63 isoforms comprise only 1% of total p63 in the IFE (Laurikkala, Mikkola et al. 2006). Low levels of TAp63 isoforms have been discovered in the suprabasal layers of the IFE, indicating a role in differentiation (Paris, Rouleau et al. 2012). This is supported by the discovery that TAp63 is critical for the cardiac differentiation of embryonic SCs (Rouleau, Medawar et al. 2011).

2.3.3 Roles of ΔNp63 isoforms

p63 is the master regulator of cell fate decision in keratinocytes during development and in adult skin (Candi, Amelio et al. 2014). The essential role of p63 in skin and craniofacial development is clearly demonstrated in p63 knockout (KO) mice which fail to develop stratified epithelium; instead they retain a single layer of ectoderm through which the underlying vasculature can be seen (Candi, Rufini et al. 2006). These p63-deficient cells remain as a monolayer of non-proliferating cells expressing K8 and K18 which are markers of early development. p63 KO mice also exhibit additional developmental abnormalities including severe limb deformation, and lack of eyelids and teeth (Mills 2006).

ΔNp63α is the predominant isoform expressed in skin and its key role is the maintenance of proliferation which it does by repressing expression of anti-proliferative genes and cell-cycle regulators such as p21 and $p16^{INK4a}$, respectively (LeBoeuf, Terrell et al. 2010). In vitro and in vivo DNA-binding assays have shown that ΔNp63α binds to the *p53* response elements in the promoters of *p21* and *14-3-3σ.* However, p63 occupancy at these promoters decreases as differentiation proceeds, consistent with the increase in p21 protein and consequent cell cycle arrest in keratinocytes (Westfall, Mays et al. 2003).

This process is also reflected in adulthood; if ΔNp63α is silenced in adult skin there is no proliferation of adult keratinocytes. Expression of ΔNp63 isoforms prevents keratinocytes from undergoing terminal differentiation. This is demonstrated in experiments using primary mouse keratinocytes overexpressing ΔNp63α which fail to differentiate following the addition of calcium which promotes epidermal differentiation under normal conditions (King, Ponnamperuma et al. 2003). The conclusion from these studies, therefore, is that in order for differentiation to proceed ΔNp63α levels must be reduced.

ΔNp63 isoforms also play roles in mediating cell adhesion and survival in contrast to their full-length (TA) counterparts. Work in mammary epithelial cells has shown that loss of ΔNp63 isoforms results in cell detachment and death which are processes that skin keratinocytes undergo during their maturation process (Carroll, Carroll et al. 2006).

2.3.4 p63 mouse models

There has been a great deal of debate over the precise role of *p63* in skin centred around two studies which generated p63 KO mice using different techniques. Mills et al. used two different targeting vectors, pTV6H(90) and pTV12E(60), which integrate into different regions of the *p63* locus and generate different *p63* mutant alleles. The allele generated using the pTV6H(90) vector encodes a p63 protein with a non-functional DNA-binding domain, whereas the pTV12E(60) vector results in a p63 protein lacking the 3' region. Embryonic stem cell clones were created and the F1 heterozygous mutant generation were intercrossed giving rise to pups with identical phenotypes from both *p63* mutant alleles (Mills, Zheng et al. 1999). Mills and colleagues described the phenotype of these neonatal mice as presenting with a single layer of cells expressing low levels of K14 and no suprabasal markers such as K1/K10, loricrin or filaggrin and based on this concluded that a lack of *p63* results in the failure of the stratification process (Mills, Zheng et al. 1999). They believed that the defects in limb development were due to disruption of ectodermal-mesenchymal communication also involved in the morphogenesis of hair follicles and teeth.

Yang et al. used a targeting vector which has a 2.3 kb region corresponding to exons 6, 7 and 8 and flanking introns, deleted and replaced with the neomycin-resistance (*neo* ^{r}) gene driven by the mouse phosphoglycerol kinase 1 (PGK1) promoter, in the reverse orientation to the *p63* gene (Yang, Schweitzer et al. 1999). The deleted exons comprised most of the DNA-binding domain of *p63* and generated a mutant *p63* allele used to create embryonic stem cell clones. Heterozygous F1 progeny were intercrossed and the p63-null progeny lacked hair follicles and other epithelial structures such as mammary glands. Yang et al. reported that the p63-deficient skin of neonatal mice and late-stage embryos possessed isolated patches of disorganised epithelial cells expressing loricrin, involucrin and filaggrin on sections of exposed dermis indicating that differentiation is indeed able to proceed albeit in a bizarre, fragmented fashion. The same authors concluded that a lack of *p63* results in the failure to regenerate the pool of proliferative progenitors in the basal layer (Yang, Schweitzer et al. 1999).

The differences in the observed phenotypes between the two different p63 KO mice were originally thought to lie in the different transgenes used to generate these mice;

however the Mills et al. mouse model has since been shown to express *p63γ* isoforms hence is not a complete KO (Wolff, Talos et al. 2009). Despite this, subsequent studies report that the authors were both right; *p63* is required to maintain a population of undifferentiated keratinocyte stem cells but it also plays roles in epidermal differentiation and these processes are dependent upon the delicate balance of *p63* isoforms. Moreover, a study by Truong et al. in regenerating human epidermis showed that loss of *p63* resulted in hypo-proliferation and a failure to undergo terminal differentiation (Truong and Khavari 2007). Simultaneous knockdown of both *p53* and *p63*, however, restored proliferation but not differentiation, indicating that these processes are regulated by p53-dependent and p53-independent mechanisms, respectively (Truong and Khavari 2007).

In mice lacking TA- and ΔNp63 isoforms a striking phenotype is observed, as described above (Figure 2.4, panel b). The reintroduction of TAp63α alone by genetic complementation produces a phenotype similar to the complete KO mouse (Figure 2.4, panels b and d). In contrast, re-introduction of ΔNp63α rescues much of the phenotype and the resultant mouse is much more similar to the wild type mouse (Figure 2.4, panels a and c). There is evidence of stratification, however limbs and eyelids are still absent and some vasculature can still be observed. This demonstrates that ΔNp63α alone is not sufficient to recover the defects caused by loss of *p63*; the other ΔNp63 isoforms also have roles to play in the proper development of the epidermis and TAp63 isoforms may have roles to play in late differentiation (Truong and Khavari 2007).

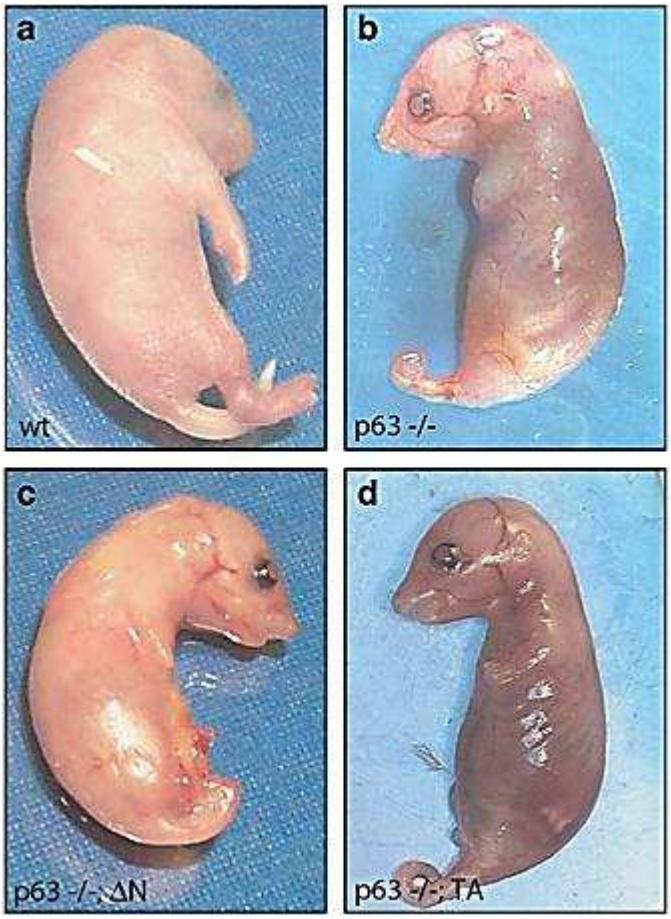

Figure 2.4 The transcription factor p63 is essential for the development of a stratified epithelium p63 was knocked out and ΔNp63α and TAp63α isoforms reintroduced by genetic complementation. (A) A wild type (WT) mouse with an intact, fully developed epidermis (B) A mouse with the TP63 gene knocked out. Skin development has been halted, resulting in a single layer of translucent ectoderm rather than a stratified epithelium, disrupted appendage formation with lack of limbs and a truncated tail and also lack of eyelids (C) Upon re-introduction of ΔNp63α much of the WT phenotype is recovered with some stratification evident, however these mice still lack limbs (D) Upon re-introduction of TAp63α the observed phenotype differs very little from the p63-null mouse with underlying vasculature still visible and a distinct lack of appendages. (Adapted from Candi et al., 2006)

p63 isoforms are not solely responsible for epidermal homeostasis. While they mediate the expression of many structural proteins, cell cycle proteins and enzymes they form part of a much larger regulatory network. This network includes Notch signalling molecules, co-factors and histone-modifying proteins and the balance between these two pathways controls the major aspects of epidermal proliferation and differentiation. These aspects will be discussed latter in the thesis.

2.4 p63 in malignancy

Strategies for treating cancer have advanced remarkably over the last few years however the clinical outcome for many patients with epithelial tumours remains poor (Hsu, Sheu et al. 2012). Few recurrent genetic aberrations have been discovered in SCC, impeding the identification of driver mutations and thus targeted therapeutic strategies (Wang, Sanborn et al. 2011).

2.4.1 Squamous cell carcinomas

Overexpression of ΔNp63α is among the most common genetic alterations observed in SCC. ΔNp63α is upregulated in approximately 80% of SCC incidences and acts as a survival factor in these cells by forming a complex with HDACs 1 and 2 which represses transcription of pro-apoptotic Bcl-2 family members such as *PUMA* (Ramsey, He et al. 2011). ΔNp63 isoforms can also bind to and repress the pro-apoptotic activity of *p73* (DeYoung, Johannessen et al. 2006).

Unlike its paralog p53, p63 is not commonly mutated in human cancers (Mills 2006). Mills et al. report that $p63^{+/-}$ mice are not prone to either spontaneous or chemically induced tumours (Mills 2006), whereas Flores *et al.* dispute this, claiming that $p63^{+/-}$ mice developed tumours (Flores, Sengupta et al. 2005).

2.4.2 Dysregulation of p63 expression in other epithelial cancers

p63 has been implicated in modulating adhesion and migration and restricting tumour cell invasion, as has p53 (Aylon and Oren 2011). Clinical evidence suggests that *p63* may play a role in inhibiting metastasis as gene expression profiling studies show clear correlations between reduced *p63* expression and progression of prostate and other cancers. Similarly, genetic mice models and cell culture data strongly point towards *p63* deficiency as a causative factor for metastatic spread because ΔNp63α expression is lost in the majority of invasive cancers and reduced *p63* expression is correlated with a reduction in cell adhesion-associated genes and consequent cell detachment in epithelial cells such as keratinocytes (Carroll, Carroll et al. 2006). Moreover, knockdown of TAp63 isoforms in human lung carcinoma also led to increased invasion (Bergholz and Xiao 2012). TAp63 isoforms have a much shorter half-life than ΔNp63 isoforms and are quickly degraded, likely to prevent aberrant induction of apoptosis (Brandt, Kaar et al. 2012). In agreement with their pro- and anti-apoptotic activities, respectively, TAp63 is often lost and ΔNp63 overexpressed in cancer cells (de Fromentel, Aberdam et al. 2012).

2.4.3 Mutations in TP63

Deregulation of epidermal development can result in blistering, inflammation, compromised barrier function and other pathological conditions in addition to cancer. Heterozygous mutations in the *TP63* gene result in several conditions collectively known as ectodermal dysplasias (EDs). These are a large group of hereditary disorders

(Vaidya, Risbud et al. 2013). Three of these syndromes are ectodactyly-ectodermal dysplasia-clefting syndrome (EEC), ankyloblepharon-ectodermal dysplasia clefting syndrome (AEC) and Rapp-Hodgkin syndrome (RHS). Patients with these syndromes often present with signs of deafness as TAp63 fails to transactivate the Notch target gene *Hes5* which is important in cochlear development (Terrinoni, Serra et al. 2013).

2.5 Notch signalling

Notch signalling is remarkably pleiotropic and influences diverse cellular processes such as proliferation, migration, self-renewal, lineage specification and differentiation (Perdigoto and Bardin 2013). Phylogenetic analyses in 35 different eukaryote species confirmed that Notch signalling is highly evolutionarily conserved in bilaterians (Gazave, Lapebie et al. 2009). Its role in development was first discovered through mutations in the *Notch* gene giving rise to heterozygous female *Drosophila* with notches in their wings (Mohr 1919). Later research demonstrated that homozygous mutations in the Notch gene resulted in cell fate changes (Poulson 1945).

2.5.1 Notch receptors

In *Drosophila melanogaster* there is only one Notch receptor whereas mammals have evolved to possess four (Notch1 to Notch4) (Panelos and Massi 2009). The four mammalian Notch receptors have a high degree of structural similarity, with Notch1 and Notch2 exhibiting the greatest (Bellavia, Checquolo et al. 2008). They are all single-pass transmembrane (TM) proteins. They are synthesised in the endoplasmic reticulum in an inactive form which is proteolytically cleaved in the trans-Golgi network, producing an active form capable of ligand binding. Notch receptors are expressed at the plasma membrane as heterodimers composed of a large extracellular domain (NECD) and a membrane-tethered intracellular domain (NICD) which interact non-covalently in a calcium-dependent manner (Perdigoto and Bardin 2013). This is important because epidermal differentiation is triggered by an increase in the extracellular concentration of calcium ions and in adult epidermis a calcium gradient is present from the basal to the cornified layers (Mauro, Bench et al. 1998).

The extracellular domain is composed of a variable number of tandem epidermal growth factor-like (EGF) repeats which mediate interactions with the Notch ligands

(Perdigoto and Bardin 2013). These are followed by three Lin-12-Notch repeats (LNR) that are involved in ligand binding and a heterodimerisation domain (HD), which together comprise the negative regulatory region (NNR) which prevents cleavage and activation of the Notch receptor in the absence of ligand. The TM domain is followed by the RBP-Jκ association module (RAM), seven ankyrin repeats (ANK), a transactivation domain containing nuclear localisation sequences (NLS) and a proline/glutamic acid/serine/threonine-rich (PEST) sequence which is involved in the stability of NICD (Figure 2.5).

2.5.2 Notch ligands and activation

In *Drosophila* Notch is activated by the ligands Delta and Serrate, whereas in mammals the equivalent ligands are Delta-like 1, 3 and 4, and Jagged 1 and 2, respectively (Perdigoto and Bardin 2013). These ligands are also TM proteins and are expressed on neighbouring cells (Perdigoto and Bardin 2013). In the absence of ligand Notch cleavage is prevented by the NRR as the cleavage site is concealed by a hydrophobic interface between the LNRs and the HD domain. Ligand binding induces a conformational change in the NRR, causing a relaxing in its structure and exposing the cleavage site (Gordon, Vardar-Ulu et al. 2007). Ligand endocytosis by the signal-sending cell is thought to generate a pulling force on the Notch receptor on the signal-receiving cell which further facilitates the exposure of the cleavage site (Nichols, Miyamoto et al. 2007). Following the first cleavage the ligand-NECD complex is endocytosed by the ligand-presenting cell to ensure that Notch signalling occurs in a linear fashion such that one receptor is activated by one ligand, not multiple (Hansson, Lanner et al. 2010).

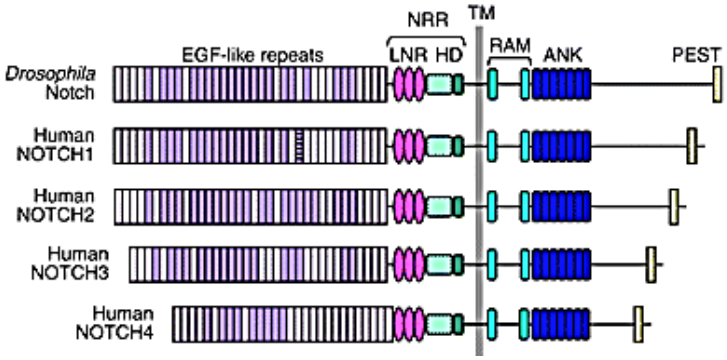

Figure 2.5 The domain architecture of the four human Notch receptors. Notch receptors are transmembrane proteins and the structural similarity of the human Notch receptors to the *Drosophila* Notch receptor is apparent. Notch receptors possess tandem epidermal growth factor (EGF)-like repeats, a negative regulatory region (NRR) composed of three Lin-12-Notch repeats (LNR) and a heterodimerisation domain (HD) in their extracellular regions, or domains. This is followed by a transmembrane (TM) region and the intracellular domain which comprises an RBP-Jκ association module (RAM), ankyrin repeats (ANK) and a proline/glutamine/serine/threonine-rich (PEST) sequence. Adapted from www.trojantec.com.

2.5.3 NICD translocation and formation of the active complex

Following activation Notch undergoes two proteolytic cleavages. The first is by ADAM10 protease and TNFα-converting enzyme at a luminal juxtamembrane site which releases the NECD. Subsequently the Notch receptor is cleaved within the TM region by presenilin-dependent-γ-secretase releasing the Notch intracellular domain (NICD) which then translocates to the nucleus in the target cell (Kopan and Ilagan 2009). Within the nucleus are the other key components required to form the active complex. These components are RBP-Jκ (a DNA-binding protein also known as CSL) and Mastermind-like 1 (MAML1). RBP-Jκ is a transcriptional repressor. The binding of NICD to RBP-Jκ in the nucleus facilitates the activation of Notch target genes. RBP-Jκ is also required for expression of markers of the spinous and granular layers of the IFE (Blanpain, Lowry et al. 2006). MAML1 is one of three members of the Mastermind-like family which function as transcriptional regulators in Notch signalling (Lindberg, Popko-Scibor et al. 2010).

In the absence of NICD Notch autoinhibition is achieved through RBP-Jκ recruiting co-repressors such as CoREST, Sin3A and histone deacetylase (HDACs). Together these proteins form a complex which represses Notch target genes (Schweisguth 2004). MAML1 can only interact with RBP-Jκ in the presence of NICD, providing supplemental autoinhibition (Kang, Yang et al. 2008). This is because neither NICD nor RBP-Jκ can

stably bind to MAML1 (Oyama, Harigaya et al. 2011). For Notch signalling to proceed RBP-Jκ –associated co-repressors must be removed in order to form the active Notch complex. Once in the nucleus NICD interacts with RBP-Jκ via its RAM domain and this interaction recruits co-activators such as p300 (a histone acetyltransferase or HAT) and MAML1, the latter of which interacts with NICD-RBP-Jκ via the Notch ankyrin repeats.

2.5.4 The pleiotropic roles and regulation of MAML1

MAML1 serves multiple functions in regulating Notch; its binding stabilises the ternary complex so it can bind to specific DNA sequences activating transcription of Notch target genes (Perdigoto and Bardin 2013). Residues 75-301 of MAML1 strongly bind to p300 which is essential for initiating transcription on chromatin. It also enhances p300 autoacetylation and HAT activity (Fryer, White et al. 2004; Lindberg, Popko-Scibor et al. 2010). HATs are recruited to facilitate the activation of Notch target genes (Mack, Anand et al. 2005). MAML1 also recruits the cyclin C and cyclin-dependent kinase 8 complex which phosphorylates the transcription activation domain and PEST sequence of NICD. This targets it for rapid proteasomal degradation via the Fbw7/Sel10 ubiquitin ligase, ensuring that Notch signalling is short-lived (Fryer, White et al. 2004).

The transcriptional activity of MAML1 is regulated in a number of ways. Glycogen synthase kinase 3 beta (GSK3β) directly interacts with the N-terminus of MAML1 and phosphorylates it, thereby inhibiting its transcriptional activity (Lindberg, Popko-Scibor et al. 2010). MAML1 activity has also been found to be regulated by SUMOylation. E3 ligating proteins attach SUMO to two consensus sites on MAML1, enhancing its interaction with HDAC7 which decreases the transcriptional activity of MAML1 (Lindberg, Popko-Scibor et al. 2010). The class IIa HDACs (HDACs 4, 5, 7 and 9, defined later) are known to possess E3 ligase activity. In particular, HDAC7 has been identified as interacting with SMRT and Sin3A, two of the co- repressors recruited by RBP-Jκ in the absence of NICD so this HDAC may prove pivotal in regulating the transcription of Notch target genes (Kao, Downes et al. 2000).

2.5.5 Notch target genes

Specific Notch target genes vary between cell types. The primary targets of Notch signalling in skin are the *Hes* and *Hey* families of basic helix-loop-helix inhibitory transcription factors which can recruit transcriptional co-repressors (Cooper, Tyler et

al. 2000). In the IFE activation of these genes ultimately results in commitment of basal keratinocytes to differentiate; for example, Notch signalling induces expression of the spinous layer marker K1 via regulation of Hes1 (Rangarajan, Talora et al. 2001). In the absence of Hes1 formation of the spinous layer is impaired. Furthermore, Hes1 is responsible for preventing the premature differentiation of spinous keratinocytes to granular keratinocytes (Moriyama, Durham et al. 2008).

There is a dynamic interplay between the Notch pathway and the epidermal lineage-specifying transcription factor p63 and this will be further discussed below.

2.5.6 Notch signalling in the epidermis

Notch signalling functions broadly in specifying cell fates, both during embryonic development and in adult tissues (Panelos and Massi 2009). Nickoloff *et al* demonstrated that transgenically expressing Notch1 under the control of the promoter of the granular layer marker involucrin promotes granular differentiation(Nickoloff, Qin et al. 2002). Other studies have also implicated Notch in late stages of differentiation. While the commitment switch for the initial induction of differentiation remained unknown, however, Fuchs *et al*. uncovered a role for active NICD and its canonical signalling partner RBP-Jκ in early differentiation (Blanpain, Lowry et al. 2006). Through loss and gain-of-function studies they showed that NICD and RBP-Jκ induce spinous fate (determined via K1 expression) while repressing basal fate at the basal/suprabasal border. Additionally *Hes1*, a downstream target of Notch signalling expressed in the spinous layer was discovered to play a role in mediating spinous gene induction as described in 2.3.4, however basal gene repression occurred via a Hes1-independent mechanism. As expected, when canonical Notch signalling is lost *Hes1* is no longer detected in the epidermis.

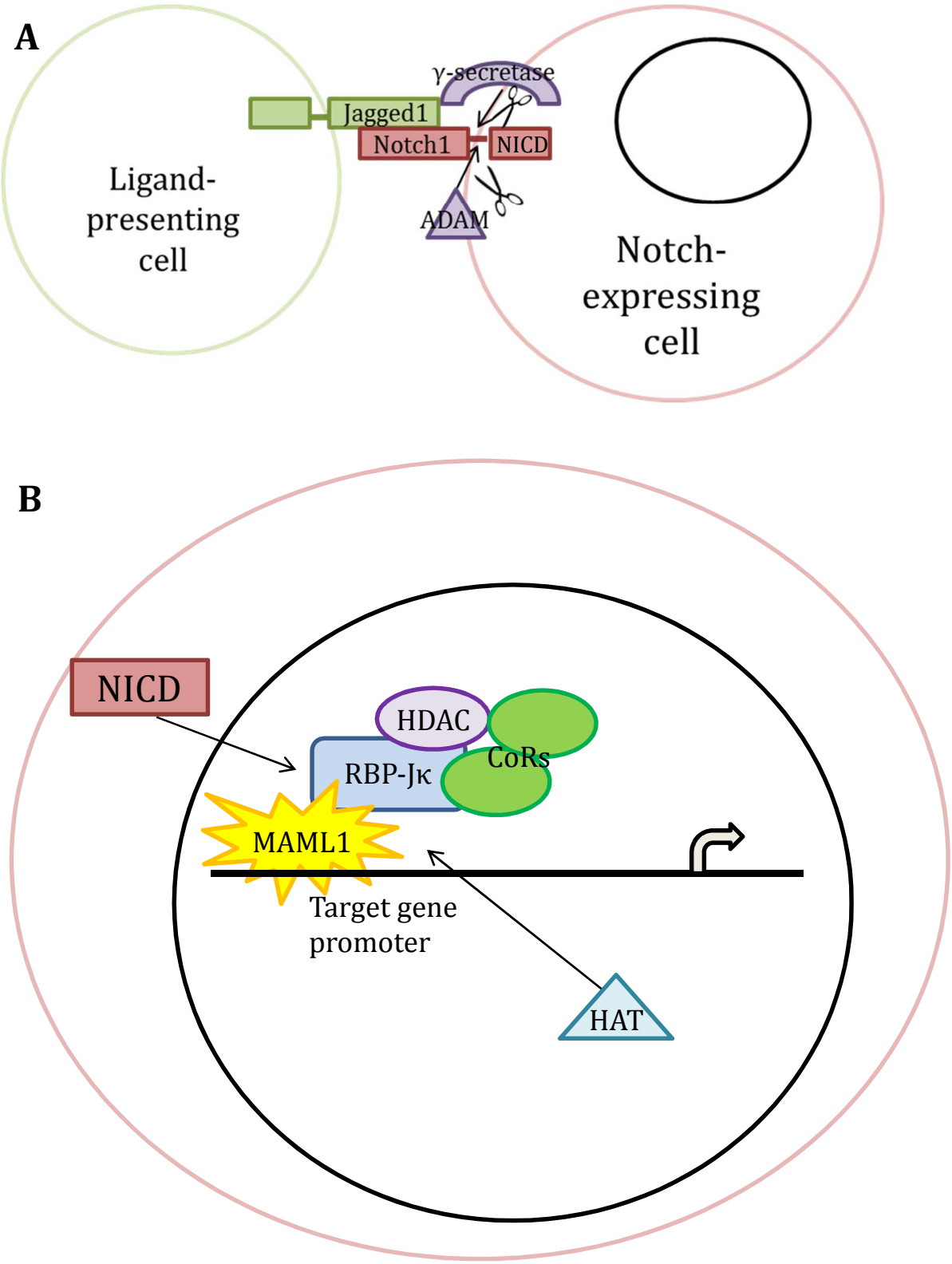

Figure 2.6 The mechanisms of Notch signalling. (A) Notch receptors interact with ligand on an adjacent cell. Notch is cleaved by ADAM metalloproteases and TNFα-converting enzyme and then by presenilin-dependent γ-secretase releasing the Notch extracellular domain. (B) The Notch intracellular domain (NICD) translocates to the nucleus where it interacts with RBP-Jκ displacing HDACs and bound co-repressors (CoRs) such as SMRT. Mastermind-like 1 (MAML1) then binds to the complex and recruits activators such as p300, a histone acetyltransferase (HAT) to the promoters of Notch target genes and transcription is initiated.

Notch and p63 expression is inversely proportional; these proteins form a reciprocal feedback loop to maintain the balance between self-renewal and differentiation (Dotto 2009). This is achieved through Notch signalling supressing *p63* expression via interferon and NF-κB signalling. RBP-Jκ binds directly to the *p21* promoter enabling its transcription in the presence of NICD (Rangarajan, Talora et al. 2001). p63 binds to the promoters of *p21* (at a different consensus site), *Hes1* and *Wnt4,* inhibiting their transcription (Dotto 2009). p63 is also able to induce expression of Jagged proteins leading to the activation of Notch.

2.5.7 Mutations in Notch

Notch signalling has been linked with a myriad of cancer types including leukaemia, melanoma, neuroblastoma, breast, pancreatic, lung and cervical cancers (Kang, Yang et al. 2008). Translocations in T cell leukaemias provided the first evidence that Notch1 may play a role in human cancers and since then mutations in Notch1 and Notch2 have been discovered in around 75% of cutaneous SCCs (Ellisen, Bird et al. 1991; Wang, Sanborn et al. 2011).

A study using whole-exome sequencing revealed that the Notch1 gene is frequently mutated in SCC, second in prevalence only to TP53, while a low mutation frequency is observed in other solid tumour types (Stransky, Egloff et al. 2011). Genes encoding Notch ligands, its binding partner RBP-Jκ, or Mastermind-like co-activators are not usually mutated in cancers (Wang, Sanborn et al. 2011).

Downregulation of Notch transcripts and signalling is well established in skin cancers, consistent with its role in promoting epithelial differentiation. Furthermore, mutations which reduce Notch receptor activity have been identified in BCCs and SCCs (Nicolas, Wolfer et al. 2003; Lefort, Mandinova et al. 2007). Recent work identified that mutations in Notch1 or Notch2 include point mutations which impact the EGL-like repeats involved in ligand binding, the HD and the RAM domains and nonsense mutations which affect the ankyrin repeats (Wang, Sanborn et al. 2011). Other mutations are thought to result in membrane-tethered, truncated receptors which retain their ligand-binding capacity and may exert dominant-negative activity as previously discovered in *Drosophila* (Rebay, Fehon et al. 1993). Furthermore, conditional ablation of Notch1 in mouse epidermis results in the development of epithelial tumours (Nicolas, Wolfer et al. 2003).

2.6 Chromatin remodelling, HATs and HDACs

Epigenetics refers to a series of phenotypic and genotypic alterations (some of which are argued to be heritable) that do not require changes in the nucleotide sequence. Epigenetics is involved in many cellular processes. The most common epigenetic modifications are methylation of CpG islands within the DNA and acetylation of histone tails.

2.6.1 Chromatin structure

Chromatin structure plays a crucial role in regulating gene expression, both in normal and cancer tissue (Yurek-George, Habens et al. 2004). Nucleosomes are the basic repeating unit of chromatin and are composed of DNA, wrapped around histone proteins. There are five histone proteins; histones H1, H2A, H2B, H3 and H4 (Hayes, Clark et al. 1991). Two copies of each of H2A, H2B, H3 and H4 form a positively charged octameric core around which 146 base pairs of negatively charged DNA wraps tightly (Figure 2.7A). Histone H1 facilitates the addition of 20 base pairs enabling two full turns of DNA around the histone core. Nucleosomes are joined by the DNA running between them and have historically been described using the "beads on a string" analogy (Figure 2.7B).

2.6.2 Histone acetylation

Chromatin structure is modulated by multiple processes, including reversible acetylation and methylation. For the purpose of this thesis I will focus on acetylation. Histone acetylation is a dynamic process regulated by two antagonistic families of enzymes –HATs which transfer acetyl groups from acetyl CoA molecules to ε-amino groups of lysine residues on histone tails forming euchromatin; and histone deacetylases (HDACs) (Hsu, Sheu et al. 2012). HDACs remove acetyl groups from histone tails and in doing so restore the inherent positive charge on lysine residues. This serves to compact the chromatin to form heterochromatin thereby reducing accessibility to transcription factors and RNA polymerase II (Figure 2.8). The regulation of histone acetylation and deacetylation thus provides a global mechanism of eukaryotic transcriptional control (Lerche, Philipsen et al. 2008).

2.6.3 Non-histone targets

In recent years researchers have started looking at non-histone proteins targeted by HDACs such as transcription factors e.g. p53, STAT1, STAT3, cytoskeletal proteins e.g. α-

tubulin and other cellular proteins such as Hsp90 (Glozak, Sengupta et al. 2005). HDAC6 is the only HDAC localised solely to the cytosol and has been implicated in the acetylation of non-nuclear proteins such as tubulin.

Acetylation forms a much larger proportion of post-translational modifications (PTMs) than previously thought and reversible acetylation plays a key role in regulating the activity of many kinases and other regulatory proteins including those involved in tumourigenesis. It also impacts protein stability (Peng and Seto 2011).

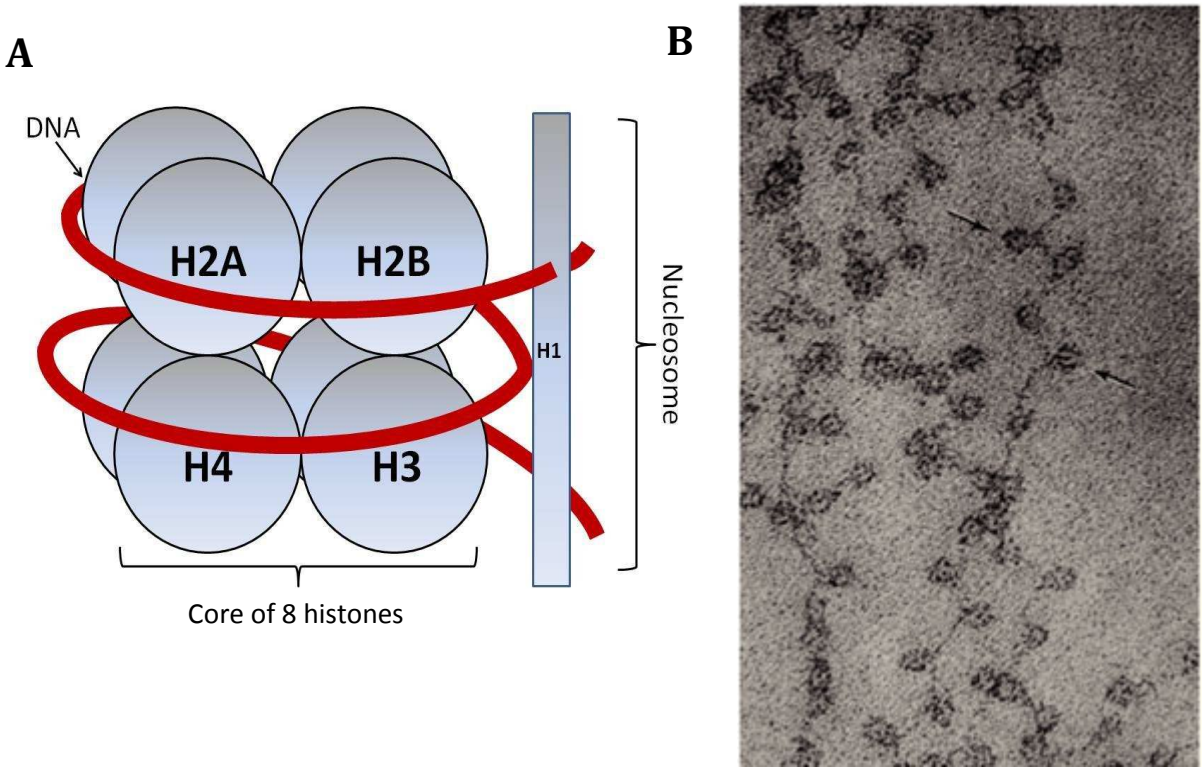

Figure 2.7 The structure of nucleosomes. (A) In order for the huge amount of DNA contained within the nuclei of cells to be compacted into the small area available DNA is wound around proteins called histones. Histones H2A, H2B, H3 and H4 form an octameric core $(H2A, H2B, H3, H4)^2$ which the DNA is wrapped around and linked by the H1 histone. The positive charge on the histones and the negative charge on DNA allows for a tight interaction and compaction of the DNA. (B) As DNA is only wound around the histones twice many are needed to accommodate the length of the entire genome in each nucleus. Nucleosomes are joined by the DNA that runs between them giving the appearance of "beads on a string" in electron micrographs such as the one shown. Arrows denote individual nucleosomes. (Olins and Olins 2003).

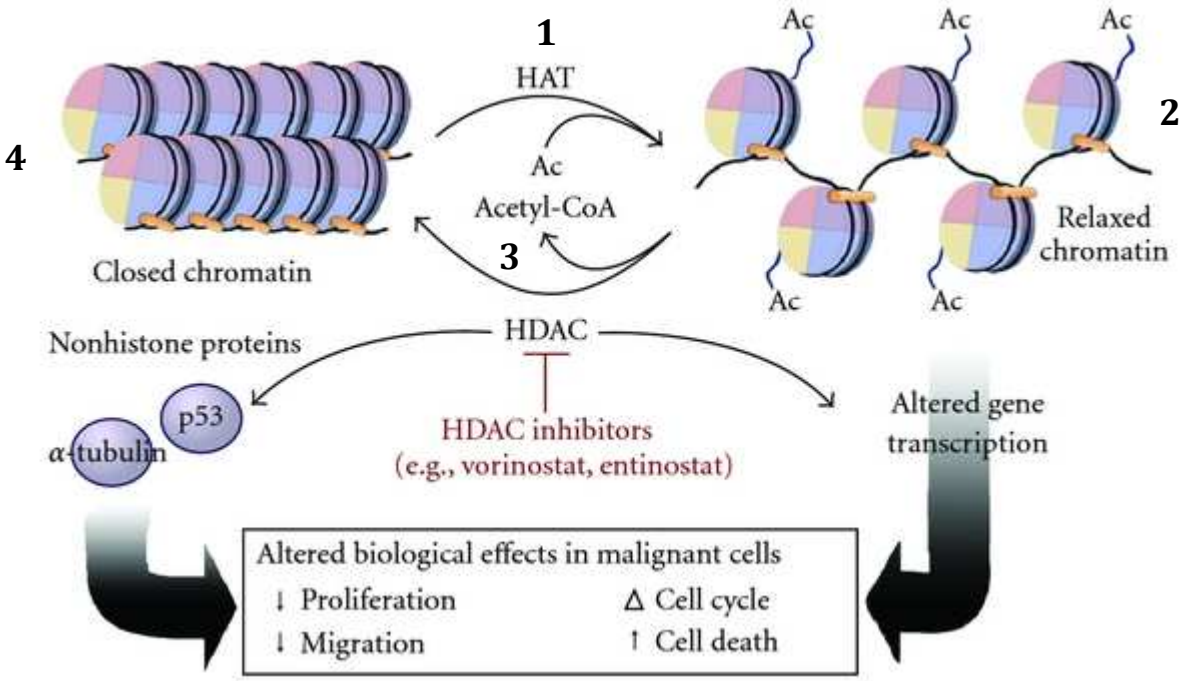

Figure 2.8 Reversible histone acetylation governs transcription in cells. 1. Histone acetyltransferases (HATs) transfer acetyl groups (Ac) from acetyl-CoA to the ε-amino group of lysine residues on the N-terminal tails of histones H3 and H4. 2. This neutralises the positive charge on lysine allowing the chromatin structure to relax and transcription factors and RNA polymerase II to gain access and activate gene transcription. 3. Histone deacetylases (HDACs) antagonise HATs, removing the acetyl groups via zinc- or NAD-dependent catalysis. 4. Lysine residues have their positive charge restored and interact strongly with the negatively charged DNA once more, compacting the chromatin structure and excluding transcription factors hence transcription is unable to initiate. 5. Histone deacetylase inhibitors such as vorinostat result in a global increase in histone acetylation. Acetylation is not limited to histones; many non-histone proteins such as α-tubulin and p53 become acetylated. Adapted from (Rodd, Ververis et al. 2012)

2.6.4 Classification of histone deacetylases

Eighteen HDACs have been identified in mammalian cells and classified into four groups based on their method of catalysis and similarity to yeast prototypes. Class I and II HDACs are zinc metalloenzymes which catalyse the hydrolysis of acetylated lysine residues, returning them to their normal protonated state, thereby facilitating chromatin condensation (Yurek-George, Habens et al. 2004).

2.6.5 Class I HDACs

Class I HDACs (HDAC1, 2, 3 and 8) each contain a deacetylase domain exhibiting from 45-93% sequence homology at the amino acid level. Class I HDACs are expressed in the nucleus in all cell types and their knockout is embryonically lethal (Montgomery, Davis et al. 2007). HDACs 1-3 form components of larger protein complexes containing co-

repressors such as Sin3 as well as methyl-binding proteins such as MeCP2 (Gurvich, Tsygankova et al. 2004). HDAC8 is the least abundant of the HDACs and is able to act independently rather than being reliant on forming a multi-protein complex. Class I HDACs are much smaller enzymes than their class II counterparts; for example HDAC8 is a 41 kDa protein and HDAC3 is 50 kDa while HDACs 4 and 6 are 120 and 160 kDa, respectively.

2.6.6 Class II HDACs

Class II HDACs are further classified into class IIa (HDAC4, 5, 7 and 9) and class IIb (HDAC6 and 10). Their expression is tissue-specific with many known roles in cardiac function (Calalb, McKinsey et al. 2009). Class II HDACs have the catalytic domain at the C-terminus. The long N-terminus contains conserved binding sites for 14-3-3 and the transcription factor myocyte enhancer factor 2 (MEF2) which renders the HDACs responsive (Haberland, Montgomery et al. 2009). They lack intrinsic DNA-binding activity and are recruited to their target promoters via their direct association with transcriptional activators, repressors or as part of a multi-protein complex e.g. CoREST (Yang and Seto 2003). Their inherent deacetylase activity against acetylated histones is also lower than that of their class I or IIb counterparts suggesting the possibility of alternate substrates (Lahm, Paolini et al. 2007).

Class IIa HDACs are able to shuttle between the nucleus and the cytoplasm and their repressive activity is dependent on this capacity which is mediated by phosphorylation (McKinsey, Zhang et al. 2000). HDACs become phosphorylated by several kinases including Aurora B kinase and calcium/calmodulin-dependent protein kinase (CaMK) (McKinsey, Zhang et al. 2000). The phosphate groups act as docking sites for proteins such as 14-3-3 which masks the nuclear localisation signal, thus facilitating localisation of the HDAC to the cytoplasm (Guise, Greco et al. 2012). The reverse mechanism is also true, with phosphatases such as PP2A removing the phosphate groups, preventing the binding of 14-3-3 thus exposing the nuclear localisation signal, directing the HDAC to the nucleus.

2.6.7 Class III and IV HDACs

The class III HDACs, or sirtuins, are different to class I and II in that they use the coenzyme NAD^+ rather than zinc-dependent catalysis to achieve deacetylation. HDAC11 is the sole member of class IV and exhibits features of both class I and class II HDACs

(Hsu, Sheu et al. 2012). It is similar in size to the class I HDACs, however has no known function. It is thought to be the ancestral member of the HDAC family. The investigation reported in this thesis focuses on class I and II HDACs.

2.6.8 Expression of HDACs in malignancy

Class I HDACs are overexpressed in various types of cancers and this is correlated with poor prognosis (Hsu, Sheu et al. 2012). HDAC inhibitors (HDACi) can cause cell cycle arrest and apoptosis in transformed cells. HDACi can attenuate metastasis in several cancer types (Taylor, Liu et al. 2010). In a colorectal cancer cell line downregulation of survivin mimicked the effects of TSA by inducing apoptosis and inhibiting cellular proliferation (Hsu, Sheu et al. 2012). A very recent study has utilised the elevated HDAC activity observed in some malignant cells to activate a cytotoxic prodrug which selectively kills cancerous cells while minimising damage to healthy tissues (Ueki, Lee et al. 2013). This may prove to be the first of a new generation of chemotherapeutic drugs as there is much scope to extend this to other cytotoxic agents and other HDACi.

2.7 HDAC regulation and inhibition

Regulation of HDAC activity occurs in part by steric hindrance; these enzymes compete with HATs for the same binding sites on some proteins such as MEF2 (Czubryt, McAnally et al. 2003). Unlike genetic mutations, epigenetic modifications such as acetylation have the potential to be reversed e.g. through upregulation of HAT activity or treatment with histone deacetylase inhibitors (HDACi, Figure 2.8). No HDACi are target-specific other than scriptaid which is HDAC6-specific; most inhibit multiple HDACs. However, some show selectivity for a particular class of HDACs. The precise mechanism of action for many HDACi is still not entirely known but the potential clinical benefits are apparent.

HDACi block the removal of acetyl groups by HDACs and tip the balance in favour of the HATs which increase histone acetylation. This results in the transcriptional activation of specific genes e.g. p21 or p27 that induce growth arrest by inactivating cyclin-dependent kinases and thereby inhibiting further cell proliferation (Ju and Muller 2003). Similarly, pro-apoptotic genes and silenced tumour suppressor genes such as

p53 may also be re-expressed which would be particularly beneficial in malignant cells as apoptosis could be initiated (Hsu, Sheu et al. 2012).

2.7.1 HDAC inhibitors

There are four main classes of HDAC inhibitors; hydroxamic acids (Figure 2.9) such as trichostatin A (TSA), SAHA (vorinostat) and LBH589 (panobinostat), depsipeptides such as FK228 (romidepsin), benzamides (derivatives of benzoic acid) and aliphatic compounds such as valproic acid and sodium butyrate. SAHA and romidepsin have been approved by the FDA for the treatment of cutaneous T cell lymphoma and many more are in clinical trials as mono- or combination therapies (Tiffon, Adams et al. 2011). The most interesting results seen during this study were in cells treated with VPA. This agent is currently under a lot of investigation for many disorders, discussed in more detail below.

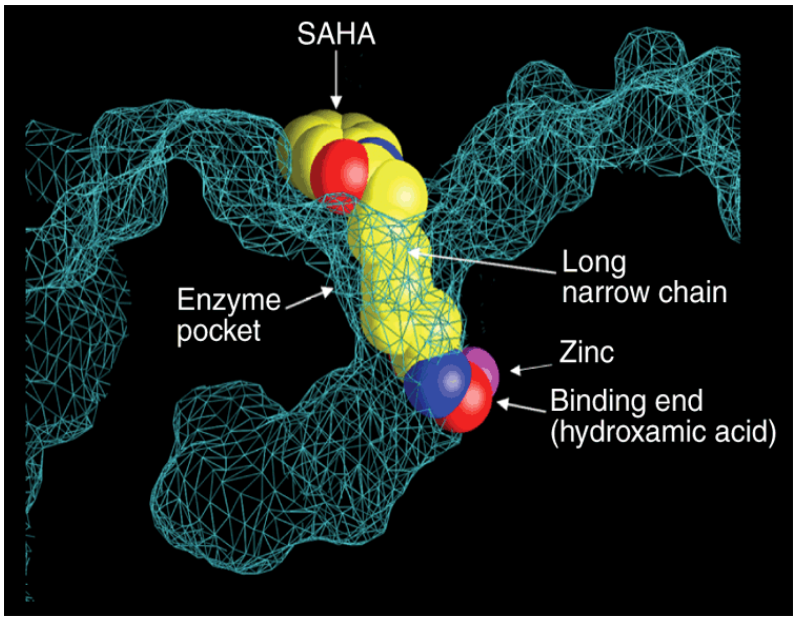

Figure 2.9 The proposed mechanism of action of the hydroxamic acid inhibitors Schematic representation of the crystal structure of HDACs. Hydroxamic acids such as SAHA snake through the 11 by 14 Angstrom cleft in HDACs and the hydroxamic acid moiety doubly coordinates the zinc atom in the catalytic centre, rendering it inactive. The hydrophobic end interacts with hydrophobic residues around the entrance to the binding pocket, strengthening the binding of the HDACi to the HDAC. Adapted from (Marks, Richon et al. 2004)

2.7.2 Valproic acid

VPA (2-propyl-pentanoic acid) is a short-chain, branched fatty acid (Figure 2.10). It was serendipitously found to have anti-convulsant effects while being used as a solvent in 1962 and has been widely used to treat epilepsy and bipolar disorder for decades, however the exact mechanisms of action remain elusive (Lee, Zahoor et al. 2012).

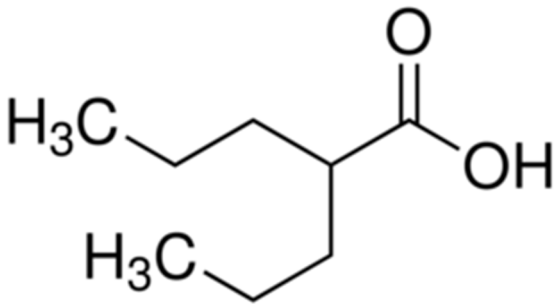

Figure 2.10 Schematic structure of the HDAC inhibitor valproic acid. VPA is an aliphatic acid compound which has been used to treat seizure disorders and depression for many years. In comparison to the other classes of HDAC it has much lower potency (mM range compared to nM).

It is a broad spectrum drug with low-to-moderate HDACi activity (Lerche, Philipsen et al. 2008). VPA has been reported to inhibit the class I HDACs 1, 2 and 3 with IC_{50} values ranging from 0.7 to 1 mM and the class IIa HDACs 4, 5 and 7 with IC_{50} values between 1 and 1.5 mM, all of which fall within the therapeutic range achieved in patients (Gurvich, Tsygankova et al. 2004).

VPA has also recently been shown to have anti-inflammatory properties as it reduced TNF-α immunostaining in inflamed rat paws, and caused a drastic reduction in the number of TNF-α positive cells in combination with the hydroxamic acid HDACi SAHA (Ximenes, de Oliveira Goncalves et al. 2013). The anti-inflammatory activity of VPA may be particularly useful in malignancies with activated HDAC4 as this is associated with aberrations in inflammatory and chemokine related genes (Cohen, Piccolo et al. 2013). VPA also has neuroprotective effects via inhibition of HDAC2 in conditions such as stroke (Lee, Zahoor et al. 2012).

VPA can induce growth arrest and differentiation of transformed cells in culture (Gurvich, Tsygankova et al. 2004). It also suppresses migration of breast cancer cells through inhibition of HDAC2 and downregulation of survivin expression (Zhang, Wang et al. 2012). Additionally VPA inhibits proliferation and migration of prostate cancer cells (Zhang, Wang et al. 2011). The serine/threonine kinase GSK3β plays important roles in skin tumourigenesis, particularly in anchorage-dependent growth and its expression is often lots in SCCs (Ma, Wang et al. 2007). In contrast to epithelial cells, VPA-mediated inhibition of GSK3β actually enhances migration of mesenchymal stem cells, highlighting the cell-specific effects this HDACi plays (Lee, Zahoor et al. 2012).

The anti-proliferative effect of VPA on malignant cells has sparked interest in its topical use for hyperproliferative skin diseases such as basal cell carcinoma or actinic keratosis (Lerche, Philipsen et al. 2008). There is also potential for using it for the treatment of

dermal malignancies such as psoriasis, because unlike retinoids which cause adverse skin reactions, its topical application does not induce any local skin irritation (Lerche, Philipsen et al. 2008). The molecular basis of this effect still remains largely unknown, hindering the development of more targeted therapies for skin malignancies.

Conclusion

Overall, Notch signalling is a highly complex process despite its linear nature. Notch signalling is entirely context-dependent; its expression in one tissue can promote proliferation while repressing it in another. Many questions remain unanswered regarding how it achieves tissue-specific effects particularly in adult stem cell systems such as the basal layer of the IFE. The multitude of p63 isoforms adds to the complexity of this network. Knowledge of this area is far from complete and the signalling pathways regulating terminal differentiation are yet to be fully revealed.

Taken together the current literature suggests that p63, Notch and HDACs have pivotal roles in epidermal homeostasis and when this is disrupted there is cancer development. Therefore the investigation of the p63/Notch/HDAC regulatory axis within the context of primary human keratinocytes, and the impact of histone deacetylase inhibitors, particularly calproic acid, is warranted.

Hypothesis

Inhibition of class I and II HDACs alters the expression levels of p63 isoforms and Notch signalling proteins in keratinocytes and epithelial tumours with consequences on proliferation and differentiation.

3. Aims and Objectives

The aims of this investigation were to determine whether differences in the expression of each HDAC, p63 isoform and Notch signalling component correlate with differentiation and proliferation. If so, to assess what role each plays in epidermal development and potentially in tumourigenesis. More specifically this investigation aimed to identify whether inhibition of class I and II HDACs plays a significant role in these processes. In order to address these questions the following objectives were set:

- Characterise which histone deacetylase enzymes are present in HaCaT cells, an immortalised keratinocyte cell line, and in primary human keratinocytes (nHEK)
- Characterise which p63 isoforms are present in nHEK cells
- Compare the expression of p63 isoforms in nHEK cells following treatment with a panel of HDAC inhibitors
- Characterise the effects of a selected panel of HDAC inhibitors on epidermal differentiation using nHEK cells

4. Materials and Methods

4.1 Cell culture

All reagents were purchased from Life Technologies unless otherwise stated.

HaCaT (a gift fromProfessor Gerry Melino, Rome) and HeLa (ATCC) cells were cultured in Dulbecco's modified Eagle's medium (DMEM + GlutaMAX) supplemented with 10% heat-inactivated fetal bovine serum (FBS). Media was changed every three days and cells were passaged at 70% confluence using 0.25% trypsin-EDTA then replated in fresh media.

Primary neonatal human epidermal keratinocytes (nHEKs, #C0015C, Invitrogen) and the immortalised keratinocyte cell line N-TERT (a gift from Professor Gareth Thomas, University of Southampton) were cultured in EpiLife medium with 60 μM calcium (MEPI500CA) supplemented with human keratinocyte growth supplement (#S0015) sterilised by filtration through a 0.2 μm filter . Media was changed every three days and cells were passaged once a week. All cells were cultured at 37°C in a humidified incubator with 5% CO_2.

4.2 Histone deacetylase inhibitors (HDACi)

Three classes of HDACis were used during this study: the hydroxamic acids trichostatin A (TSA) and LBH589, which are both pan-HDACis; the fatty acid inhibitor valproic acid (VPA, Sigma) which selectively inhibits class I HDACs; and the cyclic peptides FK228 (romidepsin) and spiruchostatin A which also selectively inhibit class I HDACs. All inhibitors were a gift of Karus Therapeutics unless otherwise stated and were used at the concentrations indicated in Figure 4.1. All HDAC inhibitors were diluted in media from a DMSO stock to treat the cells apart from VPA which was diluted directly from powder into sterile water.

4.3 Western blotting

Following treatment, cells were harvested by scraping, pelleted by centrifugation at 400 g for 8 mins and washed with ice cold PBS, then re-pelleted by spinning at 2000 g for 5 mins. Cells were lysed in laemmli buffer (63 mM Tris HCl pH 6.8, 10% glycerol, 2% SDS) and sonicated to shear the DNA (Laemmli 1970). Protein was quantified using the Pierce BCA assay (Pierce). Absorbance was measured using a plate reader at 570 nm and protein was quantified relative to a bovine serum albumin (BSA) standard curve.

Lysates were stored at -20^{0}C until use. Equal amounts of protein were separated by electrophoresis on 6-15% SDS-polyacrylamide gels (made by the author) at 100 V in a Tris-Glycine-SDS buffer (National Diagnostics, 0.25 M Tris, 1.92 M Glycine, 1% SDS). Protein was transferred to nitrocellulose membranes (GE Healthcare) at 70 V for 2 h in a Tris-Glycine transfer buffer (National Diagnostics, Tris 0.25 M, Glycine 1.92 M) then incubated in blocking buffer (5% non-fat dried milk in Tris-buffered saline (TBS) with 0.1% Tween-20 (TBST)) for 1 h at room temperature with agitation. Membranes were incubated with primary antibodies in blocking buffer at the dilutions indicated (Appendix 1) overnight at 4^{0}C with agitation , washed thrice with TBST and incubated with species-specific HRP-conjugated secondary antibody in blocking buffer at a dilution of 1:10,000 for 1 h at room temperature with agitation. Membranes were washed thrice in TBST and bound antibodies were detected by chemiluminescence using SuperSignal West Dura extended duration substrate (Thermo Scientific) on Amersham Hyperfilm ECL (GE Healthcare) developed on an Xograph Compact X4 developer.

4.4 RNA extraction

Following treatment, cells were pelleted as described previously and washed with ice cold PBS. RNA extraction was performed using the RNeasy Mini kit (Qiagen) according to the manufacturer's instructions. In brief, addition of ethanol precipitates the RNA and provides the appropriate conditions for RNA to subsequently become bound to the column membrane. Several washing steps were then performed to remove any traces of solvent before elution of the purified RNA in 30 µl RNase-free water. RNA quality and concentration were determined using a NanoDrop and ND-1000 software.

4.5 cDNA synthesis and polymerase chain reaction

cDNA was synthesised from 1 µg total RNA (unless otherwise stated) using the RevertAid H Minus First Strand cDNA synthesis kit (Thermo Scientific) using the RevertAid H Minus reverse transcriptase. Polymerase chain reaction (PCR) was performed using 1 ul of an appropriate cDNA dilution in a total reaction volume of 20 µl (2x MyTaq Red Mix, Bioline), 7 µ nuclease-free water, 1 µl forward and 1 µl reverse primers). Primer sequences, amplicon sizes, number of cycles and annealing temperatures are shown in Appendix 2. Amplification was carried out under the following conditions: enzyme activation at 95^{0}C for 10 mins, dissociation at 95^{0}C for 30

seconds, annealing at the temperatures indicated in Appendix 2 for 30 cycles unless otherwise stated then elongation at 72^{0}C for 30 secs and final extension at 72^{0}C for 10 mins. Gel electrophoresis was performed on PCR products to test the specificity of the reaction as determined by the correct amplicon size. Products were electrophoresed in a 0.8% agarose gel with GelRed (Cambridge BioScience) at 50 V for 2 h. Bands were visualised under UV light.

4.6 Real-time PCR

Quantitative PCR (q-PCR) was performed using 2 µl cDNA diluted 1:5 mixed with 7 µl nuclease-free water, 10 µl TaqMan Universal PCR MasterMix No AmpErase UNG and 1 µl gene-specific TaqMan FAM-TAMRA probe. Samples were prepared in 96 well plates and run in triplicate. No template control reactions (cDNA replaced by 1 µl nuclease-free water) were included for each primer pair. Amplification was carried out under the following conditions: 50°C for 2 mins, enzyme activation at 95°C for 10 mins, dissociation at 95°C for 15 secs and annealing at 60°C for 1 min for 40 cycles. qPCR was performed using an Applied Biosystems 7500 Real Time PCR System. 7500 System SDS software (Applied Biosystems) was used to analyse the expression of human 18S, involucrin, loricrin, p21, Notch1, Hes1, Hey1, Hey2, DLL1, Jagged1 and Mastermind-like 1 (Appendix 3). Gene expression was quantified using the comparative cycle-threshold method and levels of PCR product were expressed as a function of 18S.

4.7 Cellular viability

The viability of nHEKs was assessed via trypan blue exclusion. Briefly, 20 µl trypan blue was mixed with 20 µl cell suspension. Cells were termed viable if they excluded trypan blue and minimal viability for performing experiments was set at 70%. Cellular viability of HDACi-treated nHEKs was assessed qualitatively using phase contrast microscopy on an Olympus CKX41 fluorescence microscope at a magnification of 10x.

4.8 Epidermal differentiation

Epidermal differentiation was induced by increasing the calcium concentration of the culture media as detailed in Figure 4.1. Alterations in calcium concentration were performed by adding calcium chloride at a final concentration of 1.2 mM. Cells were harvested prior to the addition of calcium chloride (Day 0; D0) and 1, 3, 5 and 7 days afterwards (D1, 3, 5, 7). Differentiation status was confirmed by Western blotting and real-time PCR for the late differentiation marker loricrin.

4.9 Proliferation assay

To assess cellular proliferation cells were fixed on days 1, 2 and 3 with ice cold 50:50 methanol/acetone, washed with PBS and stored in PBS until use. DAPI (1 mg/ml, Sigma) was diluted 1:5000 in sterile water. 300 µl was added per well in a 24-well plate and incubated at room temperature for 10 minutes. After the incubation period cells were washed thrice with double-distilled water (ddH_2O). Cells were stored in ddH_2O until use. Fluorescence microscopy was performed using an Olympus CKX41 fluorescence microscope at a magnification of 4x. One field of view was photographed per well with 6 wells used per time point, per experimental condition. The number of cells in each well was quantified using ImageJ software.

4.10 Cell cycle analysis

Cell cycle distribution was analysed using flow cytometry to detect the cellular DNA content following propidium iodide (PI) staining. Cells were treated as described in figure legendsand harvested at days 1, 2 and 3. Cells were pelleted, resuspended in 100 µl PBS and 2 ml ice cold 70% ethanol was added dropwise to each tube while vortexing at a medium speed. Tubes were placed on ice and stored at -20°C until staining. Cells were washed with PBS and 500 µl RNase/PI solution (100 µl RNase, 3.16 mg/ml, Sigma/400 µl PI, 50 µg/ml, Sigma) was added to each FACS tube. Cells were incubated at 37°C for 30 minutes then stored on ice prior to sample acquisition. Cellular DNA content was determined using a FACS Caliber (BD) and CellQuest Pro software (BD) to generate histograms of DNA content. Changes in cell cycle after treatment were then calculated by comparison with non-treated controls.

4.11 Statistical analysis

Student's t-tests were performed using Minitab software with statistical significance judged at a p value of 0.05.

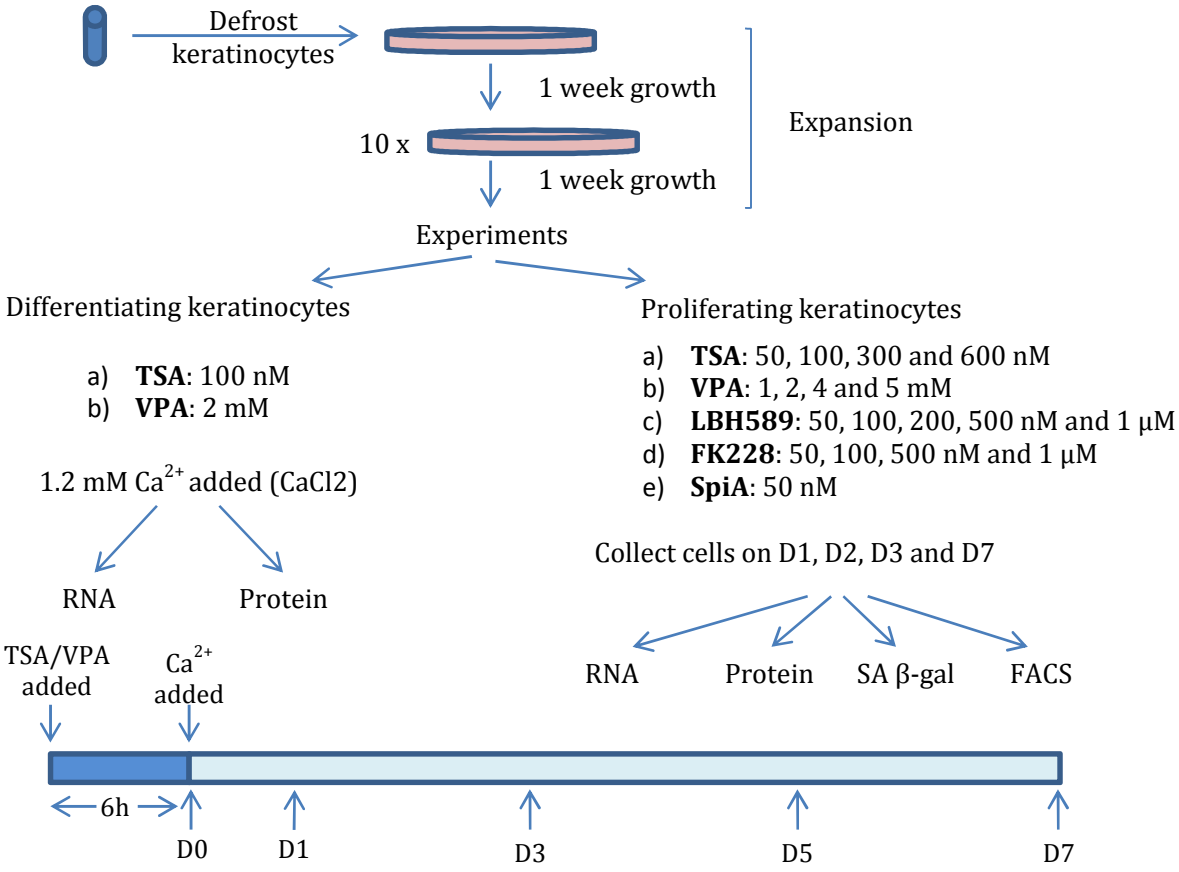

Figure 4.1 The procedures implemented to study epidermal differentiation and proliferation. nHEKs were obtained from Life Technologies and cultured in Epilife media supplemented with human keratinocyte growth supplement. When sufficient numbers were available for experimentation nHEKs were treated with trichostatin A (TSA) , valproic acid (VPA), LBH589, FK228 and spiruchostatin A (SpiA) at the concentrations indicated and harvested at the time points also indicated to assess the impact of these HDAC inhibitors on keratinocyte proliferation. Based on these results 100 nM TSA and 2 mM VPA were selected to investigate the impact of HDAC inhibitors on epidermal differentiation.

RESULTS

5.1 Expression of p63 isoforms in primary human keratinocytes

The transcription factor p63 is the master determinant of keratinocyte cell fate, therefore the first step of this investigation was to determine which p63 isoforms (TAp63, ΔNp63 isoforms or both) are expressed at the RNA level in primary human keratinocytes (nHEKs). PCR was performed as antibodies are unable to distinguish between the β and γ isoforms. To distinguish between TA- and ΔNp63 transcripts, PCR was performed using forward primers specific to the N-terminal regions of the TA- or ΔNp63 isoforms combined with a common reverse primer to the C-terminus of *p63*. Products were resolved on an agarose gel and visualised under UV light. As the N- terminus is longer in TAp63 isoforms, TAp63-specific primers were expected to amplify a larger product. 5 ng plasmid expressing TAp63α and ΔNp63α (a gift from Dr Franco Conforti) were also amplified as positive controls to test the specificity of the primers.

TAp63 isoform expression was absent in nHEKs, however ΔNp63 isoforms were highly expressed (Figure 5.1A). Subsequently PCR was performed using primers to amplify the *p63* C-termini splice variants (p63α, β and γ isoforms) and demonstrated expression of ΔNp63α, β and γ isoforms in nHEKs (Figure 5.1B). A non-specific product was amplified by the p63α primers therefore a new reverse (p63α) primer was designed (lane 2, Figure 5.1C) which successfully amplifed only p63α (lane 1, Figure 5.1C). Both primers amplified a single product which corresponded to the same size band as the amplified plasmid when run on a 1.2% agarose gel. The identity of the non-specific band amplified by the p63α reverse primer (Figure 5.1B, arrowhead) was not investigated further. Having confirmed expression of p63 isoforms in nHEKs, these cells were subsequently screened for the expression of histone deacetylase isoforms.

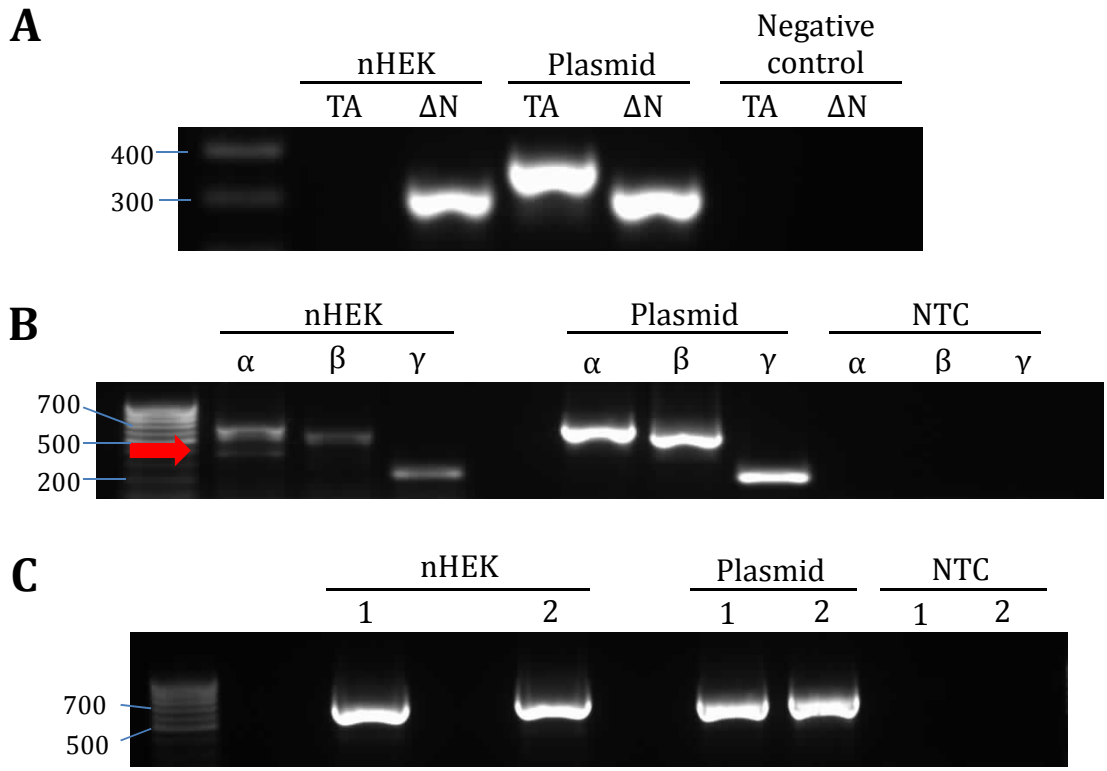

Figure 5.1 ΔNp63α, β and γ isoforms are expressed in primary human keratinocytes while TAp63 isoforms are absent. PCR was performed using primers specific to the N-terminal regions of the full length (TA) and truncated (ΔN) p63 isoforms and products were run on an agarose gel. (A) In nHEKs ΔNp63 isoforms were expressed while TAp63 isoforms are absent. TAp63α and ΔNp63α plasmids were used to confirm specificity of the amplified product. NTC=negative control. (B) PCR was performed using primers specific to the C-termini of p63 isoforms showed that p63α, β and γ isoforms were all expressed in nHEK cells at the correct sizes according to the amplified ΔNp63α, β and γ plasmids. The arrow indicates an additional product amplified by the p63α-specific primers. (C) A new reverse primer was designed to p63α (2) and PCR was performed using this alongside a p63α primer previously described to be specific to p63α (1). A single amplified product was visualised in each lane at the predicted size. NTC: No template control, nuclease-free water was added to the PCR instead of cDNA template.

5.2 Expression of HDACs in primary human keratinocytes and cell lines

The initial focus of the investigation was to identify the interactions between histone deacetylases (HDACs), specifically HDAC1 and 2 with the transcription factor p63 so experiments were undertaken to assess the expression pattern of these HDACs in nHEKs and the keratinocyte cell lines HaCaT and N-TERT. HeLa whole cell lysates were used as a positive control for HDAC expression. Immunoblotting for class I and II histone deacetylases demonstrated that HDACs 1 and 2 are expressed in nHEKs (Figure 5.2A and B). However, expression levels varied substantially between nHEKs and the two keratinocyte cell lines. The expression of HDAC1 differed the least between the cells tested; expression was incredibly similar between the two cell lines. HDAC2 exhibited more varied expression with noticeably high expression in N-TERT cells. Both HDACs had the lowest expression in nHEKs (Figure 5.2C and D).

The investigation was then extended to other HDACs to assess the expression of other classes of HDACs and expression of HDACs 3, 4 and 6 was also observed in nHEKs (Figure 5.3). The expression of these HDACs also varied between the cell lines and primary cells. Densitometry showed that expression of HDACs 3, 4 and 6 was similar in nHEKs and HaCaT cells (Figure 5.3, right hand panels). N-TERT cells exhibited the highest expression of HDAC3 (Figure 5.3A). While HDAC4 had similar expression levels in HaCaT cells and nHEKs, its expression in N-TERT cells was remarkably lower in comparison (Figure 5.3B). In contrast, expression of HDAC6 was comparable between nHEKs and cell lines, with the highest expression in nHEKs (Figure 5.3C).

The difference in HDAC expression between nHEKs and N-TERT appeared drastically different in most cases indicating that this cell line could not be used as a clear mimic of nHEKs in studies assessing the expression of HDACs, however statistical analysis revealed that the differences observed were not significant ($p>0.05$). Despite the similar levels of HDAC expression in HaCaT compared with nHEKs, HaCaT cells possess a mutant form of the transcription factor *p53* which may impact the results of investigations into the expression of *p63* isoforms therefore only nHEKs were employed for subsequent experiments investigating the expression of HDACs. Having determined the expression of p63 isoforms and both class I and II HDACs the next aim was to treat nHEKs with HDAC inhibitors (HDACi) to determine which would be suitable for investigating the impact of these agents on the expression of HDACs and p63 isoforms.

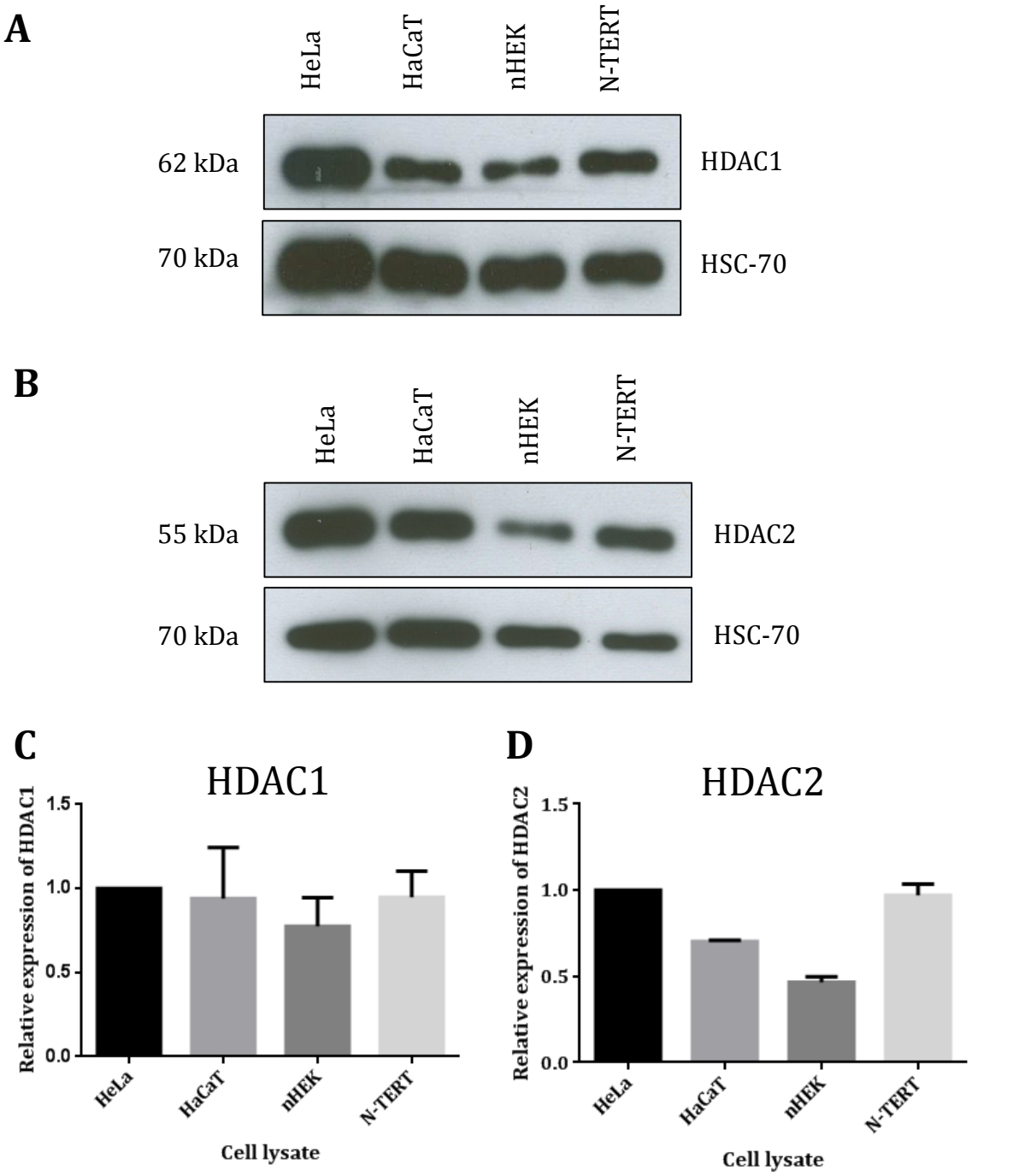

Figure 5.2 Expression of histone deacetylase 1 and 2 in primary human keratinocytes and cell lines. Whole cell lysates were prepared from nHEKs and two immortalised keratinocyte cell lines HaCaT and NTERT. Western blotting was performed to probe for HDACs. HeLa whole cell lysates were used as a positive control. HDAC1 (A) and HDAC2 (B) were expressed in nHEKs, however expression was higher in the two keratinocyte cell lines. Representative images from 3 Western blots. Densitometry was performed using ImageJ software to quantitate the expression of HDAC1 (C) and HDAC2 (D) relative to HSC-70 in each cell type and showed that HDAC expression varied between primary keratinocytes and cell lines.

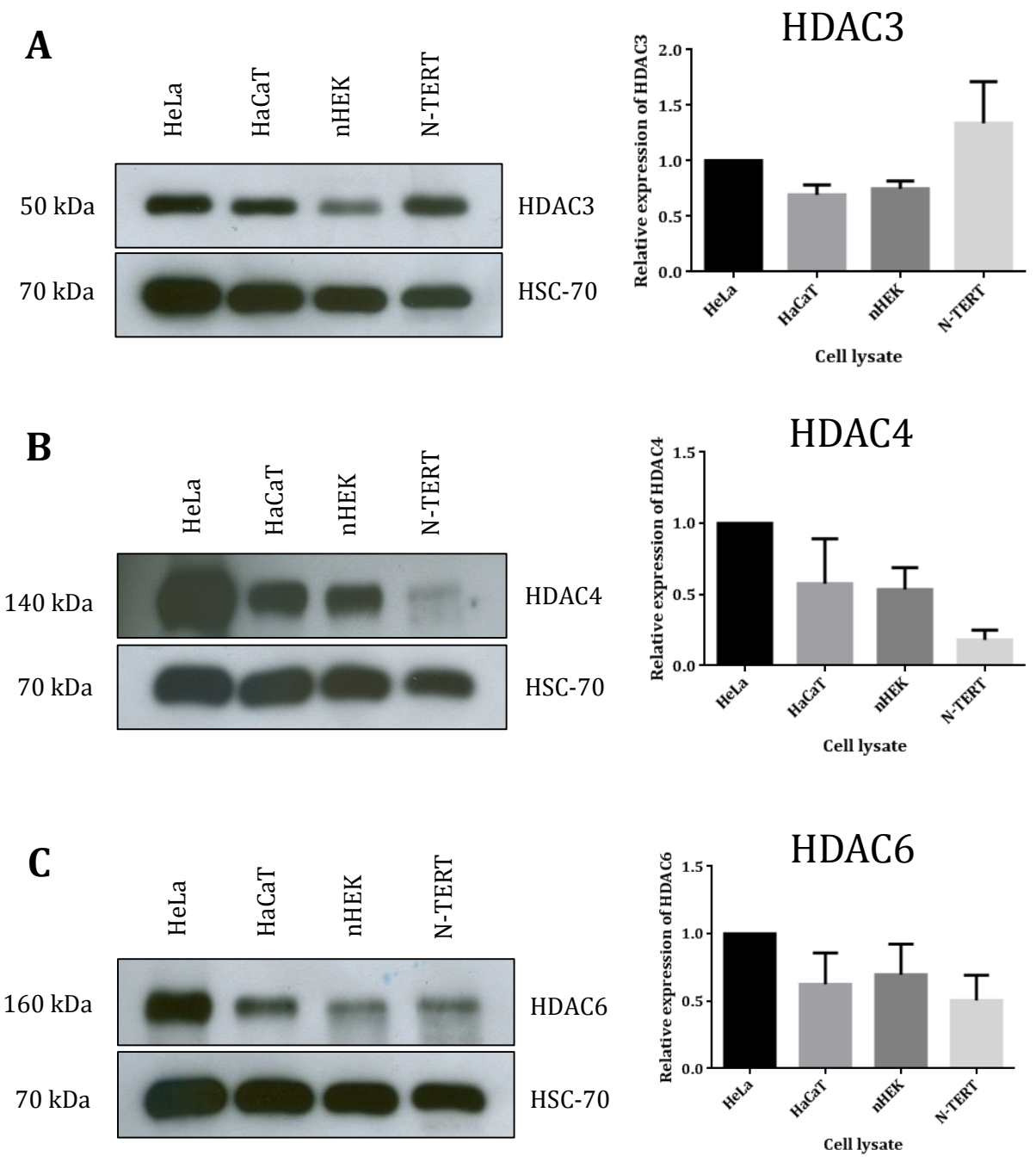

Figure 5.3 Expression of histone deacetylase 3, 4 and 6 in primary human keratinocytes and cell lines. Whole cell lysates were prepared from nHEKs and two immortalised keratinocyte cell lines HaCaT and NTERT. Western blotting was performed to probe for HDACs. HeLa whole cell lysates were used as a positive control. HDAC3 (A), HDAC4 (B) and HDAC6 (C) were expressed in all lysates tested, however, HDAC3 was the most abundant of the three HDACs in nHEKs. Representative images from 3 Western blots. Densitometry was performed using ImageJ software to quantitate the expression of HDAC3 (A, right), HDAC4 (B, right) and HDAC6 (C, right) relative to HSC-70 in each cell type and shows that expression of these HDACs was similar between nHEKs and HaCaT cells, however overall expression varied considerably between primary keratinocytes and cell lines.

5.3 The effects of HDACi on nHEKs

To address the impact of a panel of HDAC inhibitors on epidermal cells and to determine the concentrations of each drug that are non-toxic, nHEKs were treated with the short-chain fatty acid VPA, the hydroxamic acid inhibitors TSA and LBH589 and with the depsipeptide inhibitor FK228 (romidepsin) for up to three days at a range of concentrations. Phase contrast microscopy was performed to qualitatively assess cellular morphology and viability. Figure 5.4 shows that nHEKs tolerate VPA well as VPA-treated nHEKs did not appear to be undergoing increased apoptosis compared with non-treated cells.

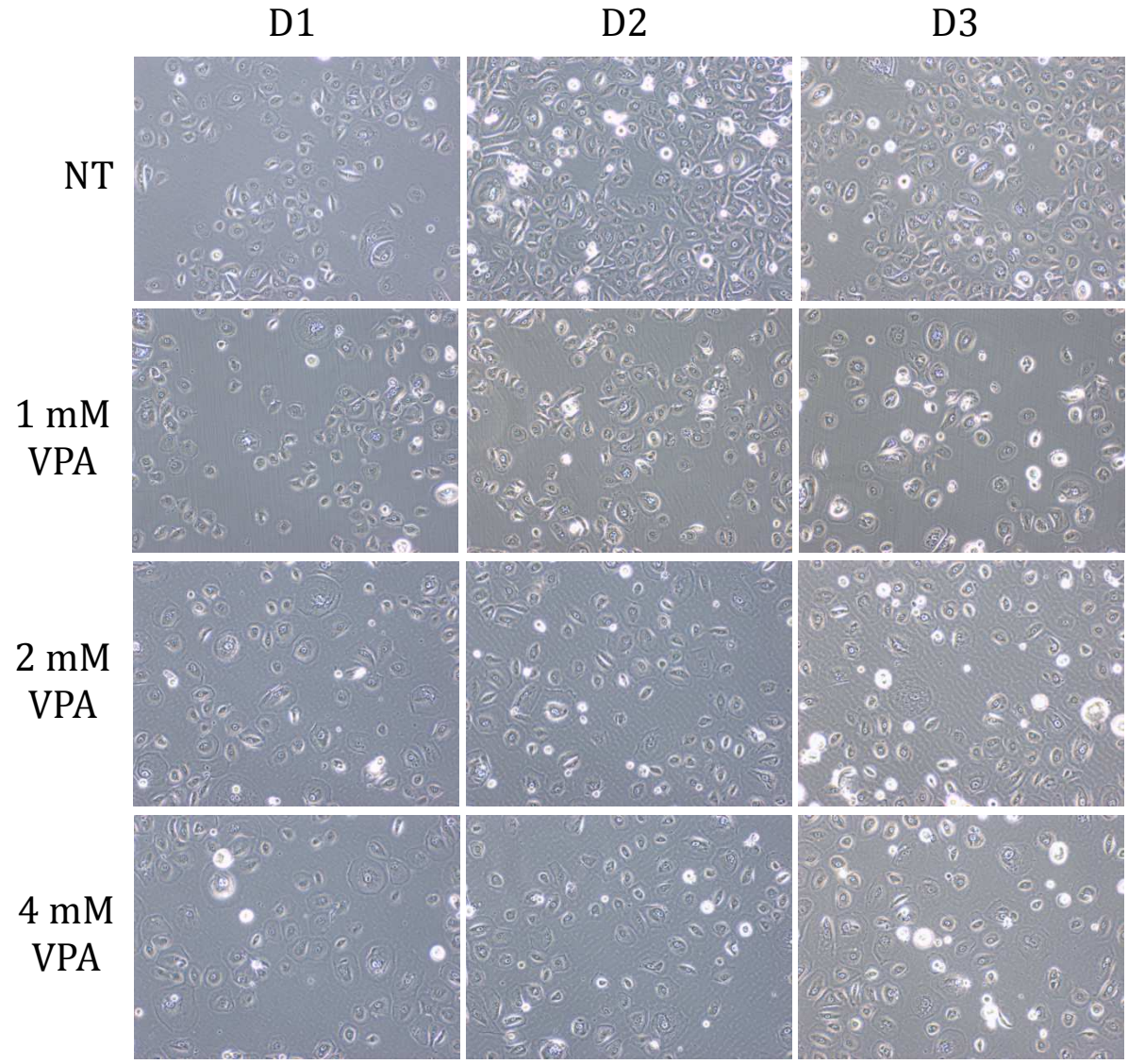

Figure 5.4 Valproic acid appeared non-toxic to primary human keratinocytes. Proliferating nHEKs were treated with 1, 2 or 4 mM VPA or left untreated (NT). Their viability was visually assessed using phase contrast microscopy over three days. Viability appeared unaffected by the addition of VPA at any of the three concentrations. Images taken at 10X magnification. n=1.

Similar to VPA, TSA appeared to be non-toxic to human keratinocytes at low concentrations however it appeared to attenuate proliferation rates. The number of TSA-treated cells accumulating over time was consistent throughout the experiment in each condition compared to the non-treated cells whose number visibly increased over time. The effects of VPA and TSA on nHEK proliferation will be discussed in further detail below.

Cells treated with 50, 100 and 300 nM TSA exhibited comparable levels of cell death to non-treated cells at days 1 (D1), 2 and 3 of treatment (Figure 5.5). On day 2 (D2) cell numbers were reduced in the 600 nM TSA condition which also showed increased cell death. By day 3 (D3) it was apparent that the number of viable cells treated with 50, 100 and 300 nM TSA was unchanged compared to D1, while cell death had only modestly increased. Cell death was extensive in cells treated with 600 nm TSA after 3 days of treatment.

As with TSA, cells treated with LBH589 seemed to exhibit a dose-dependent decrease in number by D1 (Figure 5.6). Cell numbers decreased over the next two days with all treatment concentrations, consistent with an increase in cell death in all conditions. Cell death was observed as early as D1 with all tested concentrations (50, 100, 200 and 500 nM) and increased over the course of the three days with the majority of cells treated with 200 and 500 nM LBH589 dead on D3 (Figure 5.6).

FK228 was the least well-tolerated of the four HDAC inhibitors, as demonstrated by the marked increase in cell death relative to non-treated controls at all three time points. By D3 virtually all cells treated with FK228 at any concentration were dead or dying. 500 nM FK228 caused a reduction in cell number relative to non-treated cells and lower doses by D1, while causing near-complete cell death by D2 (Figure 5.7).

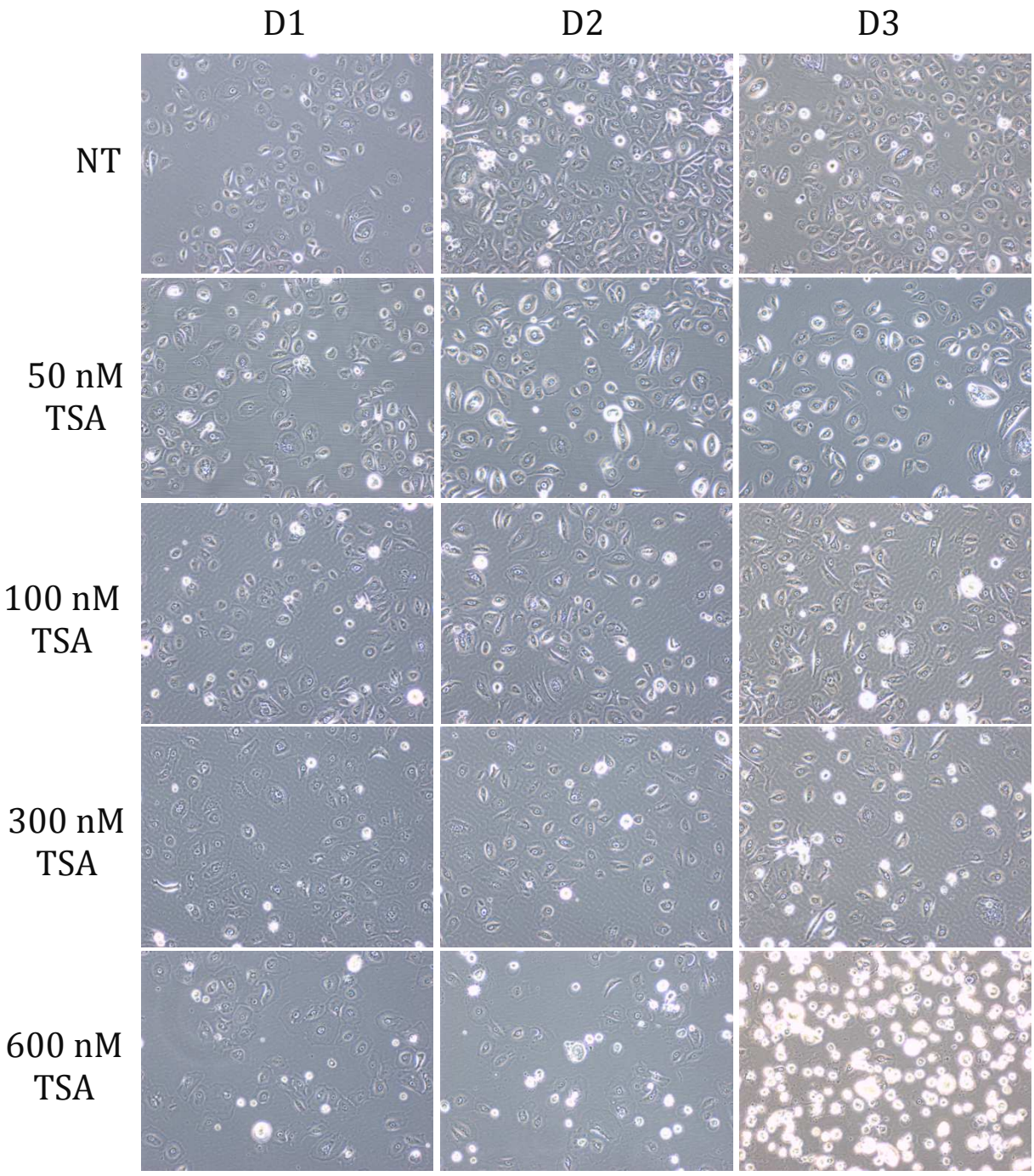

Figure 5.5 Trichostatin A is relatively non-toxic to primary human keratinocytes but seems to affect proliferation. nHEKs were cultured in EpiLife medium supplemented with human keratinocyte growth factor. Cells were treated with 50, 100, 300 or 600 nM TSA or left untreated (NT). Their viability was visually assessed using phase contrast microscopy over three days. Cells treated with 600 nM had poor viability, most evident at D3 and the number of TSA-treated cells did not increase over the course of the experiment. Images taken at 10X magnification. n=1.

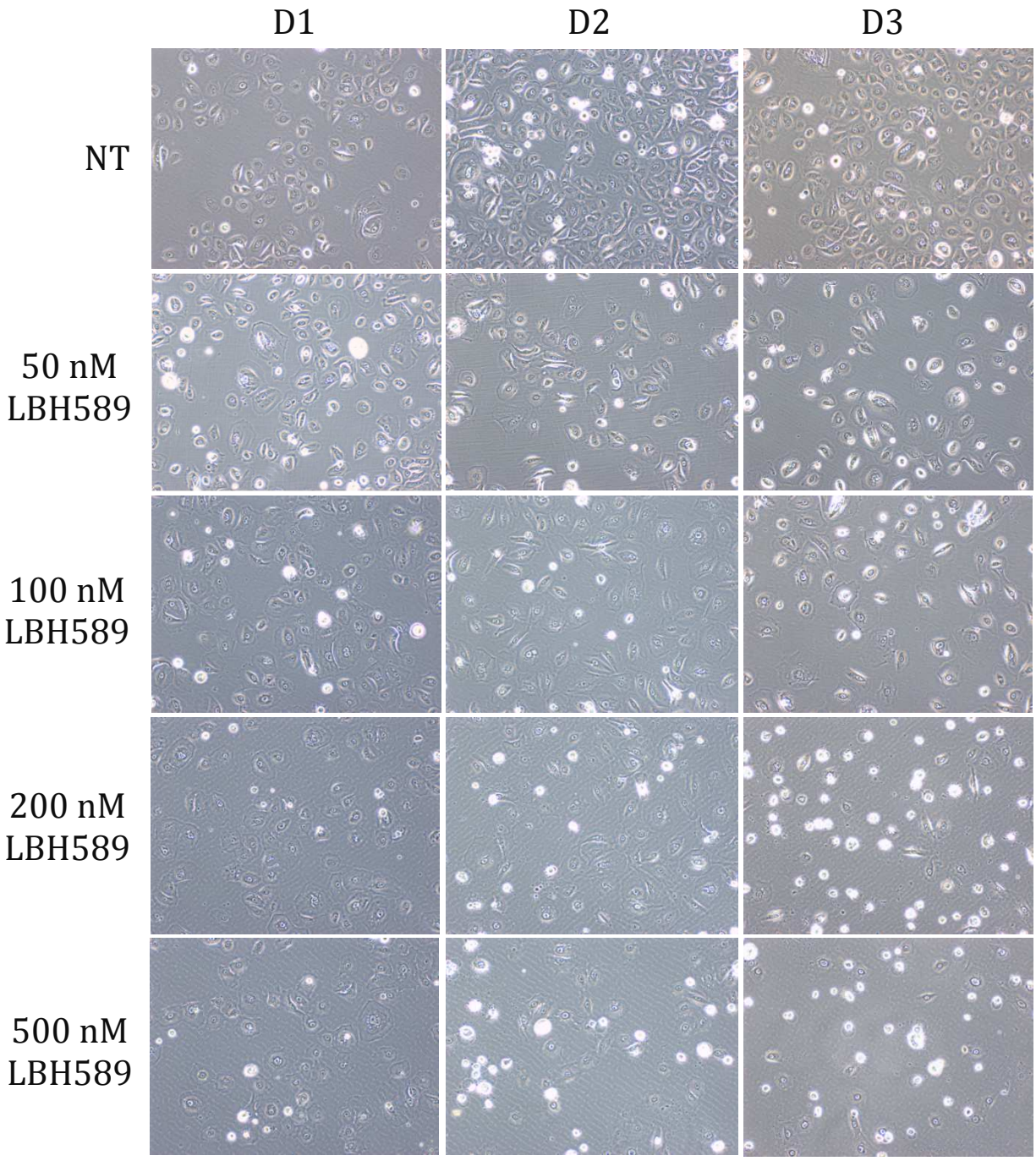

Figure 5.6 LBH589 reduced keratinocyte proliferation and was toxic even at low concentrations. nHEKs were cultured in EpiLife medium supplemented with human keratinocyte growth factor. Cells were treated with 50, 100, 200 or 500 nM LBH589 or left untreated (NT). Their viability was visually assessed using phase contrast microscopy over three days. Cells treated with 600 nM had poor viability, most evident at day 3 (D3) and proliferation was reduced with all treatments in a dose-dependent manner. Images taken at 10x magnification. n=1.

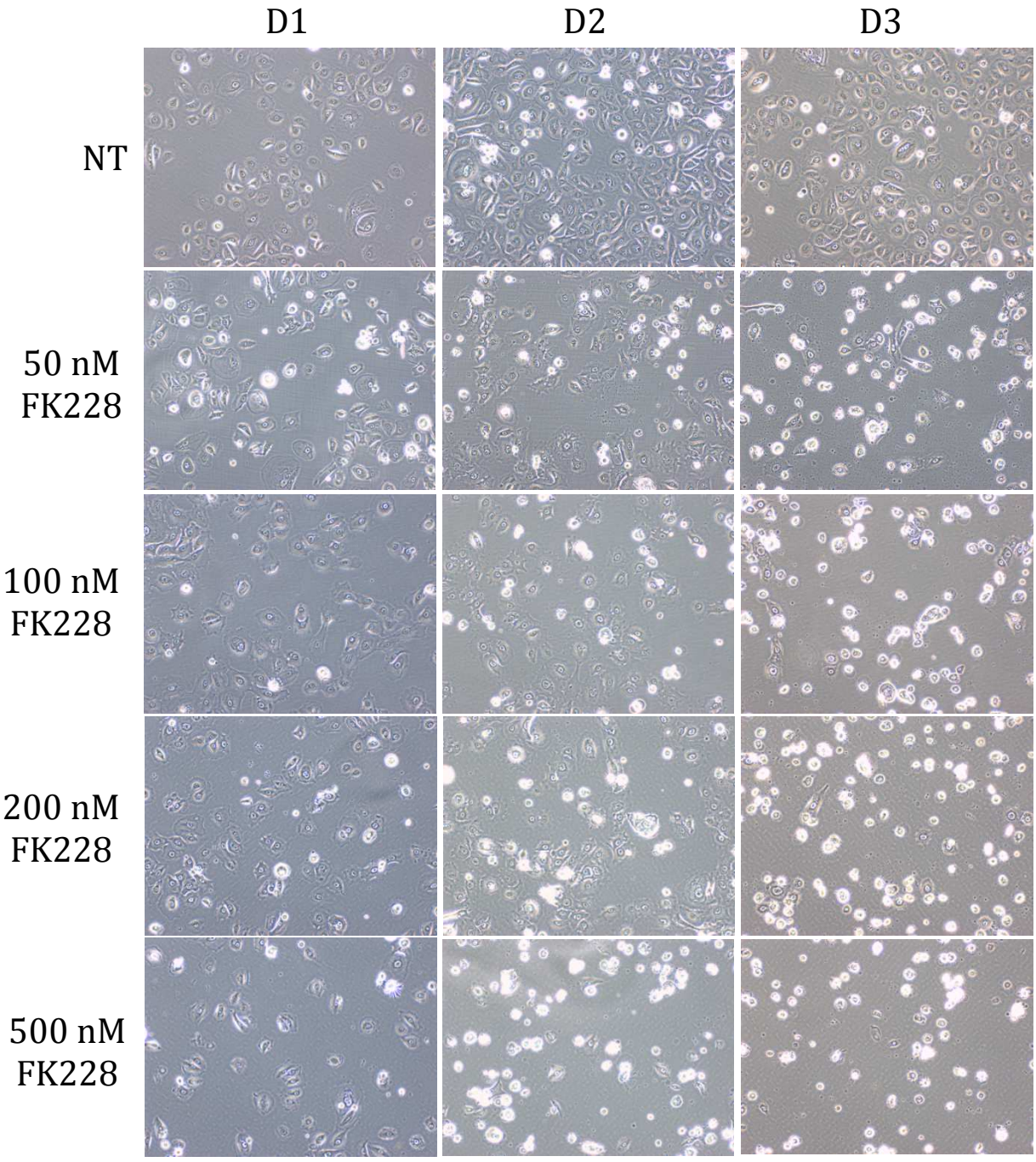

Figure 5.7 FK228 was highly toxic to primary keratinocytes. nHEKs were cultured in EpiLife medium supplemented with human keratinocyte growth factor. Cells were treated with 50, 100, 200 or 500 nM FK228 or left untreated (NT). Viability was visually assessed using phase contrast microscopy over three days. By D2 a great deal of cell death was observed with all concentrations of FK228, which increased by D3. Images taken at 10x magnification. n=1.

5.4 Cell death and cell cycle analysis

Due to the cytotoxicity of LBH589 and FK228 these were excluded from the continuing studies. VPA and TSA were chosen to further investigate the impact of HDAC inhibitors on keratinocytes due to their apparent lower toxicity (Figures 5.4 and 5.5). However, the question remained as to whether the apparent reduction in cell number observed in Figures 5.4 and 5.5 was due to an increase in cell death or a decrease in cellular proliferation. To address this flow cytometry was performed to analyse the cell cycle distribution of N-TERT cells treated with low doses of these two HDACi.

2 mM VPA and 100 nM TSA were the concentrations chosen because 1 mM VPA and 50 nM TSA were insufficient to elevate acetylation within nHEKs as demonstrated by a lack of induction of acetylated histone H4 (Ac-H4) (Figure 5.8). Therefore it was unlikely that 1 mM VPA and 50 nM TSA were sufficiently high concentrations to inhibit HDACs in these cells.

Cell death was very low in N-TERT cells treated with these agents with a maximum of 3.00 % at D3 in cells treated with 2 mM VPA and 4.23 % at D1 in cells treated with 100 nM TSA (Figure 5.9A). From the cell cycle profiles a very high proportion of cells could be observed in G_1 in all three conditions and this increased between D1 to D3 (Figure 5.10C). There was a consequent reduction in the proportion of cells in S phase in non-treated and VPA-treated cells over the three days (Figure 5.9C). The proportion of cells in G_2 decreased in all conditions over the three days (Figure 5.9D) and less than 2% of cells were polyploid in any condition (Figure 5.9E). Based on these data (n=1) it appeared that the reduction in cell number was not due to a high degree of cell death, and so the question of proliferation was next addressed.

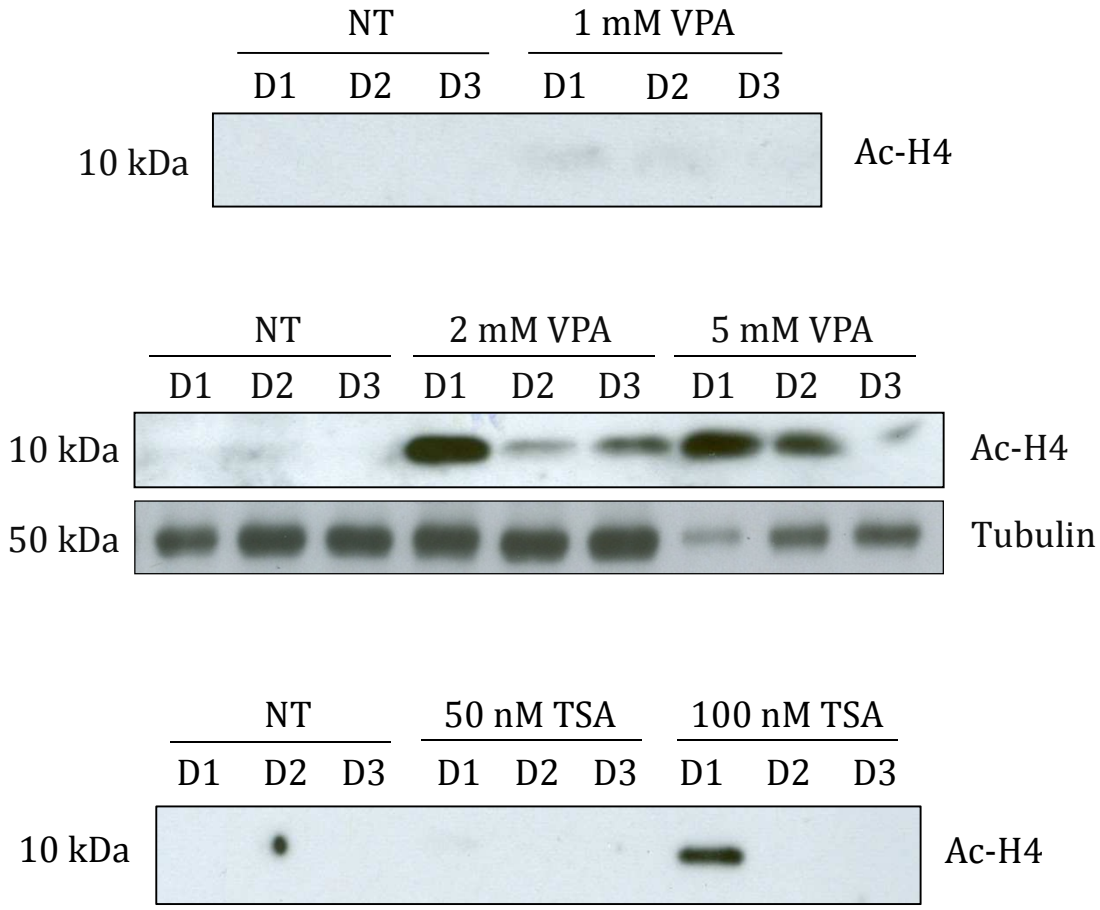

Figure 5.8. 2 mM VPA and 100 nM TSA are the minimal concentrations that increase acetylation in nHEKs. Cells were treated with 1, 2 and 5 mM valproic acid or 50 and 100 nM trichostatin A and harvested at the time points indicated for protein. Acetylated histone H4 (Ac-H4) was used to confirm that VPA had indeed inhibited deacetylase activity in these cells. 1 mM VPA had negligible effects on acetylation in nHEKs whereas 2 and 5 mM VPA drastically increased expression of Ac-H4. n=1.

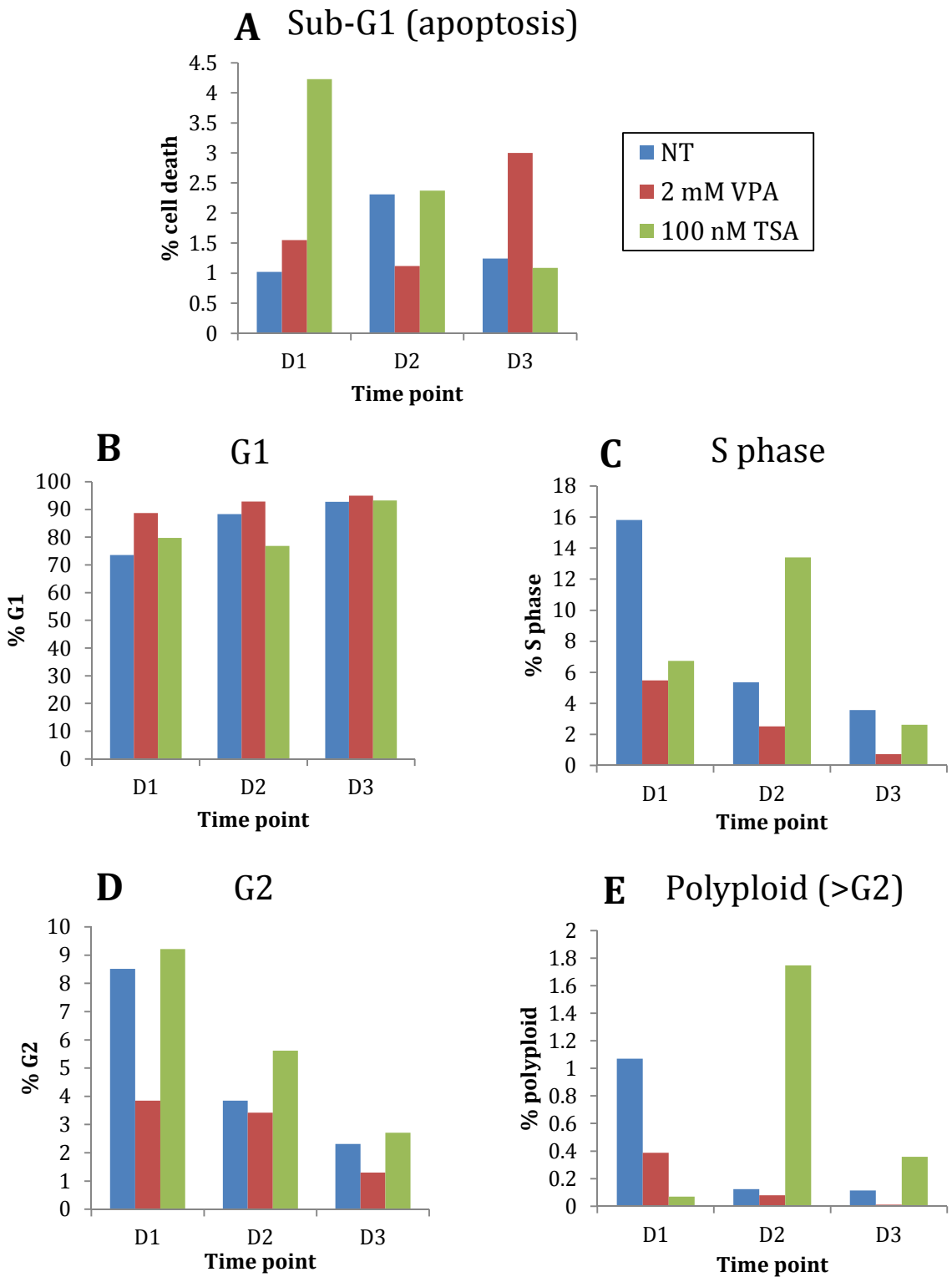

Figure 5.9 The relative proportions of N-TERT cells treated with VPA and TSA in each phase of the cell cycle. N-TERT cells were cultured as described in 4.1 and treated with 2 mM VPA, 100 nM TSA or left untreated. Cells were harvested and fixed on days 1, 2 and 3 then washed and incubated with propidium iodide and the cell cycle distribution was analysed. (A) The sub-G1 (apoptotic) fraction, (B) G1, (C) S phase, (D) G2 and (E) polyploid fractions are shown. NT, non-treated; VPA, valproic acid; TSA, trichostatin A. n=1.

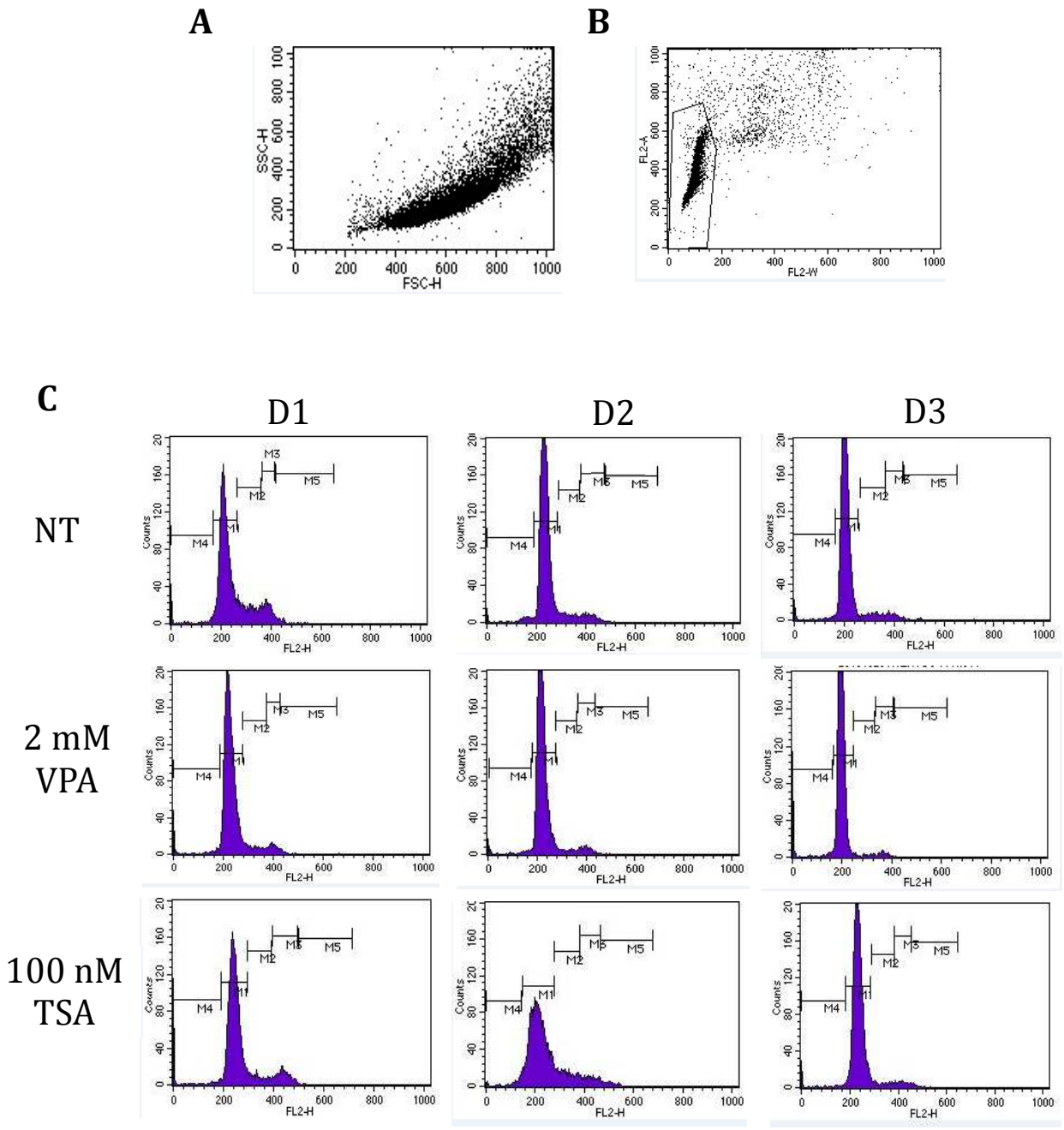

Figure 5.10 The cell cycle distribution of N-TERT cells treated with VPA and TSA is similar to non-treated cells. N-TERT cells were cultured as described in 4.1 and treated with 2 mM VPA, 100 nM TSA or left untreated. Cells were harvested and fixed on days 1, 2 and 3 then washed and incubated with propidium iodide and the cell cycle distribution was analysed. (A) Dot plot showing the distribution of non-treated cells. (B) Dot plot showing the gate that was used to select cells for analysis. This gate ensured that doublets were discriminated against such that only single cells were included in the analysis so as not to artificially elevate the proportion of cells in each phase of the cell cycle. (C) Histograms of non-treated, VPA-treated and TSA-treated cells over three days showing a clear cell cycle arrest in the G1 phase. NT, non-treated; VPA, valproic acid; TSA, trichostatin A; M1, G1; M2, S phase; M3, G2; M4, sub-G1 (apoptotic); M5, polyploid.

5.5 Valproic acid and Trichostatin A significantly reduce proliferation in keratinocytes

Initial observations showed that cells treated with all concentrations of VPA (1, 2 and 4 mM) appeared to proliferate at a reduced rate relative to the non-treated cells by D2 and showed no further increase in confluence at D3 (Figure 5.4). Likewise, on D1 a dose-dependent reduction in proliferation was observed with increasing concentrations of TSA. This pattern extended to D2 and was most pronounced in the cells treated with 600 nM TSA (Figure 5.5). The impact of the HDACi on epidermal proliferation was assessed using DAPI to stain cell nuclei and the number of nuclei were quantified using ImageJ software. VPA significantly inhibited proliferation of nHEKs ($p < 0.001$; Figure 5.11A). This was repeated in the N-TERT cell line and 100 nM TSA was included in this analysis.

In agreement with the observations from Figures 5.4 and 5.5 there was no noticeable difference in cell number between non-treated, VPA-treated or TSA-treated N-TERT cells on D1 with the HDACi concentrations used (Figures 5.11B and C). However by D2 a dramatic difference was observed in the number of non-treated cells relative to HDACi-treated cells. N-TERT proliferation was significantly reduced by treatment with 100 nM TSA ($p=0.001$) while 2 mM VPA also reduced proliferation but to a lesser extent ($p<0.01$; Figures 5.11B and C). The difference in cell numbers between TSA- and VPA-treated cells was also statistically significant at D2 ($p<0.05$; Figure 5.11D). By D3 proliferation of N-TERT cells was even more markedly reduced compared to non-treated cells. Both 100 nM TSA and 2 mM VPA reduced epidermal proliferation significantly ($p=0.001$; Figures 5.11B and C). Having established HDACi concentrations that were non-toxic to nHEKs and their effects on keratinocyte proliferation the next priority was to determine the impact of VPA and TSA on the expression of p63.

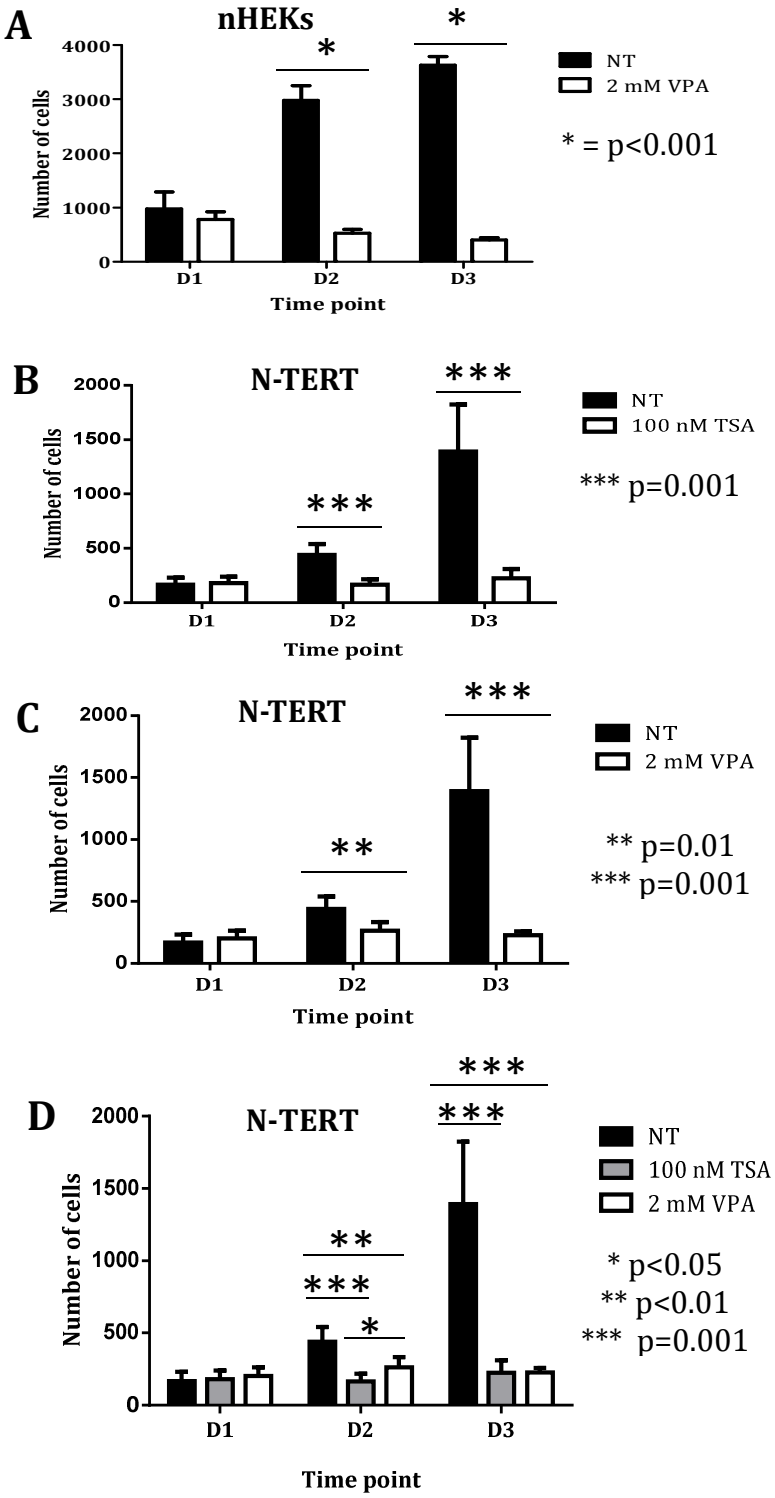

Figure 5.11 Trichostatin A and Valproic acid seem to inhibit epidermal proliferation. nHEKs and N-TERT cells were cultured as described in 4.1. nHEKs were treated with 2 mM VPA (A) whist N-TERT were treated with 100 nM TSA (B) or 2 mM VPA (C). All N-TERT results were displayed together for ease of comparison (D). Cells were fixed at D1, D2 and D3 and stained with DAPI. Fluorescence microscopy was performed and photographs were taken. ImageJ software was used to quantify the nuclei in each image and student's t-tests were performed using MiniTab software. VPA significantly reduces epidermal proliferation with $p<0.001$ in primary human keratinocytes by D2 and D3. In the N-TERT cell line both TSA and VPA significantly reduce proliferation by D2, and by D3 proliferation is inhibited with $p=0.001$. NT, non-treated; TSA, trichostatin A; VPA, valproic acid. n=2.

5.6 Alterations in expression of p63 following treatment with HDACi

Having confirmed that ΔNp63 isoforms are expressed in nHEKs and that the HDACi VPA and TSA inhibit keratinocyte proliferation with very low concurrent cell death the next aim was to characterise the effect of these HDACi on p63 isoform expression in nHEKs. nHEKs were cultured for up to three days in VPA and TSA at a range of concentrations. PCR revealed that non-treated nHEKs express ΔNp63 mRNA up until D5, the latest time point tested (Figure 5.12A) and this is not affected by the addition of 2 mM VPA. At the protein level very different results are seen; p63α is highly expressed at D0, expression decreases moderately by D1 and is dramatically reduced by D2 in non-treated nHEKs with a similar level of expression seen at D5. In contrast, p63α expression remains high in VPA-treated nHEKs (Figure 5.12B).

Intriguingly, treatment with 2 and 5 mM VPA eliminated ΔNp63 mRNA in a previous experiment (Appendix 4), however, cells treated with 2 mM VPA retained p63α protein expression (Appendix 5). The effects of VPA on protein expression were less remarkable in cells treated with 5 mM VPA (Appendix 5). VPA is a weak HDACi so to confirm the ability of VPA to inhibit HDACs, nHEK lysates were probed for acetylated histone H4 (Ac-H4, acetylated on lysines 5, 8, 12 and 16). The high levels of Ac-H4 observed on D1 in cells treated with 2 mM VPA confirmed that this agent was functioning as expected in nHEKs, and the reduction in Ac-H4 expression at D2 and D3 showed that acetylation is lost over time (Figure 5.12C).

N-TERT were cultured for up to three days with or without VPA. PCR revealed that non-treated N-TERT express ΔNp63 mRNA up until D3 (Figure 5.13A) and this is not affected by the addition of 2 mM VPA. This paralleled the data obtained in nHEKs. At the protein level very different results were also seen in N-TERT; there was a modest decrease in p63α expression between D0 and D1. After this a dramatic increase in p63α expression occurred by D2 in non-treated N-TERT and was maintained on D3 (Figure 5.13B). A similar increase in p63α expression was observed on D2 in VPA-treated N-TERT. In contrast with nHEKs, the elevated expression of p63α in VPA-treated N-TERT on D2 is not maintained but returns to a level comparable with that seen on D1 (Figure 5.13B).

The results seen in N-TERT (Figure 5.13B) are reminiscent of those seen in a previous experiment with nHEKs in which cells treated with 2 mM VPA retained p63α protein

expression (Appendix 5). To confirm the ability of VPA to inhibit HDACs in N-TERT cells, lysates were probed for Ac-H4. Interestingly, the lowest levels of Ac-H4 were observed on D1 in cells treated with 2 mM VPA, with increased expression on D2 and D3 confirming the inhibitory action on HDACs in N-TERT cells (Figure 5.13C).

nHEKs treated with 50, 100, 300 and 600 nM TSA all express ΔNp63 at the mRNA level (Figure 5.14A). Western blotting revealed that non-treated nHEKs and cells treated with 50 and 100 nm TSA also express p63α protein (Figure 5.14B). In TSA-treated cells expression appears to reduce over the course of the three days. The reduction in p63α expression is modest in cells treated with 50 nM TSA, whereas it is very pronounced with 100 nM in the Western blot and the densitometry graph (Figure 5.14B). Ac-H4 is induced in nHEKS treated with 100 nM TSA at D1; however 50 nM does not induce any observed acetylation (Figure 5.14C).

p63 is important for preventing senescence in keratinocytes therefore alterations in its expression following treatment with certain HDACi including VPA would be expected to be accompanied by increased replicative senescence (Keyes, Wu et al. 2005).

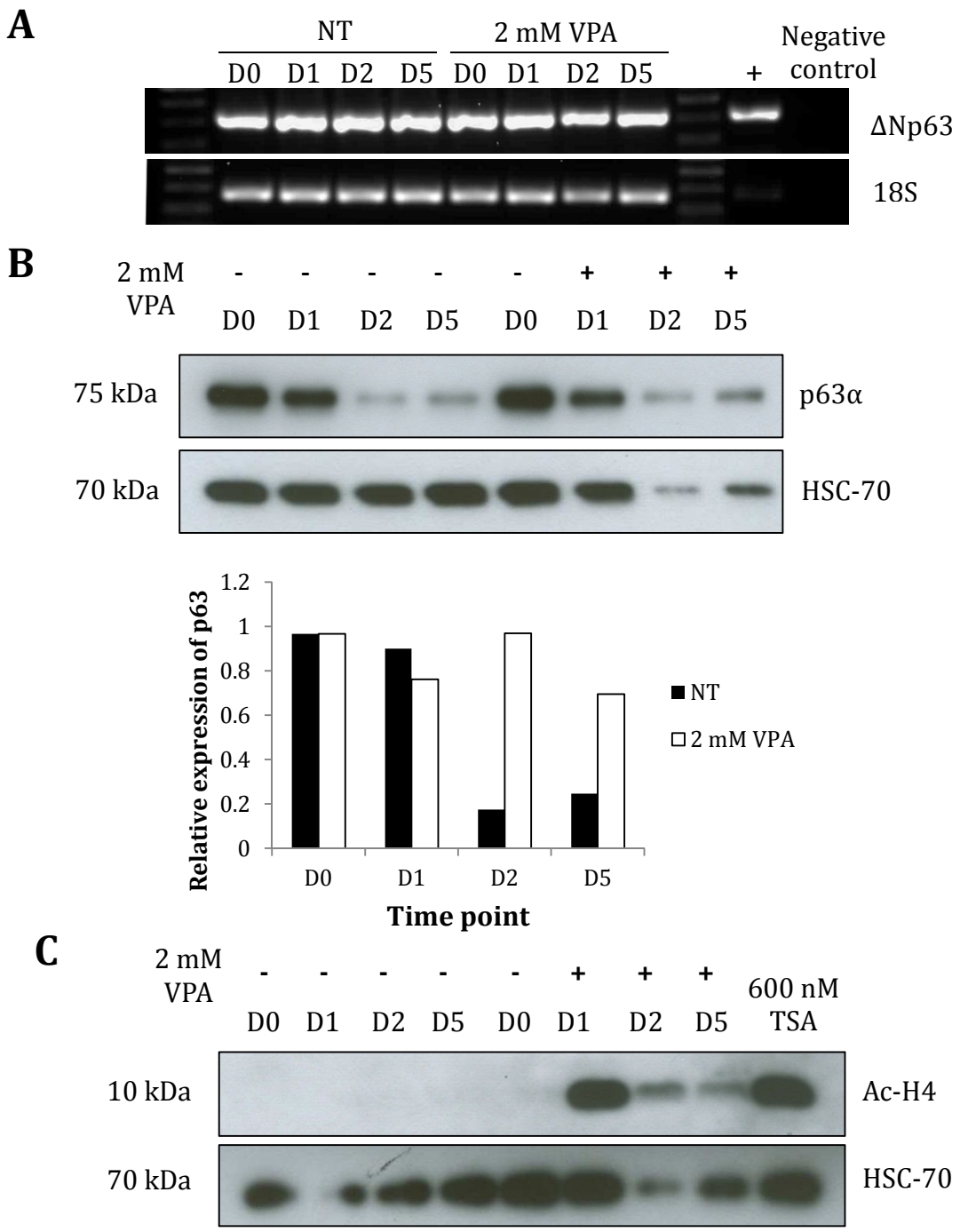

Figure 5.12 ΔNp63 is expressed at the mRNA level in non-treated nHEKs up to day 5 but protein expression is largely reduced by day 2. nHEKs were cultured as described in 4.1. RNA was isolated and 1 µg was synthesised into cDNA. PCR was performed for ΔNp63 isoforms with 18S used as a loading control. The expression of p63α isoforms and acetylated histone H4 (Ac-H4) were assessed by Western blotting. HSC-70 was used as a loading control. (A) PCR revealed the presence of ΔNp63 mRNA at all time points in treated and non-treated cells. (B) ΔNp63 expression is high at D0, decreased slightly by D1 and dramatically decreased by D2 and D5 in non-treated cells but remains high on D2 and D5 in VPA-treated cells. (C) The expression of Ac-H4 confirms the inhibitory action of VPA on HDACs. 5 ng ΔNp63α plasmid was used to confirm that amplicons were the correct size (+). Lysate from nHEKs treated with 600 nM TSA was used as a positive control for Ac-H4 expression. NT, non-treated; VPA valproic acid; Ac-H4, acetylated histone H4; TSA, trichostatin A. n=1.

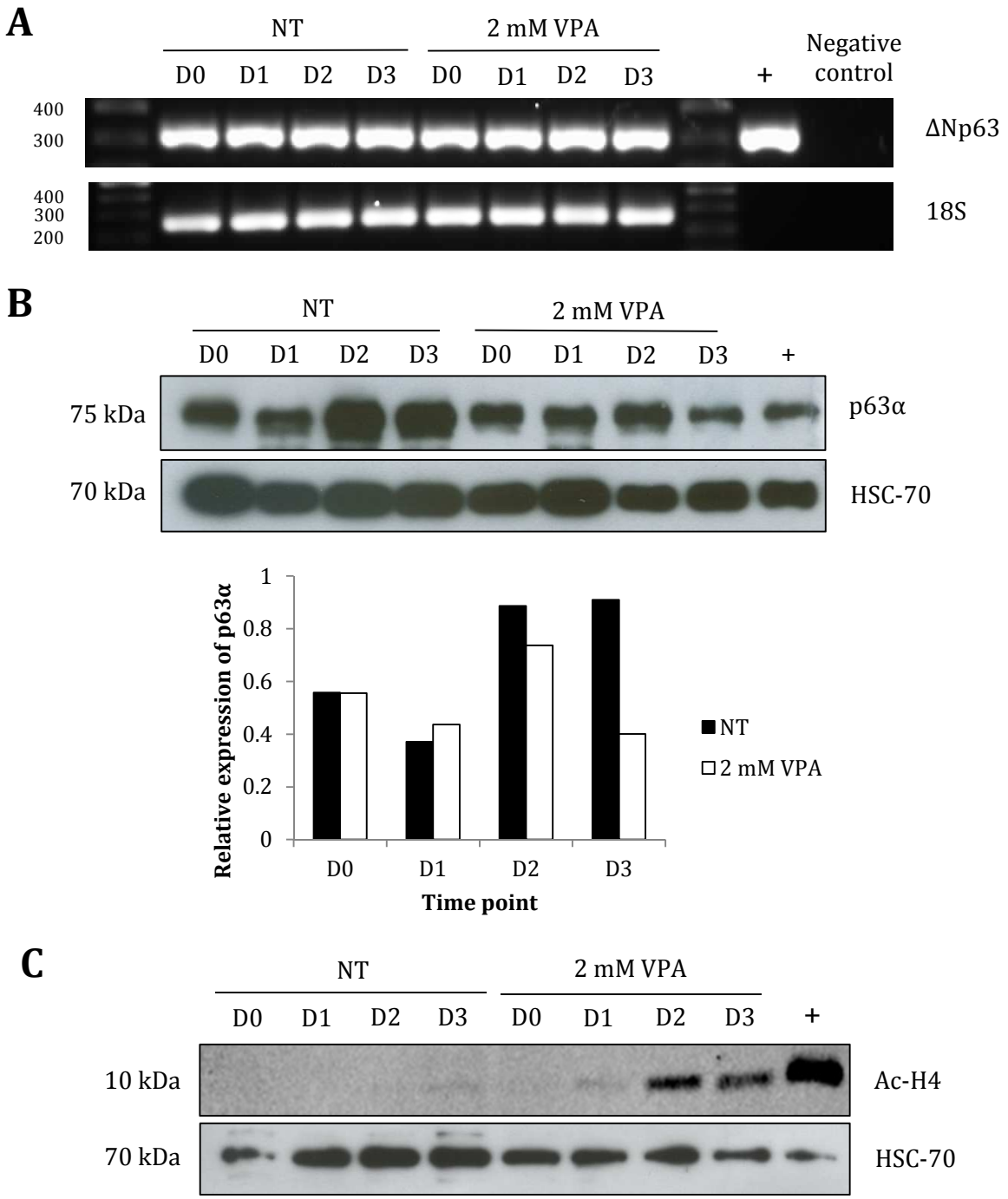

Figure 5.13 ΔNp63 is expressed at the mRNA and protein levels in non-treated N-TERT with elevated protein expression by day 2. N-TERT were cultured as described in 4.1. RNA was isolated and 1 μg was synthesised into cDNA. PCR was performed for ΔNp63 isoforms with 18S used as a loading control. The expression of p63α and acetylated histone H4 (Ac-H4) were assessed by Western blotting. HSC-70 was used as a loading control. (A) PCR revealed the presence of ΔNp63 mRNA at all time points in treated and non-treated cells. (B) ΔNp63 expression decreases slightly between D0 and D1 and dramatically elevates by D2 and D5 in non-treated cells but this increase is only observed on D2 in VPA-treated cells. (C) The expression of Ac-H4 confirms the inhibitory action of VPA on HDACs. 5 ng ΔNp63α plasmid was used to confirm that amplicons were the correct size (+). Lysate from nHEKs treated with 600 nM TSA was used as a positive control for Ac-H4 expression. NT, non-treated; VPA valproic acid; Ac-H4, acetylated histone H4; TSA, trichostatin A. n=2.

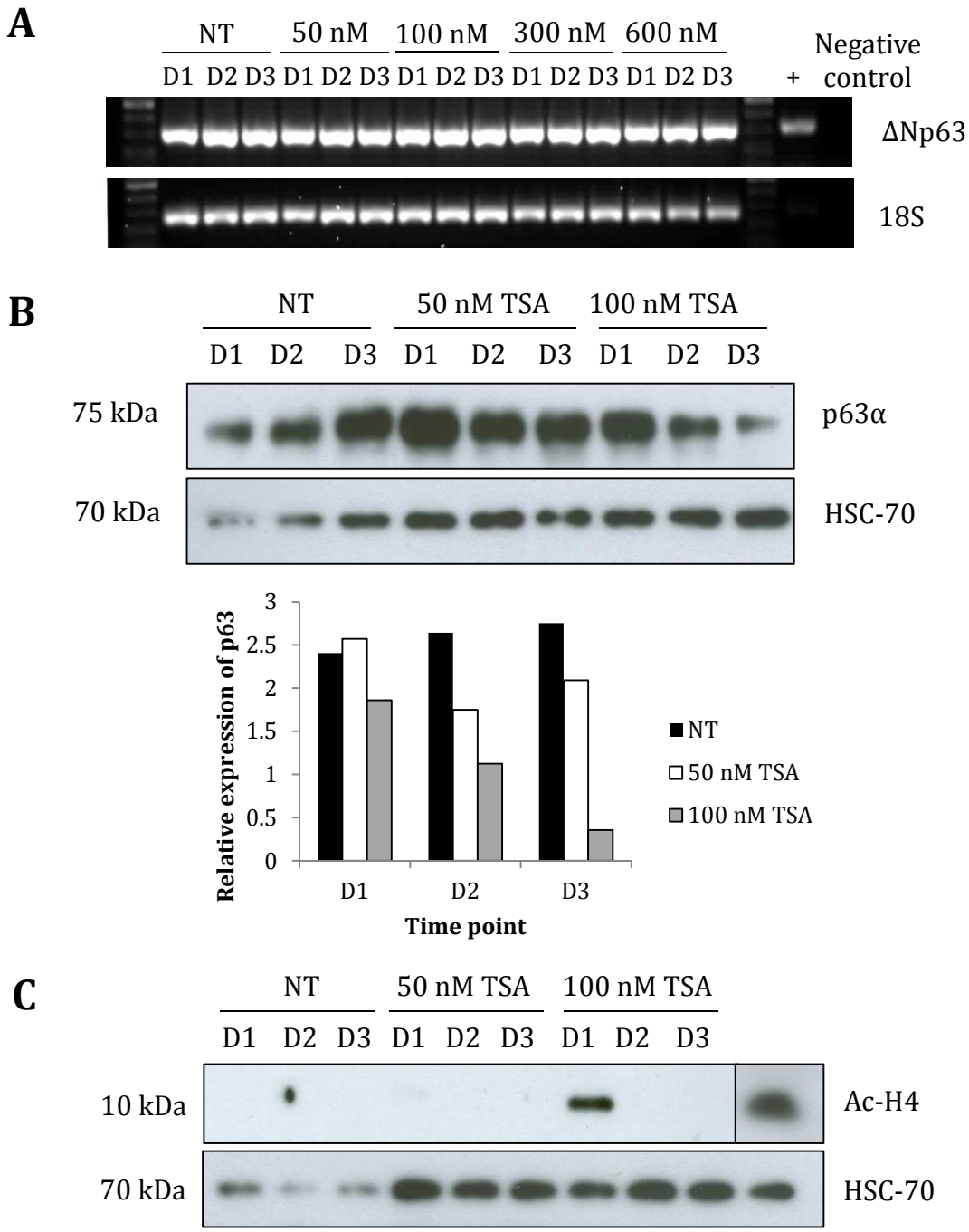

Figure 5.14 ΔNp63 is expressed at both the mRNA and protein levels in TSA-treated and non-treated nHEKs. nHEKs were cultured as described in 4.1.RNA was isolated and 1 µg was synthesised into cDNA. PCR was performed for ΔNp63 isoforms with 18S used as a loading control. The expression of p63α isoforms and acetylated histone H4 (Ac-H4) were assessed by Western blotting. HSC-70 was used as a loading control. (A) PCR revealed the presence of ΔNp63 mRNA at all time points in treated and non-treated cells. (B) ΔNp63 expression appears to increase between D1 and D3 in non-treated cells and decrease slightly over the course of the experiment in TSA-treated cells. (C) The expression of Ac-H4 confirms the inhibitory action of TSA on HDACs. Lysate from nHEKs treated with 600 nM TSA was used as a positive control for Ac-H4 expression. NT, non-treated; Ac-H4, acetylated histone H4; TSA, trichostatin A. n=1

5.7 Valproic acid may inhibit the onset of senescence in nHEKs

Having deduced that p63α protein persists in the presence of VPA but is lost in the presence of TSA, the impact of these HDACis on senescence was investigated next. Senescence was assayed by performing PCR using primers for cyclin dependent kinase inhibitor p16. This is a marker of cellular senescence and its expression at the mRNA or protein levels is indicative of this response.

No p16 expression was observed in nHEKs treated with 2 or 5 mM VPA (Figure 5.15A). In a second experiment PCR was also performed to assess the expression of p16. Non-treated nHEKs at D0 did not express p16, however p16 was detected at D1, D2 and D5 with the highest expression observed at D5 (Figure 5.15B). These differences could possibly be due to a minor variation in culture conditions or the age of the cells when they were first received from Life Technologies. In the VPA-treated nHEKs p16 was only observed at D5 and to a much lesser extent than at the same time point in non-treated nHEKs (Figure 5.15B). PCR showed no noticeable induction of p16 mRNA in TSA-treated nHEKs (Figure 5.15C).

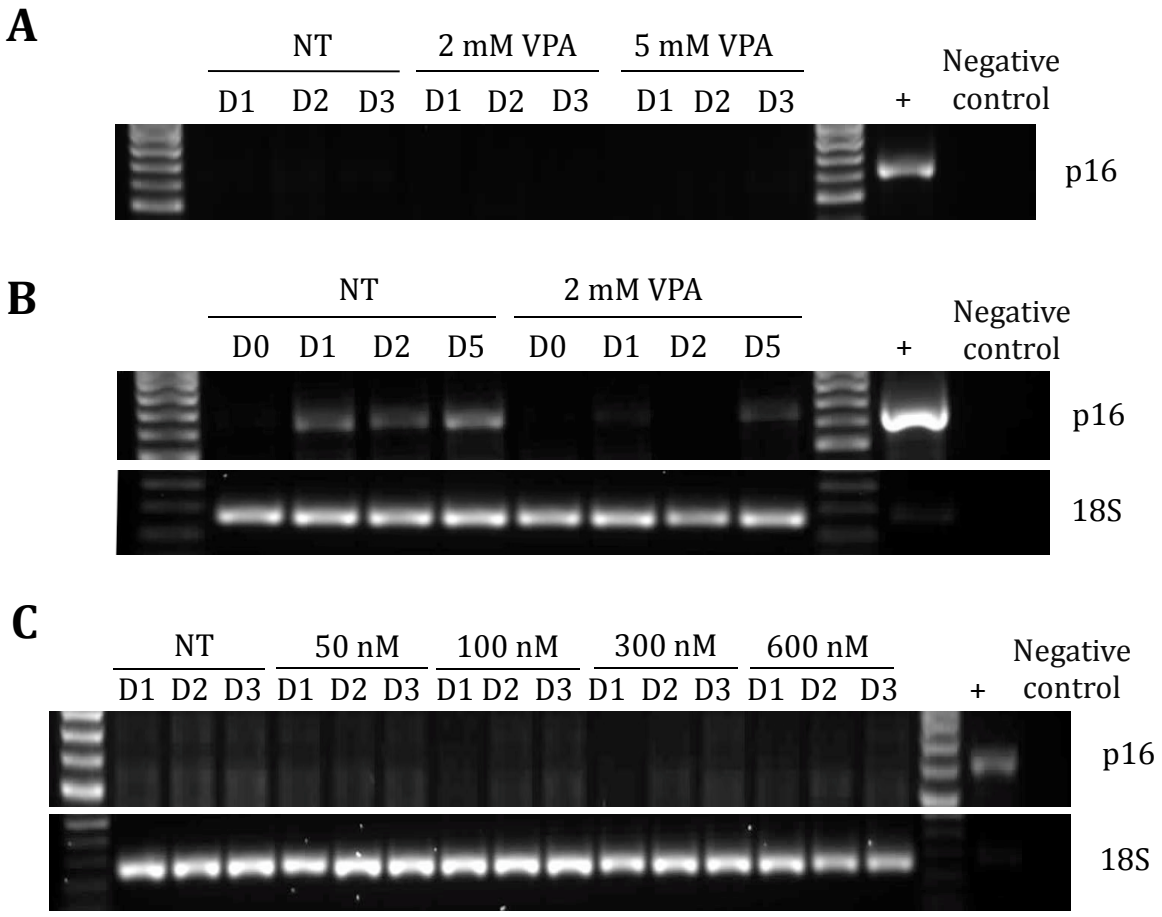

Figure 5.15 Senescence appears delayed in nHEKs by treatment with VPA but seemingly unaffected by TSA. Proliferating nHEKs were treated with 2 or 5 mM VPA or left untreated. In a separate experiment nHEKs were treated with 50, 100, 300 or 600 nM TSA or left untreated. nHEKs were harvested at the time points indicated for RNA isolation. 1 µg RNA was reverse transcribed to cDNA and PCR was performed for p16. (A) No p16 was observed in the nHEKs. (B) A small amount of p16 was detected in both VPA-treated and non-treated cells with the greatest p16 transcript observed at D5 in non-treated nHEKs. (C) PCR for p16 did not reveal any p16 expression in TSA-treated cells. Non-treated nHEKs at passage 6 were used as a positive control for p16 (+). NT, non-treated; VPA, valproic acid; TSA, trichostatin A. VPA n=2; TSA n=1.

5.8 Valproic acid appears to inhibit epidermal differentiation

In the interfollicular epidermis the cells within the basal layer proliferate and when stimulated to, undergo cell cycle arrest and delamination subsequently differentiating and migrating outwards to form the upper layers. This procedure can be mimicked in vitro by culturing cells as a monolayer and increasing the calcium concentration of the medium to 1.2 mM to stimulate nHEKs to differentiate. Complete differentiation takes 9 days in a cell culture environment therefore the two least toxic HDAC inhibitors (VPA and TSA) were chosen to test the effect of HDAC inhibition on keratinocyte differentiation.

100 nM TSA and 2 mM VPA were the concentrations chosen to treat cells because these concentrations were sufficient to induce the expression of acetylated histone H4 while being non-toxic to nHEKs. Furthermore the degree of acetylation induced by 2 mM VPA is similar to that induced by 100 nM TSA in several cell lines (Goettlicher, Minucci et al. 2001). To induce differentiation, cells were pre-treated for 6 h with either 100 nM TSA or 2 mM VPA then the calcium concentration was raised to 1.2 mM and cells were cultured and harvested at various intervals (Figure 4.1). 6 h was the chosen time for pre-treatment as previously published research suggests that the acetylation induced by TSA only lasts for up to 8 h in some cell types (Gurvich, Tsygankova et al. 2004).

Loricrin is expressed in the outermost cornified cells of the epidermis and serves as a marker of late epidermal differentiation. Under normal conditions its expression increases throughout differentiation (Figure 5.16A). VPA-treated cells failed to upregulate loricrin at both the mRNA and the protein levels, having a maximal induction of 4.2-fold at D3 (Figure 5.16A, left and B). Expression of keratin 1, a marker of the spinous layer, was upregulated over the seven days of differentiation in non-treated cells, however VPA-treated nHEKs also failed to upregulate expression of this suprabasal protein to the same extent in this instance (Figure 5.16C).

In contrast, cells treated with TSA followed the normal pattern of differentiation albeit at slightly reduced magnitude, with a 26–fold induction of loricrin mRNA compared to the 31.8-fold induction in non-treated cells at D7 (Figure 5.16A, right). Loricrin protein expression was also slightly lower than the non-treated cells at all time points in this experiment (Figure 5.16B).

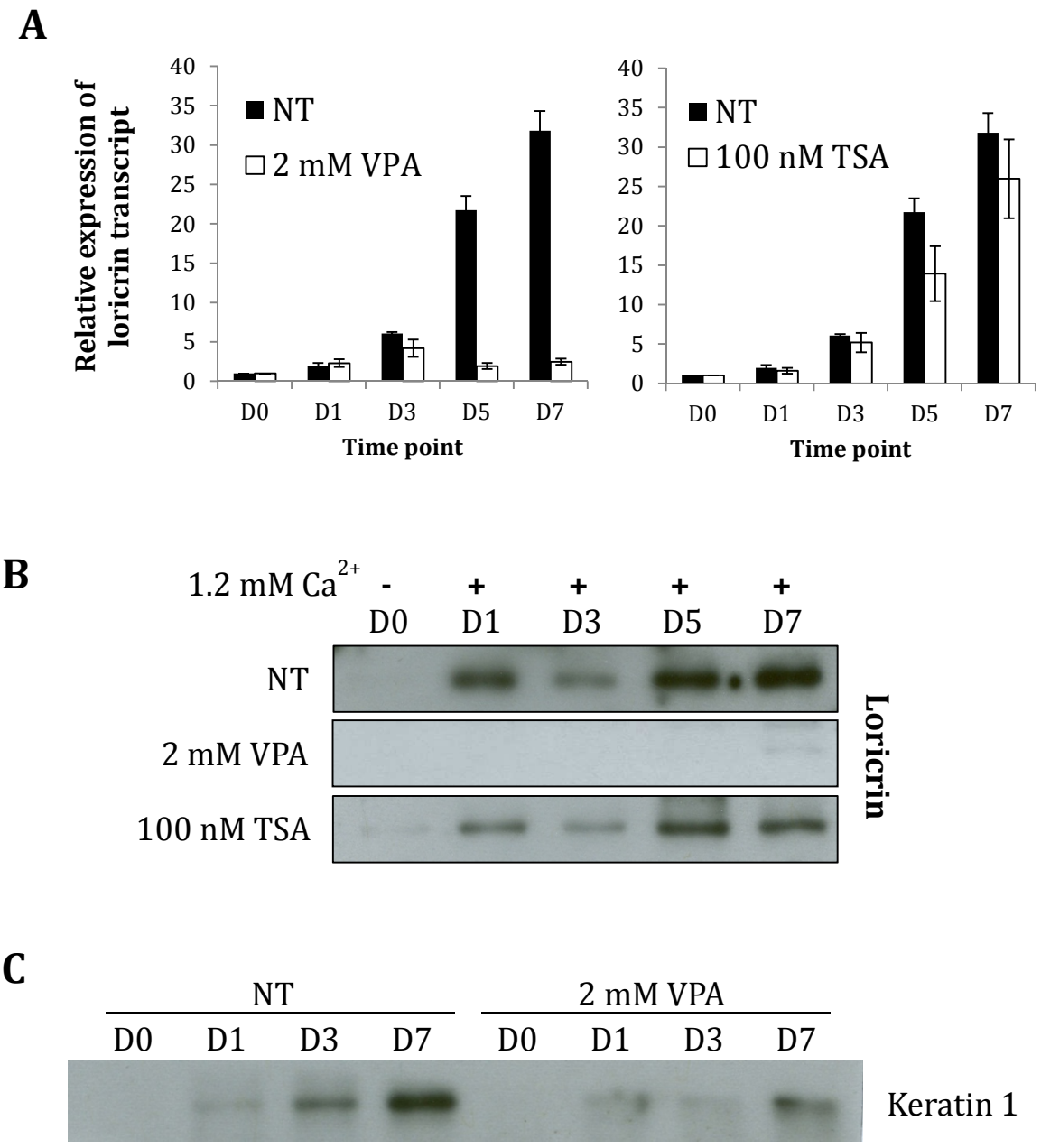

Figure 5.16 Treatment of nHEK with valproic acid appears to inhibit differentiation. nHEKs were pre-treated for 6 h with 100 nM TSA, 2 mM VPA or left untreated. After this time the calcium concentration was raised to 1.2 mM by the addition of calcium chloride and cells were harvested at the time points indicated to collect RNA (A) or protein (B). (A) 1 µg RNA was isolated and used to synthesise cDNA which was used in real-time PCR using TaqMan primers for loricrin. In non-treated cells loricrin expression increases throughout differentiation. Pre-treatment with VPA causes loricrin levels to remain low (left). Pre-treatment with TSA (right) causes a reduction in loricrin expression relative to the control, however expression continues to increase over time. (B) Expression of loricrin protein increases during the course of the experiment in non-treated cells and those treated with 100 nM TSA, whereas it is absent in cells treated with 2 mM VPA.(C) Western blotting for the suprabasal marker keratin 1 showed a gradual increase in expression in non-treated cells but not in VPA-treated nHEKs. n=1.

5.9 Valproic acid may inhibit differentiation via affecting Notch signalling

For epidermal differentiation to occur basal cells must detach from the basal membrane and exit the cell cycle. Notch signalling has been implicated in regulating the commitment switch during epidermal differentiation. In order to determine whether Notch signalling is involved in the apparent failure of VPA-treated keratinocytes to execute a programme of terminal differentiation its expression at the earliest time points was assessed by Western blotting.

The active component of Notch is the intracellular domain (NICD). There is a dramatic reduction in NICD protein expression in VPA-treated cells between D0 and D1 compared to non-treated cells which maintain a similar level of expression at both time points (Figure 5.17A). Furthermore the decrease in Notch1 at the mRNA level is much greater in VPA-treated cells than non-treated; on D0 Notch1 has reduced to 0.44 relative to non-treated (1) with a further reduction at D1 to 0.23-fold relative to 0.37 (Figure 5.17B).

Cell cycle arrest must occur in order for differentiation to proceed. Therefore to assess the biological effect of Notch downregulation by VPA expression of the key cell cycle regulator p21 was assessed. When p21 expression was determined using qPCR its expression was slightly higher in VPA-treated nHEK at D0 and D1, however it failed to increase much more. After this time, expression was considerably higher in the non-treated cells with a 6.2-fold induction at D7 compared with the 3.2-fold induction observed in VPA-treated cells indicating that treatment impaired cell cycle arrest (Figure 5.17C).

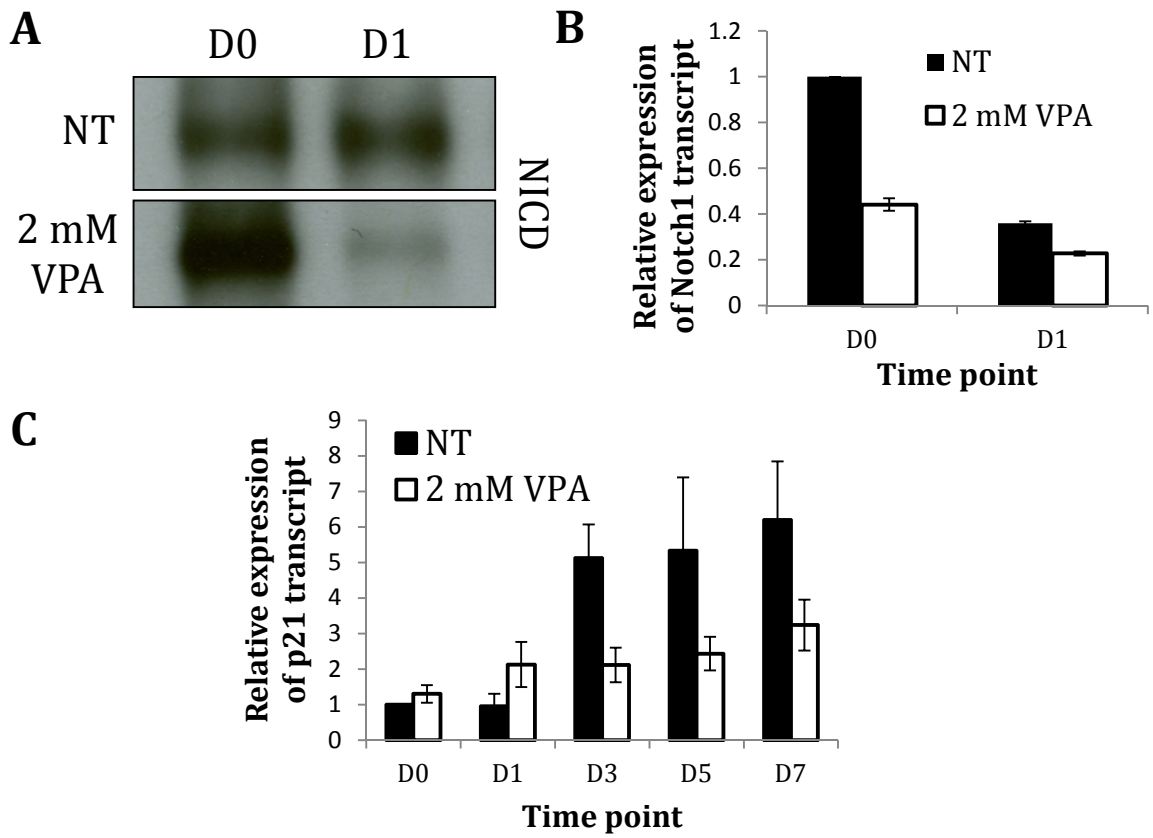

Figure 5.17 Valproic acid causes a reduction in expression of Notch1 and p21. nHEKs were pre-treated for 6 h with 2 mM VPA or left untreated. After this time the calcium concentration was raised to 1.2 mM by the addition of calcium chloride and cells were harvested at the time points indicated. Western blotting was performed for the Notch intracellular domain (NICD). Additionally 1 µg RNA was isolated and used to synthesise cDNA. 2 µl 1:5 cDNA was used in qPCR using TaqMan primers for Notch1 and p21. (A) Expression of NICD decreased between D0 and D1 in VPA-treated cells, however remained high in non-treated cells. (B) Expression of Notch1 mRNA decreased between D0 and D1 in the non-treated cells, however the VPA-induced decrease in Notch1 was far greater. (C) Expression of p21 is higher in VPA-treated cells at D0 and D1 and then consistently lower than in non-treated cells from D3 onwards. n=1

5.10 Valproic acid appears to alter expression of Notch target genes

After observing that treatment with VPA was followed by a reduction in Notch protein the expression of several downstream targets was investigated. Hes1 and Hey1 are both basic helix-loop-helix transcription factors and are the key effectors of Notch signalling therefore expression of these markers was assessed by qPCR. Hes1 was upregulated 1.8-fold by D1 in non-treated nHEKs, however expression was reduced at both D0 and D1 in VPA-treated cells (Figure 5.18, left). In contrast Hey1, another downstream target of Notch1, was dramatically elevated with a 31.6-fold induction in VPA-treated cells that persisted until D1 albeit at the lower magnitude of a 15.4-fold induction (Figure 5.18, middle). The Notch co-activator Mastermind-like 1 (MAML1) was also considerably upregulated in VPA-treated nHEKs with a 7.8- fold induction at D1 (Figure 5.18, right). Like Hey1 the expression of MAML1 was still noticeably elevated at D1 in VPA-treated cells relative to the non-treated condition, however induction was reduced to 2.6-fold. The vast induction in Hey1 and MAML1 but not Hes1 suggests that VPA may be exerting its effects via non-canonical Notch signalling, possibly bypassing Notch entirely.

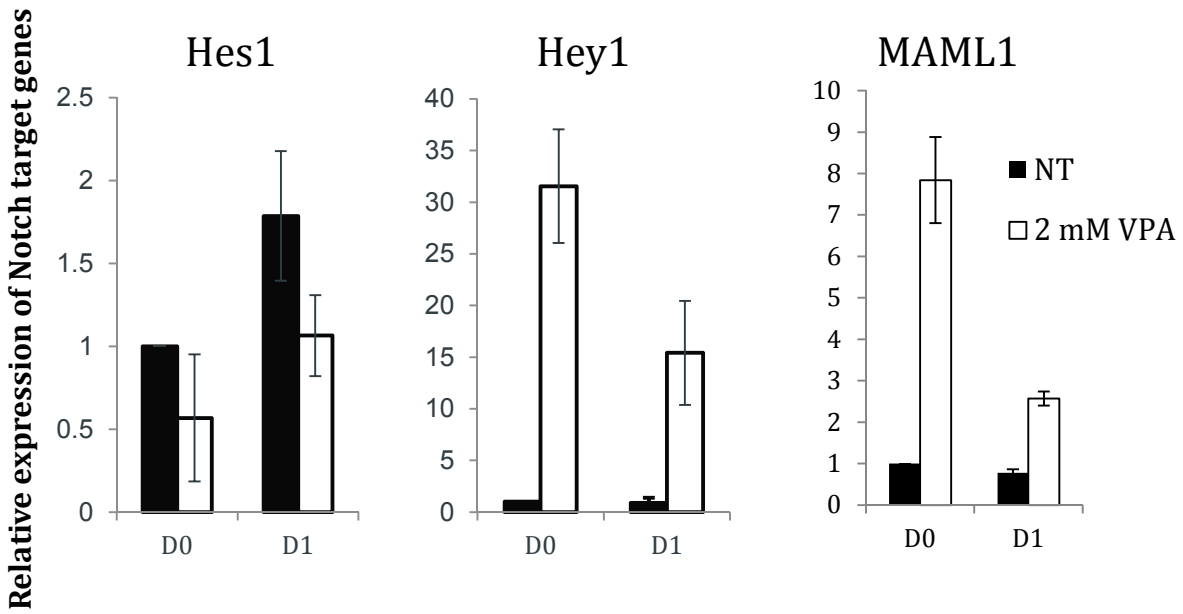

Figure 5.18 Expression of Notch target genes Hes1 and Hey is altered, as is expression of the co-activator Mastermind-like 1. nHEKs were pre-treated for 6 h with 2 mM VPA or left untreated. After this time the calcium concentration was raised to 1.2 mM by the addition of calcium chloride and cells were harvested at the time points indicated. 1 µg RNA was isolated and used to synthesise cDNA. 2 µl 1:5 cDNA was used in qPCR using TaqMan primers for Hes1, Hey1 and Mastermind-like 1 (MAML1). Expression of Hes1 increased at D1 in all cells relative to D0, however expression of Hes1 much lower in VPA-treated cells than in non-treated cells at both D0 and D1. Hey1 expression, on the other hand, was markedly induced at D0 relative to non-treated cells, and remained elevated at D1 although to a lesser extent. MAML1 expression was also noticeably induced at D0 in VPA-treated cells and expression remained higher at D1 than in non-treated nHEKs. n=1

In summary the results of this research indicate that the histone deacetylase inhibitor valproic acid has a considerable impact on both keratinocyte proliferation and differentiation via altering the expression of several genes responsible for specifying keratinocyte cell fate. The genes affected include the p53-family member p63, Notch1, its co-activator Mastermind-like 1 and a number of Notch downstream targets, in particular Hey1. Although preliminary, the data presented here suggest several possible mechanisms for the effects observed in VPA-treated keratinocytes. Canonical Notch signalling cannot be excluded, however non-canonical Notch signalling is the most likely primary mediator of VPA based on the vast induction of the Notch co-activator MAML1 and the Notch downstream target Hey1 in contrast to much more modest alterations in Notch expression.

6. Discussion

One of the initial objectives of this investigation was to characterise which p63 isoforms were present in primary human keratinocytes. ΔNp63 isoforms were highly expressed in the nHEKs tested whereas TAp63 isoforms were absent (Figure 5.1A). This result concurs with data showing that ΔNp63 isoforms are the predominant ones expressed in the epidermis (LeBoeuf, Terrell et al. 2010). PCRs analysis using reverse primers specific to the C-terminal regions of the p63α, β and γ isoforms confirmed the expression of all three isoforms allowing the conclusion that nHEKs express ΔNp63α, β and γ (Figure 5.1B). ΔNp63α and β isoform expression was expected as previous research denotes that these isoforms in particular are essential for correct skin and limb development, however the role of the p63γ isoforms remains unclear (Wolff, Talos et al. 2009).

After confirming which p63 isoforms were present in nHEKs the next aim was to confirm which histone deacetylase enzymes were present in nHEKs and two cell lines: HaCaT and N-TERT. The primary focus was to confirm the expression of HDAC1 and 2 as these have previously been shown to interact with p63 in the epidermis and in SCC. nHEK, HaCaT and N-TERT whole cell lysates were assayed for HDAC1 and 2 via Western blotting. HeLa whole cell lysate was also used as a positive control for HDAC expression. Figure 5.2 illustrates that the expression of HDAC1 was very similar across the cells tested whereas expression of HDAC2 varied substantially between primary cells and the two cell lines.

The investigation was extended to the remaining class I HDACs and the class II HDACs. The class I HDACs 1, 2 and 3 were expressed in nHEKs, as were the class II HDACs 4 and 6 (Figure 5.1B). Expression of HDAC8 was not observed. This was unsurprising as it has previously been described as the least abundant HDAC in most other cell types, requiring overexpression for its detection in the nucleus (Van den Wyngaert, de Vries et al. 2000). Of the lysates tested, HDACs 1 and 2 had the lowest expression in nHEKs. The expression level was, however, most similar to that observed in HaCaT cells (Figure 5.2). Interestingly, HDACs 3, 4 and 6 were expressed at similar levels in nHEKs and HaCaT cells (Figure 5.3). However, because HaCaT cells possess a mutant form of the transcription factor *p53* only nHEKs were employed for subsequent experiments to eliminate the possibility of the mutant *p53* impacting the expression of *p63* isoforms.

The impact of a panel of HDAC inhibitors on nHEKs was investigated by treating them with varied concentrations of each drug. Cell death was first assessed using phase contrast microscopy. nHEKs treated with 1, 2 and 4 mM VPA for up to three days showed no evidence of increased cell death when observed using phase contrast microscopy (Figure 5.4). This result was unexpected as VPA has previously been shown to induce apoptosis via the intrinsic pathway which includes the activation of caspase-3 (Yagi, Fushida et al. 2010). To further investigate any impact of VPA on cell death, flow cytometry was performed using N-TERT cells to quantify the percentage of cells which fall within the sub-G_1 fraction (degraded DNA) using hypotonic propidium iodide staining. The maximum cell death observed in cells treated with 2 mM VPA over 3 days was 3% (Figure 5.8A) confirming its low cytotoxicity.

The proliferation rate of VPA-treated nHEKs appeared to be reduced compared with non-treated cells (Figure 5.4). Previous studies have reported that VPA has shown anti-proliferative effects. Specifically, it induced cell cycle arrest in G_1 and was associated with increased expression of *p21* (Catalano, Fortunati et al. 2005; Yagi, Fushida et al. 2010). The cell cycle profile of N-TERT cells treated with 2 mM VPA showed an arrest in the G_1 phase (Figure 5.10C) with a modest increase in the proportion of cells in G_1 over a three day treatment period (Figure 5.9B). The proportion of N-TERT cells in S phase and G_2 decreased between D1 and D3, reflecting the increase in G_1 (Figure 5.9C and D), however the proportion of cells in G_1 may have been artificially elevated due to over-confluence and as the data come from n=1 further repeats would be required to validate the observed effects.

The impact of VPA on keratinocyte proliferation was investigated using DAPI staining and ImageJ software to quantify the number of nuclei. VPA was indeed found to significantly inhibit nHEK proliferation $p < 0.001$ (Figure 5.11A). When repeated with N-TERT cells very similar results were seen. There was no difference in cell numbers on D1 but by D2 proliferation was reduced significantly in VPA-treated cells ($p=0.01$) and this difference extended further by D3 with significance determined as $p=0.001$ (Figure 11.B). To further probe the mechanism of action of VPA and determine whether VPA induces cell cycle arrest in the G_1 phase or promotes the exit of keratinocytes from the cell cycle into a quiescent G_0 state, flow cytometry could be performed using acridine

orange as quiescent cells exhibit higher levels of fluorescence with this dye than cycling cells (Darzynkiewicz, Traganos et al. 1979).

Lee *et al*. state that VPA stimulated cell proliferation during wound healing (determined by Ki67 staining) and also suppressed apoptosis, as determined by TUNEL staining (Lee, Zahoor et al. 2012). Their work contradicts this body of research in terms of proliferation, however as both Ki67 and DAPI stain cell nuclei the difference in methodology is unlikely to be the cause of this discrepancy. Their work concurs with the lack of apoptosis observed in nHEKs and N-TERT cells following VPA treatment. Their data is based on healing wounds in mice treated with 500 mM VPA which is a substantially higher concentration than was used in this research. Additionally, the data presented here is based on human cells so these differences are likely either due to differences between human and murine cells, to the much higher treatment dose or to the presence of additional cytokines and growth factor stimuli *in vivo*.

Lee *et al*. also suggested that VPA increases the motility of keratinocytes, however their work was based on HaCaT, a keratinocyte cell line. This and the aforementioned considerations must be factored in, however investigating the motility of nHEKs by using transwell assays could be an appealing future venture to determine how topical treatments may impact upon the interfollicular epidermis.

As observed with VPA, TSA was well tolerated by the nHEKs tested and also seemed to inhibit proliferation (Figure 5.5). The anti-proliferative effect of TSA was more readily observed, however, with the number of TSA-treated cells failing to increase during the course of the experiment despite cell death remaining at low levels and comparable to the non-treated cells. This anti-proliferative effect appeared dose-dependent, becoming noticeable on D1 (Figure 5.5). This was in accordance with a previous report stating that TSA also inhibits growth of HeLa cells in a time- and dose-dependent manner (Xu, Wang et al. 2006).

High doses of TSA such as 600 nM were highly toxic by D3 as judged by the lack of viable cells at this time point, therefore is not a suitable treatment concentration (Figure 5.5). This is likely due to the high binding affinity of TSA to HDACs. This results in a longer-lasting interaction, with TSA taking a relatively long time to dissociate. During

the work leading to the development of SAHA (vorinostat) similar toxicity was observed with the analogues possessing the highest binding affinity (Marks and Breslow 2007).

As previously stated, the higher concentrations of TSA were deemed cytotoxic. 50 nM TSA did not induce acetylation in nHEKs (Figure 5.8) therefore 100 nM was the concentration chosen to investigate further. TSA has been described to reduce the proportion of cells in S phase and increase the proportions in G_0/G_1 and G_2/M phases (Xu, Wang et al. 2006). The initial focus of quantifying the extent of cell death induced by 100 nM TSA was carried out as part of cell cycle analysis using flow cytometry.

The low cytotoxicity of 100 nM TSA was confirmed by 4.23% maximum cell death in N-TERT cells (Figure 5.9A). G_1 arrest was observed in the cell cycle profiles of TSA-treated N-TERT cells (Figure 5.10C). The proportions of TSA-treated cells in G_1 increased between D1 and D3 (Figure 5.9B) while the proportion in S phase decreased (Figure 5.8C), in agreement with Xu *et al*. On D2 the proportion of cells in G_1 was lower than D1 while in S phase was higher (Figures 5.9B and C). This was likely due to minor variation as these data were obtained from n=1 and the data from D1 and D3 follow the pattern we would expect to see. In contrast to Xu *et al*. the proportion of cells in G_2 decreased over the course of the experiment (Figure 5.9D), as expected given that the majority of cells arrested in G_1. However, as previously stated, the high proportion of cells in G_1 may be due to over confluence and had the cells been at a lower confluence we may also have seen an increase in the proportion of TSA-treated cells in G_2. Overall, the flow cytometry data suggest that the reduction in cell number observed in Figure 5.5 is not due to a high degree of cell death but further work would be required to confirm this.

Next, cell proliferation effects with TSA were assessed using N-TERT cells in the same way as VPA. The same result was seen on D1 with no difference in cell number between TSA-treated and non-treated N-TERT cells but a large difference becoming apparent by D2 ($p=0.001$) and proliferation being further reduced by D3 also with significance determined as $p=0.001$ (Figure 5.11C). The difference in cell numbers between TSA- and VPA-treated cells was also statistically significant at D2 with $p<0.05$ (Figure 5.11D). These data confirm the anti-proliferative effect of TSA and suggest it is more potent than VPA in this respect.

LBH589-treated cells also seemed to exhibit a dose-dependent decrease in number by D1. All four treatment concentrations (50, 100, 200 and 500 nM LBH589) resulted in cell death even at this stage which increased over the course of this single experiment (Figure 5.6). LBH589 is a hydroxamic acid like TSA and also a pan-HDACi. Both HDACi have IC_{50} values in the nanomolar range so the difference in toxicity between these two inhibitors was unexpected (Beckers, Burkhardt et al. 2007). It is likely the greater toxicity of LBH589 is due to it being more selective than TSA. Research has shown that some HDACi exhibit selectivity for different class I HDACs, therefore if LBH589 is more selective than TSA for HDAC or HDAC2 this could explain the increased toxicity (Hu, Dul et al. 2003). Ideally, this experiment would have been repeated to confirm the relatively higher cytotoxicity of LBH589 compared with TSA, however time and availability of resources did not permit this.

FK228 is a bicyclic peptide and was the least well-tolerated of the four HDACi, clearly demonstrated by the striking increase in cell death on all three days relative to the non-treated cells (Figure 5.7). Furthermore, phase contrast microscopy showed that by D3 virtually all FK228-treated cells were dead or dying, irrespective of the concentration used while 500 nM FK228 resulted in near-complete cell death by D2 (Figure 5.7). This remarkable cytotoxicity can potentially be attributed to the relative selectivity of FK228 for HDACs 1 and 2, the induction of pro-apoptotic proteins such as Bax and the downregulation of anti-apoptotic proteins such as Bcl-2 observed in other cell types (Dickinson and Prince 2012).

Subsequently studies were performed using VPA and TSA to assess their effects on p63 expression. The studies involving VPA had very conflicting results. One experiment showed that treatment of nHEKs with 2 and 5 mM VPA eliminated p63 mRNA (Appendix 4), whereas the second experiment revealed that non-treated nHEKs express ΔNp63 mRNA up until D5, the latest time point tested and the addition of 2 mM VPA did not have any impact on its expression (Figure 5.12A). The data from the second set of experiments in nHEKs is supported by the N-TERT data. Non-treated and VPA-treated N-TERT cells also expressed ΔNp63 mRNA up until the latest time point tested, D3 (Figure 5.13A).

Variation also exists within the protein data. ΔNp63 mRNA was eliminated by VPA-treatment in nHEKs but p63α protein was still present at D1, D2 and D3 albeit a reduction in expression was observed by D3 (Appendix 5). In line with this data, the results of the following experiment showed p63α protein was highly expressed at D0 and expression decreased considerably by D2 with a similar level of expression seen at D5 in non-treated nHEKs (Figure 5.12B). Although the reduction in p63α protein expression in Figure 5.12B is greater and occurs sooner than in Appendix 5, a reduction in expression over time is apparent in both cases. In nHEKs treated with 2 mM VPA expression of p63α protein is retained in both cases (Figure 5.12B and Appendix 5).

In non-treated N-TERT cells there was a modest decrease in p63α expression between D0 and D1 (Figure 5.13B), consistent with the decrease in expression over time observed in nHEKs. However, expression of p63α actually increased at the later time points in non-treated N-TERT cells (Figure 5.13B), conflicting with the nHEK data. The expression profiles of p63α protein were very similar in both VPA-treated nHEKs and N-TERT cells; expression modestly decreased between D0 and D1, increased by D2 and dropped again at the later time points (Figures 5.12B and 5.13B). These results are also reminiscent of the first experiment in nHEKs (Appendix 5) in which cells treated with 2 mM VPA retained p63α protein expression. It is difficult to make any firm conclusions from this as the data are rather conflicting. Additionally, results are representative of n=1 so the observed increases in p63α protein expression cannot decisively be attributed to a particular treatment and as these cells are very sensitive to changes, even changing the media may have had an impact on p63α protein expression.

In TSA-treated cells ΔNp63 mRNA was expressed on D1, D2 and D3 in all conditions (Figure 5.14A). p63α protein was also expressed at all time points, however treatment with 100 nM TSA reduced p63α protein expression over the course of the three days (Figure 5.14B). Treatment with 50 nM TSA had little impact on p63α; a modest reduction in expression was observed (Figure 5.14B). The results of TSA treatment come from n=1, therefore in order to obtain more reliable data these experiments would need to be repeated with new cultures of nHEKs. This was planned, however, could not take place due to external circumstances; specifically a new group moving into the tissue culture facility and numerous subsequent infections followed by moving to a different tissue culture facility.

In non-treated nHEKs p63α protein is postulated to have a half-life of around 24 hours (personal communication, B Sayan). ΔNp63α protein is considerably more kinetically stable than its β and γ isoforms, and also much more stable than its paralog p53 (Brandt, Kaar et al. 2012). These data, although preliminary in nature, suggest that the stability of p63α protein may be altered by post-translational modifications. VPA appeared to stabilise p63α protein whilst TSA treatment resulted in accelerated degradation. Treatment with TSA and VPA are both reported to increase endogenous p53 acetylation and based on the high degree of homology between p53 and p63 it is possible that p63 may also become acetylated in the presence of histone deacetylase inhibitors (Phiel, Zhang et al. 2001). To investigate this possibility immunoprecipitation was performed on VPA-treated nHEKs to look for acetylated p63 protein but to little avail. Future work exploring the clinical potential of VPA could explore this in more detail as the broad-spectrum actions of HDACis are still being uncovered.

To confirm that VPA and TSA were active and inhibiting HDACs, nHEK and N-TERT lysates were probed for acetylated histone H4 (Ac-H4, acetylated on lysines 5, 8, 12 and 16). The very high levels of Ac-H4 observed on D1 in cells treated with 2 mM VPA (Figure 5.12C) and the induction of Ac-H4 on D1 by 100 nM TSA-treated cells (Figure 5.14C) confirmed that these agents were functioning as expected in nHEKs, and the reduction in Ac-H4 expression showed that acetylation was transient. Unusually, the induction of Ac-H4 was at its lowest on D1 in VPA-treated N-TERT, increasing by D2 (Figure 5.13C). Further Western blots would need to be performed to determine if this was a true reflection of VPA treatment in these cells. Despite this unexpected expression pattern, the presence of Ac-H4 confirms the inhibitory action of VPA on HDACs in N-TERT cells.

p63 is important for preventing senescence in keratinocytes (Keyes, Wu et al. 2005) therefore the data suggesting that p63α protein persists in the presence of VPA but is lost in the presence of TSA had important implications for cellular senescence. As p63α protein appears stabilised in the presence of VPA (Figure 5.12B) it would follow that senescence is inhibited. The cyclin dependent kinase inhibitor p16 is a marker of cellular senescence. During the initial investigation PCR for p16 revealed no expression of this marker in nHEKs treated with 2 or 5 mM VPA (Figure 5.15A).

A further investigation showed that non-treated nHEKs did not express p16 at D0, however p16 was detected at D1, D2 and D5 with the highest expression observed at D5 (Figure 5.15B) indicating an increase in cellular senescence. In VPA-treated nHEKs p16 was only observed on D5 and to a much lesser extent than at the same time point in non-treated nHEKs (Figure 5.15C), consistent with VPA inhibiting the onset of senescence in nHEKs, at least when using *p16* as a marker. The link may not be as straightforward as this, however. Data and other studies previously discussed suggested that VPA induces cell cycle arrest in nHEKs, so it may simply be that nHEKs in a state of arrest upregulate other markers such as *p21* but not *p16* as they have not entered a senescent state. Due to the limited data set and the inconsistencies mentioned, it is not possible to make a firm conclusion regarding the impact of VPA on cellular senescence in nHEKs.

PCR showed no noticeable induction of *p16* mRNA in TSA-treated nHEKs (Figure 5.15C) despite decreased expression of p63α protein in TSA-treated nHEKs (Figure 5.14B). These data suggest that TSA does not impact on senescence in nHEKs, however are only preliminary.

Following on from the data obtained on proliferating keratinocytes the investigation was extended to encompass the effects of HDACi on differentiation. In these studies cells were pre-treated for 6 h with either 100 nM TSA or 2 mM VPA then the calcium concentration was raised to 1.2 mM to induce epidermal differentiation and cells were cultured and harvested at various intervals. 6 h was the chosen time for pre-treatment as research suggests that the acetylation induced by TSA only lasts for up to 8 h in some cell types (Gurvich, Tsygankova et al. 2004). 100 nM TSA and 2 mM VPA were chosen because these induced expression of acetylated histone H4 at concentrations that were non-toxic to nHEKs.

Expression of loricrin mRNA in non-treated nHEKs increased over the course of 7 days in non-treated cells in accordance with it being a marker of late epidermal differentiation. VPA treatment resulted in a near-complete failure of cells to upregulate loricrin at either the mRNA or protein levels (Figures 5.16A, left and C). Furthermore VPA-treated cells failed to upregulate expression of keratin 1, a marker of the spinous layer lending further support to the notion that VPA inhibits epidermal differentiation

because as keratinocytes mature they downregulate expression of K5 and 14 and upregulate expression of K1 and K10 but K1 cannot be detected in VPA-treated cells (Figure 5.16C). The increase in loricrin expression in TSA-treated cells was of slightly lower magnitude than in non-treated cells (26-fold compared with 31.8-fold at D7 and less loricrin protein throughout), implying that TSA does not exert a great deal of effect on epidermal differentiation (Figures 5.16A, right and B). Whilst these results have important implications, the data are from isolated experiments so require further confirmation.

Lee *at al.* recently published their findings on the effect of VPA in cutaneous wound healing and reported the induction of keratin 14, a marker of the undifferentiated basal layer (Lee, Zahoor et al. 2012). This lends support to this body of work in suggesting that VPA inhibits epidermal differentiation.

Notch signalling has been implicated in the commitment switch during epidermal differentiation so following the discovery that VPA may inhibit differentiation, Notch expression was assessed to determine its involvement. The active component of Notch is the intracellular domain (NICD) and there was a dramatic reduction in its expression in VPA-treated cells between D0 and D1 whereas non-treated cells maintained similar expression at both time points (Figure 5.17A).

Detachment from the basement membrane and withdrawal from the cell cycle (which is regulated by the cyclin-dependent kinase inhibitor *p21*) are required for basal keratinocytes to execute a programme of terminal differentiation (Conforti, Li Yang et al. 2012). The failure of VPA-treated cells to upregulate *p21* with a maximal induction of 3.2-fold compared to 6.2-fold in non-treated cells indicates impaired cell cycle arrest, supporting the idea that VPA inhibits differentiation (Figure 5.17C). Unfortunately, these data, while interesting, cannot be used to conclusively determine the role of VPA in keratinocyte differentiation, if any, due to their limited quantity.

Treatment with HDACi such as VPA could cause genotoxic stress (DNA damage). Under normal conditions this would induce terminal differentiation of epidermal cells via p53-dependent transactivation of Notch1, which is antagonised by ΔNp63α (Figure 6.1) (Stransky, Egloff et al. 2011). However these data indicate that in differentiating nHEKs

Notch1 expression is reduced so this means of inducing differentiation would be prevented.

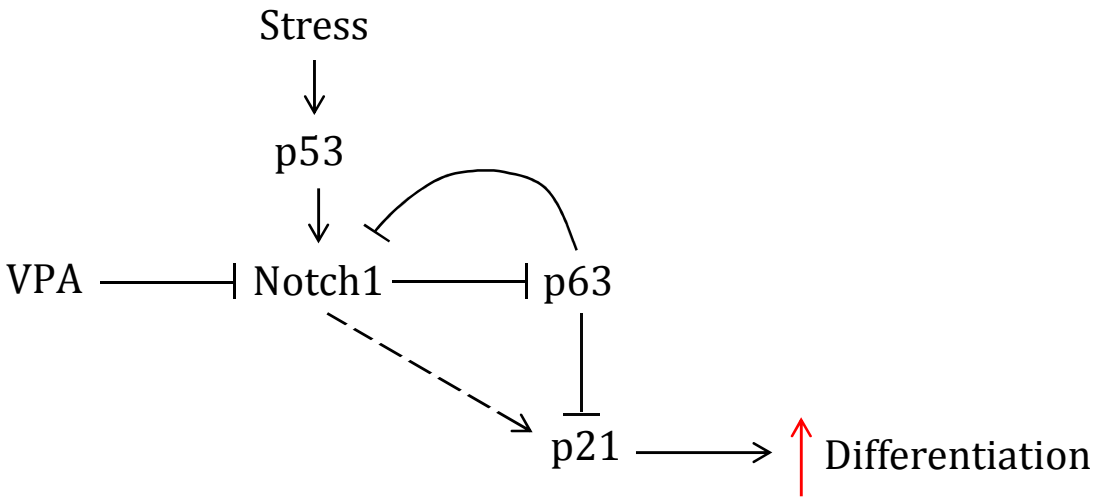

Figure 6.1 A schematic of the process of differentiation in the interfollicular epidermis
Detection of stress causes an increase in p53 which in turn transactivates Notch1. Notch1 signalling is initiated and inhibits p63. The p63-dependent repression of p21 is relieved so its expression increases, leading to cell cycle arrest and facilitating the initiation of terminal differentiation. A reciprocal negative feedback loop exists between Notch proteins and p63, maintaining the delicate balance between proliferation and differentiation. The addition of VPA disrupts this balance, favouring the expression of p63 and the consequent inhibition of differentiation.

The expression of several downstream targets of Notch was investigated in an attempt to elucidate the mechanism via which VPA exerts its apparent effects. Notch signalling is transduced via the Hes and Hey families of transcription factors. The expression of Hes1 was upregulated 1.8-fold by D1 in non-treated nHEKs, but like Notch its expression was also reduced at both D0 (6h treatment with VPA but prior to the addition of calcium) and D1 in VPA-treated cells (Figures 5.18, left and Figure 5.17B). In stark contrast Hey1 was greatly induced in VPA-treated cells by 31.6-fold at D0 and 15.4-fold at D1 (Figure 5.18, middle). Such a remarkable difference in the expression of individual members of these two transcription families was totally unexpected because in canonical Notch signalling a reduction in Notch1 itself would be paralleled by a consequent reduction in expression of its downstream targets due to the linear nature of the signalling pathway. These unexpected results require further validation, however, point towards non-canonical Notch signalling mediating the observed effects.

The Notch co-activator Mastermind-like 1 (MAML1) was also considerably upregulated in VPA-treated cells with a 7.8-fold induction at day 1 (Figure 5.18, right). The profile of MAML1 resembles that of Hey1 with expression still noticeably elevated at D1 in VPA-treated cells relative to the non-treated condition, albeit reduced to 2.6-fold. This is particularly interesting as work in melanoma cells using siRNA specifically targeting MAML1 blocked downstream expression of the transcriptional repressor Hey1 (Kang, Yang et al. 2008). The vast induction in Hey1 and MAML1 but not Notch1 or Hes1 suggests that VPA may be exerting its effects via non-canonical Notch signalling.

A probable explanation for the increase in MAML1 following VPA treatment is that VPA inhibits the kinase GSK3β (Lindberg, Popko-Scibor et al. 2010). Under normal circumstances GSK3β phosphorylates MAML1 and targets it for degradation, however the addition of VPA inhibits GSK3β, consequently reducing its activity including targeting MAML1 for degradation. The increase in Hey1 may rely on a similar mechanism which is unknown as yet. As previous work described a reduction in Hey1 expression in siMAML1-treated melanoma cells (Kang, Yang et al. 2008) it would be necessary to use siRNA to MAML1 to see if these effects were replicated in nHEKs. The next step would be using a GSK3β inhibitor to see if this upregulated MAML1 and if so, compare the increase with VPA-treated nHEKs. If Hey1 was also upregulated, then this would suggest a link between expression of these two genes. The increased expression of Hey1 could also be investigated through the use of siRNA to see if its silencing had any noticeable effects on mRNA levels of other genes of interest. For example, loricrin could be studied in order to elucidate the role of Hey1 in commitment to differentiation.

Decreased recruitment of HDACs and a consequent increase in histone acetylation has been found concomitant with increased expression of Notch target genes including Hey1 and Hes1 in oligodendrocyte precursor cells following inhibition of differentiation (Wu, Hernandez et al. 2012). The data in this investigation suggest that VPA inhibits differentiation (Figure 5.16, left) and elevates histone acetylation (Figure 5.12C). In this investigation the use of the HDACi VPA may be equivalent to decreased recruitment of HDACs. Therefore the marked increase in expression of Hey1 and MAML1 in nHEKs observed following treatment with 2 mM VPA may indeed be due to greater histone acetylation. The degree of acetylation induced by 100 nM TSA was not as high as that

induced by 2 mM VPA (Figure 5.13C) so this dose may not be high enough to mimic decreased recruitment of HDACs.

However this does not explain the reduction in Notch1 and Hes1 expression, thereby increasing the possibility that the effects observed upon VPA treatment are due to non-canonical Notch signalling and may bypass Notch1 itself entirely. Support for this theory comes from studies of the nervous system and muscle development which demonstrate that RBP-Jκ and MAMLs can operate independently of Notch1 (Hori, Cholewa-Waclaw et al. 2008; McElhinny, Li et al. 2008).

In order to verify the role of Notch1 in differentiation, keratinocytes could be treated with the γ-secretase inhibitor *N*-[(3,5-Difluorophenyl)acetyl]-L-alanyl-2-phenyl]glycine-1,1-dimethylethyl ester (DAPT). Inhibition of γ-secretase also inhibits Notch1 as one of the proteolytic cleavages required for the activation of Notch1 is prevented (Imbimbo and Giardina 2011). If the data could be replicated in the presence of DAPT or siRNA to Notch1 it would lend further support to the notion that Notch1 is not involved in mediating the inhibitory effects of VPA on epidermal differentiation and that VPA acts directly on downstream targets of Notch.

Straightforward inhibition of Notch has not proven to be a viable option for treatment of squamous cell carcinomas as demonstrated by a clinical trial of a γ-secretase inhibitor which was cut short due to an increased frequency of skin cancers in the treatment arm of the patients (Stransky, Egloff et al. 2011). Studies using conditional ablation of Notch1 in murine epidermis also show that knockout of Notch1 promotes formation of epidermal tumours, thus indicating that Notch inhibition alone would not be a promising treatment for skin cancers and other skin disorders (Nicolas, Wolfer et al. 2003), however may be a useful tool in identifying which signalling molecules mediate the effects of VPA in nHEKs. siRNA targeting MAML1 has been shown to specifically block Notch signalling in melanoma cells so this warrants further investigation for cancer therapy (Kang, Yang et al. 2008).

Notch signalling inhibits neuronal differentiation in zebrafish via activation of Hes genes (Yamaguchi, Tonou-Fujimori et al. 2005). In the zebrafish retina HDAC1 is required for the switch from proliferation to differentiation as it suppresses Notch signalling. In the epidermis we see the reverse; Notch is responsible for the commitment to terminal

differentiation via suppression of p63. The strong resemblance between the p63- and HDAC1-null epidermis in mice strongly implies that HDAC1 also plays an important role in epidermal development and may interact with Notch and its target genes therefore the impact of HDAC inhibitors on HDAC1 expression during epidermal differentiation warrants further investigation (LeBoeuf, Terrell et al. 2010).

In C6 glioma cells VPA treatment caused changes in the mRNA expression of HDACs 1, 2 and 3 whereas TSA did not (Kim, Castro et al. 2008). As our preliminary data already shows reduced expression of HDAC2 in nHEKs (data not shown) this further necessitates examining the impact of VPA on other HDACs. Future experiments could involve the silencing of HDACs, specifically HDACs 1 and 2 during differentiation to try to dissect out the contribution of each individual HDAC to this process as a degree of redundancy exists between these two isoforms. HDAC7 could also be silenced as it has been shown to interact with MAML1 and its inhibition by VPA could be a factor in the upregulation observed following VPA treatment.

It would be interesting to determine if VPA results in a difference in HDAC enzyme activity in nHEKs, particularly if treatment with VPA alters the expression of any HDACs in addition to HDAC2. If other HDACs also showed alterations in expression following VPA treatment the HDAC activity should be determined as alterations in HDAC expression and/or activity may contribute to the apparent failure of VPA-treated cells to undergo terminal differentiation. This in turn may be linked to the differences observed in expression of Notch1, its target genes and its co-activator MAML1. In order to confirm these ideas Western blotting of HDAC2 and Notch target genes would need to be undertaken to see if any alterations in expression could be correlated and HDAC activity would need to be assayed e.g. by using a Fluor-de-Lys HDAC fluorometric activity assay (Enzo Life Sciences).

Early work seeking to elucidate the mechanism of action of VPA identified parallels between this molecule and TSA with both inducing hyperacetylation of histones in cultured cells, transcription from diverse promoters and similarities in their teratogenic effects (Phiel, Zhang et al. 2001). These early observations lend strength to using TSA as a comparison to VPA to demonstrate that the effects observed in this limited investigation are likely to be specific to VPA.

Many questions have been raised by this investigation and in the future attempts could be made to address these. In conclusion this body of work determined that the class I HDACs 1, 2 and 3 are present in nHEKs, as are the class II HDACs 4 and 6. ΔNp63α, β and γ isoforms are all expressed in the epidermis however TAp63 isoforms were not detected. Valproic acid, a drug that has already been in use for many years as an anticonvulsant and mood stabiliser, seemingly has remarkable effects upon epidermal proliferation and differentiation. It appears to significantly inhibit proliferation in keratinocytes and inhibit epidermal differentiation, although further work is required to confirm these findings.

As p63α protein seems to persist in VPA-treated cells the likely mechanism for the apparent inhibition of differentiation seen is that VPA treatment results in increased stability of the p63α protein and consequently, expression of *p21* and *p16* remain repressed, preventing cell cycle arrest and replicative senescence, respectively. The discrepancy with this theory is that ΔNp63α promotes proliferation. VPA treatment results in prolonged p63α expression which should result in prolonged proliferation; however we see a significant reduction in nHEK proliferation following the addition of VPA (in the absence of additional calcium i.e. to induce differentiation). It follows that this substantial reduction in proliferation would be accompanied by the induction of terminal differentiation, however we see the opposite. One explanation for this could be that the observed effects of VPA on differentiation may occur via non-canonical Notch signalling, acting directly on downstream targets such as Mastermind-like 1, however this would require further work to identify and dissect out the contribution of individual proteins in this signalling pathway.

Overall this HDACi seems to have pleiotropic effects and with further work to elucidate its mechanism(s) of action it may be a promising therapy for skin cancers and other skin disorders either alone or in combination with other treatments.

7. References

Agrawal, N., M. J. Frederick, et al. (2011). "Exome Sequencing of Head and Neck Squamous Cell Carcinoma Reveals Inactivating Mutations in NOTCH1." Science 333(6046): 1154-1157.

Aylon, Y. and M. Oren (2011). "New plays in the p53 theater." Current Opinion in Genetics & Development 21(1): 86-92.

Barker, N., S. Bartfeld, et al. (2010). "Tissue-Resident Adult Stem Cell Populations of Rapidly Self-Renewing Organs." Cell Stem Cell 7(6): 656-670.

Beckers, T., C. Burkhardt, et al. (2007). "Distinct pharmacological properties of second generation HDAC inhibitors with the benzamide or hydroxamate head group." International Journal of Cancer 121(5): 1138-1148.

Bellavia, D., S. Checquolo, et al. (2008). "Notch3: from subtle structural differences to functional diversity." Oncogene 27(38): 5092-5098.

Bergholz, J. and Z.-X. Xiao (2012). "Role of p63 in Development, Tumorigenesis and Cancer Progression." Cancer microenvironment : official journal of the International Cancer Microenvironment Society 5(3): 311-322.

Blanpain, C. and E. Fuchs (2009). "Epidermal homeostasis: a balancing act of stem cells in the skin." Nature Reviews Molecular Cell Biology 10(3): 207-U267.

Blanpain, C., W. E. Lowry, et al. (2006). "Canonical Notch signaling functions as a commitment switch in the epidermal lineage." Genes & Development 20(21): 3022-3035.

Boldrup, L., P. J. Coates, et al. (2011). "Differences in p63 expression in SCCHN tumours of different sub-sites within the oral cavity." Oral Oncology 47(9): 861-865.

Brandt, T., J. L. Kaar, et al. (2012). "Stability of p53 Homologs." Plos One 7(10).

Byrne, C., M. Tainsky, et al. (1994). "PROGRAMMING GENE-EXPRESSION IN DEVELOPING EPIDERMIS." Development 120(9): 2369-2383.

Calalb, M. B., T. A. McKinsey, et al. (2009). "Increased Phosphorylation-Dependent Nuclear Export of Class II Histone Deacetylases in Failing Human Heart." Cts-Clinical and Translational Science 2(5): 325-332.

Candi, E., I. Amelio, et al. (2014). "MicroRNAs and p63 in epithelial stemness." Cell Death and Differentiation.

Candi, E., A. Rufini, et al. (2006). "Differential roles of p63 isoforms in epidermal development: selective genetic complementation in p63 null mice." Cell Death and Differentiation 13(6): 1037-1047.

Carroll, D. K., J. S. Carroll, et al. (2006). "p63 regulates an adhesion programme and cell survival in epithelial cells." Nature Cell Biology 8(6): 551-561.

Catalano, M. G., N. Fortunati, et al. (2005). "Valproic acid induces apoptosis and cell cycle arrest in poorly differentiated thyroid cancer cells." Journal of Clinical Endocrinology & Metabolism 90(3): 1383-1389.

Clayton, E., D. P. Doupe, et al. (2007). "A single type of progenitor cell maintains normal epidermis." Nature 446(7132): 185-189.

Cohen, A., S. Piccolo, et al. (2013). "Genomic pathway analysis reveals that EZH2 and HDAC4 represent mutually exclusive epigenetic pathways across human cancers." BMC Medical Genomics.

Conforti, F., A. Li Yang, et al. (2012). "PIR2/Rnf144B regulates epithelial homeostasis by mediating degradation of p21WAF1 and p63." Oncogene.

Cooper, M. T. D., D. M. Tyler, et al. (2000). "Spatially restricted factors cooperate with Notch in the regulation of Enhancer of split genes." Developmental Biology 221(2): 390-403.

Coulombe, P. and C. Lee (2012). "Defining keratin protein function in skin epithelia: epidermolysis bullosa simplex and its aftermath." Journal of Investigative Dermatology 132: 763-775.

Czubryt, M. P., J. McAnally, et al. (2003). "Regulation of peroxisome proliferator-activated receptor gamma coactivator 1 alpha (PGC-1 alpha) and mitochondrial function by MEF2 and HDAC5." Proceedings of the National Academy of Sciences of the United States of America 100(4): 1711-1716.

Dale, B. A., K. A. Resing, et al. (1985). "FILAGGRIN - A KERATIN FILAMENT ASSOCIATED PROTEIN." Annals of the New York Academy of Sciences 455: 330-342.

Darzynkiewicz, Z., F. Traganos, et al. (1979). "DIFFERENT SENSITIVITY OF CHROMATIN TO ACID DENATURATION IN QUIESCENT AND CYCLING CELLS AS REVEALED BY FLOW CYTOMETRY." Journal of Histochemistry & Cytochemistry 27(1): 478-485.

de Fromentel, C. C., E. Aberdam, et al. (2012). "The two faces of p63, Janus of the p53 gene family." M S-Medecine Sciences 28(4): 381-387.

DeYoung, M. P., C. M. Johannessen, et al. (2006). "Tumor-specific p73 up-regulation mediates p63 dependence in squamous cell carcinoma." Cancer Research 66(19): 9362-9368.

Dickinson, M. and H. Prince (2012). "Romidepsin for Relapsed and Refractory Cutaneous T-Cell Lymphoma." Clinical Medical Insights: Dermatology 5: 21-28.

Dotto, G. P. (2009). "Crosstalk of Notch with p53 and p63 in cancer growth control." Nature Reviews Cancer 9(8): 587-595.

Doupe, D. P., A. M. Klein, et al. (2010). "The Ordered Architecture of Murine Ear Epidermis is Maintained by Progenitor Cells with Random Fate." Developmental Cell 18(2): 317-323.

Ellisen, L. W., J. Bird, et al. (1991). "TAN-1, THE HUMAN HOMOLOG OF THE DROSOPHILA NOTCH GENE, IS BROKEN BY CHROMOSOMAL TRANSLOCATIONS IN T-LYMPHOBLASTIC NEOPLASMS." Cell 66(4): 649-661.

Flores, E. R., S. Sengupta, et al. (2005). "Tumor predisposition in mice mutant for p63 and p73: Evidence for broader tumor suppressor functions for the p53 family." Cancer Cell 7(4): 363-373.

Fryer, C. J., J. B. White, et al. (2004). "Mastermind recruits CycC : CDK8 to phosphorylate the notch ICD and coordinate activation with turnover." Molecular Cell 16(4): 509-520.

Gazave, E., P. Lapebie, et al. (2009). "Origin and evolution of the Notch signalling pathway: an overview from eukaryotic genomes." Bmc Evolutionary Biology 9.

Ghazizadeh, S. and L. B. Taichman (2001). "Multiple classes of stem cells in cutaneous epithelium: a lineage analysis of adult mouse skin." Embo Journal 20(6): 1215-1222.

Glozak, M. A., N. Sengupta, et al. (2005). "Acetylation and deacetylation of non-histone proteins." Gene 363: 15-23.

Goettlicher, M., S. Minucci, et al. (2001). "Valproic acid defines a novel class of HDAC inhibitors inducing differentiation of transformed cells." EMBO (European Molecular Biology Organization) Journal 20(24): 6969-6978.

Gordon, W. R., D. Vardar-Ulu, et al. (2007). "Structural basis for autoinhibition of Notch." Nature Structural & Molecular Biology 14(4): 295-300.

Goudas, L. C., R. Bloch, et al. (2005). "The epidemiology of cancer pain." Cancer Investigation 23(2): 182-190.

Guise, A. J., T. M. Greco, et al. (2012). "Aurora B-dependent Regulation of Class IIa Histone Deacetylases by Mitotic Nuclear Localization Signal Phosphorylation." Molecular & Cellular Proteomics 11(11): 1220-1229.

Gurvich, N., O. M. Tsygankova, et al. (2004). "Histone deacetylase is a target of valproic acid-mediated cellular differentiation." Cancer Research 64(3): 1079-1086.

Haberland, M., R. L. Montgomery, et al. (2009). "The many roles of histone deacetylases in development and physiology: implications for disease and therapy." Nature Reviews Genetics 10(1): 32-42.

Hansson, E. M., F. Lanner, et al. (2010). "Control of Notch-ligand endocytosis by ligand-receptor interaction." Journal of Cell Science 123(17): 2931-2942.

Hayes, J. J., D. J. Clark, et al. (1991). "HISTONE CONTRIBUTIONS TO THE STRUCTURE OF DNA IN THE NUCLEOSOME." Proceedings of the National Academy of Sciences of the United States of America 88(15): 6829-6833.

Hettiaratchy, S. and P. Dziewulski (2004). "ABC of burns. Introduction." British Medical Journal 328: 1366-1368.

Hori, K., J. Cholewa-Waclaw, et al. (2008). "A nonclassical bHLH-Rbpj transcription factor complex is required for specification of GABAergic neurons independent of Notch signaling." Genes & Development 22(2): 166-178.

Hsu, Y.-F., J.-R. Sheu, et al. (2012). "Trichostatin A and sirtinol suppressed survivin expression through AMPK and p38MAPK in HT29 colon cancer cells." Biochimica Et Biophysica Acta-General Subjects 1820(2): 104-115.

Hu, E. D., E. Dul, et al. (2003). "Identification of novel isoform-selective inhibitors within class I histone deacetylases." Journal of Pharmacology and Experimental Therapeutics 307(2): 720-728.

Imbimbo, B. and G. Giardina (2011). "γ-secretase inhibitors and modulators for the treatment of Alzheimer's disease: disappointments and hopes." Current Topics in Medicinal Chemistry 11(12): 1555-1570.

Ju, R. and M. T. Muller (2003). "Histone deacetylase inhibitors activate p21(WAF1) expression via ATM." Cancer Research 63(11): 2891-2897.

Kang, S., C. Yang, et al. (2008). "Induction of CCL2 by siMAML1 through upregulation of TweakR in melanoma cells." Biochemical and Biophysical Research Communications 372(4): 629-633.

Kao, H. Y., M. Downes, et al. (2000). "Isolation of a novel histone deacetylase reveals that class I and class II deacetylases promote SMRT-mediated repression." Genes & Development 14(1): 55-66.

Kerr, J. B., K. J. Hutt, et al. (2012). "DNA Damage-Induced Primordial Follicle Oocyte Apoptosis and Loss of Fertility Require TAp63-Mediated Induction of Puma and Noxa." Molecular Cell 48(3): 343-352.

Keyes, W. M., Y. Wu, et al. (2005). "p63 deficiency activates a program of cellular senescence and leads to accelerated aging." Genes & Development 19(17): 1986-1999.

Kim, B., L. M. R. Castro, et al. (2008). "Clinically relevant concentrations of valproic acid modulate melatonin MT(1) receptor, HDAC and MeCP2 mRNA expression in C6 glioma cells." European Journal of Pharmacology 589(1-3): 45-48.

King, K. E., R. M. Ponnamperuma, et al. (2003). "Delta Np63 alpha functions as both a positive and a negative transcriptional regulator and blocks in vitro differentiation of murine keratinocytes." Oncogene 22(23): 3635-3644.

Kopan, R. and M. X. G. Ilagan (2009). "The Canonical Notch Signaling Pathway: Unfolding the Activation Mechanism." Cell 137(2): 216-233.

Koster, M. I., D. Dai, et al. (2007). "p63 induces key target genes required for epidermal morphogenesis." Proceedings of the National Academy of Sciences of the United States of America 104(9): 3255-3260.

Koster, M. I., S. Kim, et al. (2006). "TAp63 alpha induces AP-2 gamma as an early event in epidermal morphogenesis." Developmental Biology 289(1): 253-261.

Koster, M. I. and D. R. Roop (2008). "Sorting out the p63 signaling network." Journal of Investigative Dermatology 128(7): 1617-1619.

Laemmli, U. (1970). "Cleavage of structural proteins during the assembly of the head of bacteriophage T4." Nature 227: 680-685.

Lahm, A., C. Paolini, et al. (2007). "Unraveling the hidden catalytic activity of vertebrate class Ila histone deacetylases." Proceedings of the National Academy of Sciences of the United States of America 104(44): 17335-17340.

Laurikkala, J., M. L. Mikkola, et al. (2006). "p63 regulates multiple signalling pathways required for ectodermal organogenesis and differentiation." Development 133(8): 1553-1563.

LeBoeuf, M., A. Terrell, et al. (2010). "Hdac1 and Hdac2 Act Redundantly to Control p63 and p53 Functions in Epidermal Progenitor Cells." Developmental Cell 19(6): 807-818.

Lee, S.-H., M. Zahoor, et al. (2012). "Valproic acid induces cutaneous wound healing in vivo and enhances keratinocyte motility." Plos One 7(11): e48791-e48791.

Lefort, K., A. Mandinova, et al. (2007). "Notch1 is a p53 target gene involved in human keratinocyte tumor suppression through negative regulation of ROCK1/2 and MRCK alpha kinases." Genes & Development 21(5): 562-577.

Lerche, C. M., P. A. Philipsen, et al. (2008). "Photocarcinogenesis of topical tazarotene and isotretinoin alone and in combination with valproic acid in hairless mice." Experimental Dermatology 17(11): 972-974.

Lindberg, M. J., A. E. Popko-Scibor, et al. (2010). "SUMO modification regulates the transcriptional activity of MAML1." Faseb Journal 24(7): 2396-2404.

Ma, C., J. Wang, et al. (2007). "The role of glycogen synthase kinase 3 beta in the transformation of epidermal cells." Cancer Research 67(16): 7756-7764.

Mack, J. A., S. Anand, et al. (2005). "Proliferation and cornification during development of the mammalian epidermis." Birth Defects Research 75(4): 314-329.

Madan, V., J. T. Lear, et al. (2010). "Non-melanoma skin cancer." Lancet 375(9715): 673-685.

Marks, P. A. and R. Breslow (2007). "Dimethyl sulfoxide to vorinostat: Development of this histone deacetylase inhibitor as an anticancer drug." Nature Biotechnology 25(1): 84-90.

Marks, P. A., V. M. Richon, et al. (2004). "Histone deacetylase inhibitors." Advances in Cancer Research, Vol 91 91: 137-+.

Marques-Pereira, J. P. and C. P. Leblond (1965). "Mitosis and differentiation in the stratified squamous epithelium of the rat esophagus." Amer J Anat 117((1)): 73-87.

Mascre, G., S. Dekoninck, et al. (2012). "Distinct contribution of stem and progenitor cells to epidermal maintenance." Nature 489(7415): 257-+.

Mauro, T., G. Bench, et al. (1998). "Acute barrier perturbation abolishes the ca(2+) and k(+) gradients in murine epidermis: Quantitative measurement using PIXE." Journal of Investigative Dermatology 111(6): 1198-1201.

McElhinny, A. S., J. L. Li, et al. (2008). "Mastermind-like transcriptional co-activators: emerging roles in regulating cross talk among multiple signaling pathways." Oncogene 27(38): 5138-5147.

McKinsey, T. A., C. L. Zhang, et al. (2000). "Signal-dependent nuclear export of a histone deacetylase regulates muscle differentiation." Nature 408(6808): 106-111.

Medawar, A., T. Virolle, et al. (2008). "Delta Np63 Is Essential for Epidermal Commitment of Embryonic Stem Cells." Plos One 3(10).

Mills, A. A. (2006). "p63: oncogene or tumor suppressor?" Current Opinion in Genetics & Development 16(1): 38-44.

Mills, A. A., B. H. Zheng, et al. (1999). "p63 is a p53 homologue required for limb and epidermal morphogenesis." Nature 398(6729): 708-713.

Mohr, O. L. (1919). "Character Changes Caused by Mutation of an Entire Region of a Chromosome in Drosophila." Genetics 4(3): 275-282.

Montgomery, R. L., C. A. Davis, et al. (2007). "Histone deacetylases 1 and 2 redundantly regulate cardiac morphogenesis, growth, and contractility." Genes & Development 21(14): 1790-1802.

Moriyama, M., A.-D. Durham, et al. (2008). "Multiple roles of notch signaling in the regulation of epidermal development." Developmental Cell 14(4): 594-604.

Nichols, J. T., A. Miyamoto, et al. (2007). "DSL ligand endocytosis physically dissociates Notch 1 heterodimers before activating proteolysis can occur." Journal of Cell Biology 176(4): 445-458.

Nickoloff, B. J., J. Z. Qin, et al. (2002). "Jagged-1 mediated activation of notch signaling induces complete maturation of human keratinocytes through NF-kappa B and PPAR gamma." Cell Death and Differentiation 9(8): 842-855.

Nicolas, M., A. Wolfer, et al. (2003). "Notch1 functions as a tumor suppressor in mouse skin." Nature Genetics 33(3): 416-421.

Nowak, J. A., L. Polak, et al. (2008). "Hair follicle stem cells are specified and function in early skin morphogenesis." Cell Stem Cell 3(1): 33-43.

Olins, D. E. and A. L. Olins (2003). "Chromatin history: our view from the bridge." Nature Reviews Molecular Cell Biology 4(10): 809-814.

Oyama, T., K. Harigaya, et al. (2011). "Mastermind-like 1 (MamL1) and mastermind-like 3 (MamL3) are essential for Notch signaling in vivo." Development 138(23): 5235-5246.

Panelos, J. and D. Massi (2009). "Emerging role of Notch signaling in epidermal differentiation and skin cancer." Cancer Biology & Therapy 8(21): 1986-1993.

Paris, M., M. Rouleau, et al. (2012). "Regulation of skin aging and heart development by TAp63." Cell Death and Differentiation 19(2): 186-193.

Peng, L. and E. Seto (2011). "Deacetylation of nonhistone proteins by HDACs and the implications in cancer." Handbook of experimental pharmacology 206: 39-56.

Perdigoto, C. N. and A. J. Bardin (2013). "Sending the right signal: Notch and stem cells." Biochimica Et Biophysica Acta-General Subjects 1830(2): 2307-2322.

Phiel, C. J., F. Zhang, et al. (2001). "Histone deacetylase is a direct target of valproic acid, a potent anticonvulsant, mood stabilizer, and teratogen." Journal of Biological Chemistry 276(39): 36734-36741.

Potten, C. S. (1974). "EPIDERMAL PROLIFERATIVE UNIT - POSSIBLE ROLE OF CENTRAL BASAL-CELL." Cell and Tissue Kinetics 7(1): 77-88.

Poulson, D. (1945). "Chromosomal control of embryogenesis in Drosophila." The American Naturalist 79: 340-363.

Ramsey, M. R., L. He, et al. (2011). "Physical Association of HDAC1 and HDAC2 with p63 Mediates Transcriptional Repression and Tumor Maintenance in Squamous Cell Carcinoma." Cancer Research 71(13): 4373-4379.

Rangarajan, A., C. Talora, et al. (2001). "Notch signaling is a direct determinant of keratinocyte growth arrest and entry into differentiation." Embo Journal 20(13): 3427-3436.

Rebay, I., R. G. Fehon, et al. (1993). "SPECIFIC TRUNCATIONS OF DROSOPHILA NOTCH DEFINE DOMINANT ACTIVATED AND DOMINANT-NEGATIVE FORMS OF THE RECEPTOR." Cell 74(2): 319-329.

Rodd, A., K. Ververis, et al. (2012). "Current and emerging therapeutics for cutaneous T cell lymphoma: histone deacetylase inhibitors." Lymphoma 2012.

Roshan, A. and P. H. Jones (2012). "Act your age: Tuning cell behavior to tissue requirements in interfollicular epidermis." Seminars in Cell & Developmental Biology 23(8): 884-889.

Rouleau, M., A. Medawar, et al. (2011). "TAp63 Is Important for Cardiac Differentiation of Embryonic Stem Cells and Heart Development." Stem Cells 29(11): 1672-1683.

Sandilands, A., C. Sutherland, et al. (2009). "Filaggrin in the frontline: role in skin barrier function and disease." Journal of Cell Science 122(9): 1285-1294.

Schweisguth, F. (2004). "Regulation of notch signaling activity." Current Biology 14(3): R129-R138.

Stransky, N., A. M. Egloff, et al. (2011). "The Mutational Landscape of Head and Neck Squamous Cell Carcinoma." Science 333(6046): 1157-1160.

Taylor, M. D., Y. Liu, et al. (2010). "Combined proteasome and histone deacetylase inhibition attenuates epithelial-mesenchymal transition through E-cadherin in esophageal cancer cells." Journal of Thoracic and Cardiovascular Surgery 139(5): 1224-U1160.

Terrinoni, A., V. Serra, et al. (2013). "Role of p63 and the Notch pathway in cochlea development and sensorineural deafness." Proceedings of the National Academy of Sciences of the United States of America 110(18): 7300-7305.

Tiffon, C. E., J. E. Adams, et al. (2011). "The histone deacetylase inhibitors vorinostat and romidepsin downmodulate IL-10 expression in cutaneous T-cell lymphoma cells." British Journal of Pharmacology 162(7): 1590-1602.

Truong, A. B. and P. A. Khavari (2007). "Control of keratinocyte proliferation and differentiation by p63." Cell Cycle 6(3): 295-299.

Ueki, N., S. Lee, et al. (2013). "Selective cancer targeting with prodrugs activated by histone deacetylases and a tumour-associated protease." Nature communications In Press.

Vaidya, S., M. Risbud, et al. (2013). "Hereditary ectodermal dysplasia: Report of 11 patients from a family." Indian journal of dental research : official publication of Indian Society for Dental Research 24(4): 502-506.

Van den Wyngaert, I., W. de Vries, et al. (2000). "Cloning and characterization of human histone deacetylase 8." Febs Letters 478(1-2): 77-83.

Van Keymeulen, A. and C. Blanpain (2012). "Tracing epithelial stem cells during development, homeostasis, and repair." Journal of Cell Biology 197(5): 575-584.

Vanbokhoven, H., G. Melino, et al. (2011). "p63, a Story of Mice and Men." Journal of Investigative Dermatology 131(6): 1196-1207.

Wang, N. J., Z. Sanborn, et al. (2011). "Loss-of-function mutations in Notch receptors in cutaneous and lung squamous cell carcinoma." Proceedings of the National Academy of Sciences of the United States of America 108(43): 17761-17766.

Westfall, M., D. Mays, et al. (2003). "The ΔNp63α Phosphoprotein Binds the p21 and 14-3-3σ Promoters In Vivo and Has Transcriptional Repressor Activity That Is Reduced by Hay-Wells Syndrome-Derived Mutations." Molecular and Cellular Biology 23: 2264-2276.

Wolff, S., F. Talos, et al. (2009). "The alpha/beta carboxyterminal domains of p63 are required for skin and limb development. New insights from the Brdm2 mouse which is not a complete p63 knockout but expresses p63 gamma-like proteins." Cell Death and Differentiation 16: 1108-1117.

Wolff, S., F. Talos, et al. (2009). "The alpha/beta carboxy-terminal domains of p63 are required for skin and limb development. New insights from the Brdm2 mouse which is not a complete p63 knockout but expresses p63 gamma-like proteins." Cell Death and Differentiation 16(8): 1108-1117.

Wu, M., M. Hernandez, et al. (2012). "Differential Modulation of the Oligodendrocyte Transcriptome by Sonic Hedgehog and Bone Morphogenetic Protein 4 via Opposing Effects on Histone Acetylation." Journal of Neuroscience 32(19): 6651-6664.

Ximenes, J. C., D. de Oliveira Goncalves, et al. (2013). "Valproic acid: an anticonvulsant drug with potent antinociceptive and anti-inflammatory properties." Naunyn Schmiedebergs Arch Pharmacol Epub ahead of print.

Xu, Z., Y. Wang, et al. (2006). "TRICHOSTATIN A INHIBITS PROLIFERATION, INDUCES APOPTOSIS AND CELL CYCLE ARREST IN HELA CELLS." Chinese Journal of Cancer Research 18(3): 188-192.

Yagi, Y., S. Fushida, et al. (2010). "Effects of valproic acid on the cell cycle and apoptosis through acetylation of histone and tubulin in a scirrhous gastric cancer cell line." Journal of Experimental & Clinical Cancer Research 29.

Yamaguchi, M., N. Tonou-Fujimori, et al. (2005). "Histone deacetylase 1 regulates retinal neurogenesis in zebrafish by suppressing Wnt and Notch signaling pathways." Development 132(13): 3027-3043.

Yang, A., M. Kaghad, et al. (2002). "On the shoulders of giants: p63, p73 and the rise of p53." Trends in Genetics 18(2): 90-95.

Yang, A., R. Schweitzer, et al. (1999). "p63 is essential for regenerative proliferation in limb, craniofacial and epithelial development." Nature 398(6729): 714-718.

Yang, X. J. and E. Seto (2003). "Collaborative spirit of histone deacetylases in regulating chromatin structure and gene expression." Current Opinion in Genetics & Development 13(2): 143-153.

Yurek-George, A., F. Habens, et al. (2004). "Total synthesis of spiruchostatin A, a potent histone deacetylase inhibitor." Journal of the American Chemical Society 126(4): 1030-1031.

Zhang, L., G. Wang, et al. (2012). "VPA inhibits breast cancer cell migration by specifically targeting HDAC2 and down-regulating Survivin." Molecular and Cellular Biochemistry 361(1-2): 39-45.

Zhang, L., G. Wang, et al. (2011). "Valproic acid inhibits prostate cancer cell migration by up-regulating E-cadherin expression." Pharmazie 66(8): 614-618.

Zhu, H., A. Li, et al. (2012). "The new function of p53 family and its pathway related proteins in female reproduction." Yichuan 34(8): 943-949.

8. Appendices

Appendix 1. Detailed list of the antibodies used in this investigation

Target protein	Species raised in	Dilution	Predicted molecular weight (kDa)	Company	Catalogue number
HDAC1	Rabbit	1: 2000	55/62	Abcam	Ab19845
HDAC2	Rabbit	1: 1000	55/60	Abcam	Ab16032
HDAC3	Rabbit	1: 1000	50	Abcam	Ab16047
HDAC4	Rabbit	1: 2000	140	Cell Signalling	7628
HDAC6	Rabbit	1: 1000	160	Cell Signalling	7558
HDAC7	Rabbit	1: 500	102	Abcam	Ab23657
HDAC8	Rabbit	1: 500	41	Abcam	Ab23658
p63α (H-129)	Rabbit	1: 1000	77	Santa Cruz	sc-8344
Ac-H4	Mouse	1:2000	10	Millipore	06-598
Ac-tubulin	Mouse	1: 2000	50	Sigma	T6793
B-tubulin (H-235)	Rabbit	1: 1000	55	Santa Cruz	sc-9104
Notch1	Rabbit	1: 1000	120	Santa Cruz	sc-6014
Involucrin	Mouse	1: 20000	120-170	Sigma	I9018
Loricrin	Rabbit	1: 3000	42	Sigma	AV41738
Keratin 1 (AF-109)	Rabbit	1: 1000	67	Covance	PRB-165P
Secondary antibodies					
Anti-mouse IgG HRP-linked		1: 10000		Cell Signalling	7076
Anti-rabbit IgG HRP-linked		1: 10000		Cell Signalling	7074

Appendix 2. Primer sequences, amplicon sizes, number of cycles and annealing temperatures used for PCR studies

Primer	Forward5'-3'	Reverse 5'-3'	Amplicon size (bp)	No. of cycles	Annealing temp (^{0}C)
TAp63	CCATCAGAAGATGGTGCGAC	GTTCAGTGGAATACGTCCAGG	355	30	60
ΔNp63	CCTGGAAAACAATGCCCAGAC		295	30	60
p63α	CACACATGGTATCCAGATGAC	GCTCAATCTGATAGATGGTGG	590	30	60
p63α (2)		CTTGCCAGATCATCCATGGAG	693	30	62
p63β		GCCAGATCCTGACAATGCTG	492	30	60
p63γ		GGCTGAAAGGAGATGTTTCTG	218	30	60
18S	CAGCCACCCGAGATTGAGCA	TAGTAGCAGCGGGCGGTGTG	253	22	58

Appendix 3. TaqMan primers used for qPCR

Target gene	Primer catalogue number
18S	Hs99999901_s1
Involucrin	Hs00846307_s1
Loricrin	Hs01894962_s1
p21	Hs00355782_m1
Notch1	Hs01062014_m1
Hes1	Hs00172878_m1
Hey1	Hs01114113_m1
Hey2	Hs00232622_m1
DLL1	Hs00194509_m1
Jagged1	Hs01070032_m1
Mastermind-like 1	Hs01070499_m1

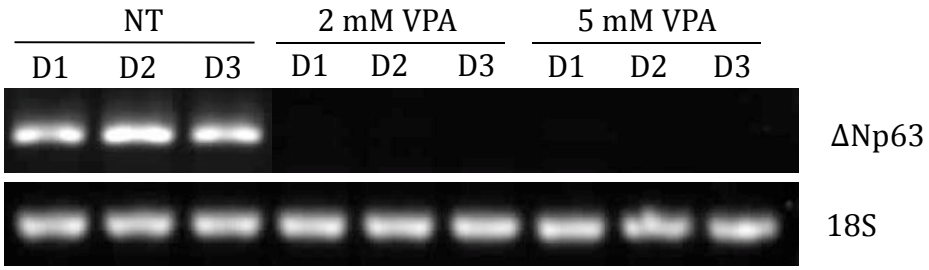

Appendix 4. Valproic acid results in the elimination of p63 mRNA. Cells were treated with 2 and 5 mM valproic acid and harvested at the time points indicated for RNA extraction and cDNA synthesis. In non-treated nHEKs ΔNp63 mRNA is present at D1, 2 and 3 while in cells treated with either 2 or 5 mM VPA there is a complete lack of ΔNp63 mRNA. The ribosomal RNA 18S was used to confirm equal loading and the integrity of the cDNA used. NT, non-treated; VPA, valproic acid. n=1.

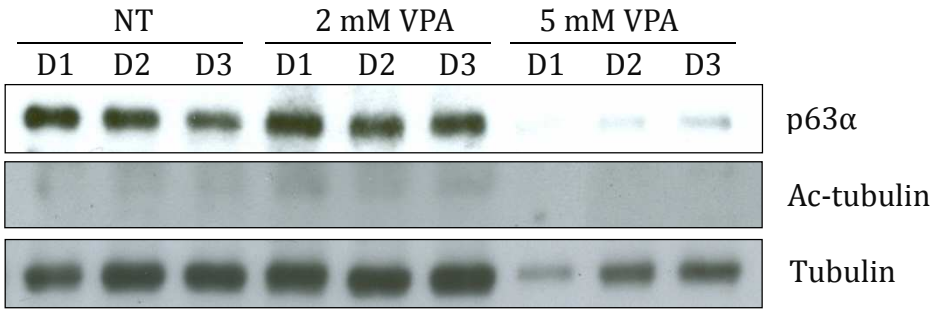

Appendix 5. Valproic acid has dose-dependent effects on p63 protein expression. Cells were treated with 2 and 5 mM valproic acid and harvested at the time points indicated for protein. In non-treated nHEKs p63α protein was observed at the three time points, although at D3 expression was reduced. Cells treated with 2 mM VPA also retained p63α protein at all three time points without a reduction at D3, whereas p63α expression was virtually lost in cells treated with 5 mM VPA. NT, non-treated; VPA, valproic acid. n=1.